

Constrained Symplectic Quantization I: the Quantum Harmonic Oscillator

Martina Giachello^{a,b} Francesco Scardino^{c,d} Giacomo Gradenigo^e

^a*Gran Sasso Science Institute, Viale F. Crispi 7, 67100 L’Aquila, Italy*

^b*INFN-Laboratori Nazionali del Gran Sasso, Via G. Acitelli 22, 67100 Assergi (AQ), Italy*

^c*Physics Department, INFN Roma1, Piazzale A. Moro 2, Roma, I-00185, Italy*

^d*Physics Department, Sapienza University, Piazzale A. Moro 2, Roma, I-00185, Italy*

^e*Physics and Astronomy Department “Galileo Galilei”, Università di Padova, Via Marzolo 8, 35131 Padova, Italy*

E-mail: martina.giachello@gssi.it, francesco.scardino@roma1.infn.it,
giacomo.gradenigo@gssi.it

ABSTRACT: Symplectic quantization is a functional approach to quantum field theory that allows sampling of quantum fluctuations directly in Minkowski space-time by means of a generalized microcanonical ensemble similar to the one of the standard microcanonical approach to lattice field theory. In a previous paper [1] we showed that, for an interacting scalar field theory in 1+1-dimensions, this formalism allows to capture numerically some crucial real-time features inaccessible to any Euclidean approach to lattice field theory. Yet, the new approach was plagued by two main limitations: an ill-defined non-interacting limit and the absence of a direct formal correspondence between its correlation functions and those generated by the Feynman path integral approach. In this paper, we introduce the new “*constrained symplectic quantization*” approach, for which the perfect equivalence with the Feynman path integral is proved and which is perfectly well defined for the free theory. This new approach is characterized by the analytical continuation of all fields and of the action from \mathbb{R} to \mathbb{C} and the presence of some constraints which guarantee the stability of the generalized Hamiltonian dynamics and the convergence of the corresponding generalized microcanonical partition function, hence the name of the theory. We show the application of this formalism to the quantum harmonic oscillator on a Minkowskian-time lattice, finding perfect agreement between one- and two-point numerical correlators and the exact quantum-mechanical results. We observe genuine real-time features such as the oscillatory propagator and the discrete excited-state energy spectrum. Our results provide strong numerical evidence that constrained symplectic quantization can sample real-time quantum-mechanical observables, offering a concrete route to overcome the limitations of Euclidean-time importance sampling.

Contents

1	Introduction	2
2	Fields and Action: analytic continuation from \mathbb{R} to \mathbb{C}	4
3	Microcanonical action and the Feynman Path Integral	6
4	Harmonic Oscillator: constrained equations of motion	11
5	Constrained symplectic dynamics: numerical algorithm	19
6	Constrained symplectic dynamics: numerical results	24
6.1	Average position $\langle \hat{q}(x_0) \rangle$ finite- $\Delta\tau$ effects (periodic boundaries)	25
6.2	Two-point correlation function (periodic boundaries)	28
6.3	Uncertainty principle	31
6.4	Discrete spectrum of $\langle \hat{q}^{2k}(x_0) \rangle$ or Dirichlet boundary conditions	34
7	Conclusions	40
A	Asymptotic properties of the coefficients $c_j(M, n)$	43
B	Two-point function on a periodic domain (continuum and discrete)	45
B.1	Continuum derivation from the tower of eigenstates	45
B.2	Periodic lattice derivation (discrete Fourier modes)	47
C	Lattice functional derivation of the commutator identity	49
D	Dirichlet modes and diagonalisation of the quadratic action	51
E	Continuum Dirichlet expression for $\langle \hat{q}^2(x_0) \rangle_{\text{D.B.}(T)}$	53
F	Dirichlet correlators on the lattice	60
G	Expectation values of $\langle \hat{q}^{2k}(x_0) \rangle_{\text{D.B.}(T)}$ with Dirichlet boundaries	62
G.1	\hat{q}^4	62
G.2	\hat{q}^6	64
H	Resonant enhancement of Dirichlet correlators on the lattice and relation to truncated even-state sums	66

1 Introduction

Symplectic quantization is the proposal of a new functional approach to quantum field theory put forward in a recent series of conceptual papers [2–4] and backed by some encouraging numerical evidence, presented in [1, 5, 6], showing that symplectic quantization allows for a numerical sampling of the real-time dynamics of a field theory closely related to ordinary scalar field theory on a lattice. The present paper aims to fully clarify from the theoretical viewpoint the relation between symplectic quantization and the Feynman path integral approach to quantum mechanics, showing how, at least in the case of the harmonic oscillator, it allows one to reproduce features of the quantum dynamics that are inaccessible to importance sampling algorithms based on imaginary time quantum mechanics [7–9]. Symplectic quantization, which is closely inspired by the microcanonical approach to quantum field theory [10–12], is a functional deterministic approach built on an extended variable space, where the quantum fluctuations of fields are parametrized by an additional time parameter τ , referred to as the *intrinsic time* in [2–4], and governed by an intrinsic Hamiltonian dynamics. For instance, in the symplectic quantization approach, the position quantum operator $\hat{q}(t)$ is replaced by the fluctuating field $q(t, \tau)$ [8, 13], such that the quantum fluctuations at a given Minkowskian time t are those generated by the Hamiltonian equations

$$\frac{\partial q(t, \tau)}{\partial \tau} = \frac{\delta \mathbb{H}[q, \pi]}{\delta \pi(t, \tau)}, \quad \frac{\partial \pi(t, \tau)}{\partial \tau} = -\frac{\delta \mathbb{H}[q, \pi]}{\delta q(t, \tau)}, \quad (1.1)$$

where $\mathbb{H}[q, \pi]$ is a generalized Hamiltonian of the system of the form

$$\mathbb{H}[\pi, q] = \mathbb{K}[\pi] - S[q], \quad (1.2)$$

with $S[q]$ the standard action of the problem considered, playing the role of a potential, and $\mathbb{K}[\pi]$ is a generalized kinetic energy, quadratic in the additional momenta $\pi(t, \tau) \propto \partial q(t, \tau) / \partial \tau$. It is immediate to see that if one replaces quantum mechanics with quantum field theory, $q(t, \tau) \rightarrow \phi(x, \tau)$, where x is a coordinate in Minkowski space-time, the above construction is completely analogous to the microcanonical approach to quantum fields used in numerical lattice field theory [12, 14, 15], with the only difference that the potential terms is not the Euclidean action $S_E[\phi]$ but minus the Minkowskian action $-S[\phi]$. The striking result of [1, 5, 6] is that the above procedure, when realized as a numerical protocol to sample the quantum fluctuations of a $\lambda\phi^4$ theory on a $1 + 1$ lattice allows for a qualitative reproduction of the shape of the free Feynman propagator when a small non-linear coefficient λ is employed.

Despite this numerical success, in [1] we have also explained the theoretical limitations of this approach. Assuming a bona fide ergodic hypothesis for the trajectories generated by Eq. (1.1), ubiquitous in the microcanonical approach to quantum field theory, one claims that the quantum fluctuations sampled are those corresponding to the microcanonical measure:

$$\varrho_{\text{micro}}[q, \pi] = \frac{1}{\Omega(\mathcal{A})} \delta(\mathbb{H}[q, \pi] - \mathcal{A}), \quad (1.3)$$

where the normalization is

$$\Omega[\mathcal{A}] = \int \mathcal{D}q \mathcal{D}\pi \delta(\mathbb{H}[q, \pi] - \mathcal{A}). \quad (1.4)$$

In [1, 5], as a corollary of the numerical results, it is proved that, for a system with M degrees of freedom, in the large- M limit the microcanonical measure corresponds to a canonical one of the kind

$$M \rightarrow \infty \implies \varrho_{\text{micro}}[q, \pi] \rightarrow \exp\{S[q]/\hbar\}, \quad (1.5)$$

where $\hbar = A/M$ is the unit of action. The equivalence of Eq. (1.5) contains two important pieces of information: first, it is perfectly consistent with the numerical results contained in the same paper, where we found a Hamiltonian dynamics which is stable only for a lower-bounded non-linear potential in the action, while it is unstable for a free action: it must be in fact recalled that a free relativistic action $S[\phi]$ is not positive definite. Second, the procedure does not directly sample the Feynman path integral measure, which is proportional to $\exp(iS[\phi/\hbar])$, but a different object, $\exp(S[\phi/\hbar])$.

The purpose of the present discussion is to demonstrate how the symplectic quantization approach can be further extended with respect to the form in which we have proposed it in [1, 5, 6]. This extension furnishes a stable dynamics capable of numerically sampling quantum fluctuation on a lattice, even in the case of a free action and, most importantly, provides expectation values which are precisely those obtained from the Feynman path integral approach [16]. The logic followed by the extension of the symplectic quantization formalism proposed here is simple and in agreement with recent developments to circumvent the sign problem in numerical field theory [17]: to sample the correct quantum fluctuations we consider an analytic prolongation to the complex plane of all fields. For instance, for the position field in quantum mechanics, we consider $q(t, \tau) \in \mathbb{C}$ rather than $q(t, \tau) \in \mathbb{R}$, so that we also have $S[q] \in \mathbb{C}$. Then, we consider a *real* generalized Hamiltonian and a *constrained* deterministic dynamics such that stability is guaranteed, as well as a direct correspondence with the path integral measure. It is worth noticing that the logic of the constrained symplectic quantization approach has profound analogies with the evaluation of path integrals with the Lefschetz-Thimbles strategy [17–20], which considers the analytic continuation of all fields/variables in the complex plane [21], and then performs the integration along constrained paths to guarantee the convergence of functional integrals. The main difference between Symplectic Quantization and the Lefschetz-Thimble's approach is that while in the latter one puts constraints on the path integral evaluation, where the path integral plays the role of a partition function, in the symplectic quantization approach, one puts constraints directly on the microscopic dynamical processes which generate the path integral "measure". As such, and by virtue of its striking ability to reproduce quantum mechanical expectation values, we believe that the present approach could be a new interesting proposal to handle the sign problem in many instances in numerical field theoretical and many-body quantum dynamics [22–24].

This paper is therefore dedicated to illustrating all the analytical subtleties of our new *constrained symplectic quantization* approach and to numerically validate it in a prototypical

reference case: the quantum harmonic oscillator.

The theoretical characterization of the constrained symplectic quantization approach proceeds in two main steps. First, we define the analytic continuation of fields and action to the complex plane and introduce a generalized Hamiltonian, proving that the associated microcanonical measure generates connected field correlators that are equivalent to those obtained from the Feynman path integral. These points are discussed in Sec. 2 and demonstrated in Sec. 3. Second, we identify the class of microscopic constraints that bound the Hamiltonian dynamics, which define the corresponding integration contours allowing the sampling of the microcanonical partition function and by extension the Feynman path-integral. This is discussed in detail in Sec. 4, with a focus—both for clarity and for practical purposes—on the system studied in this work: the quantum harmonic oscillator. Sec. 5 then explains how the constrained dynamics introduced in Sec. 4 is implemented within the numerical symplectic algorithm used to integrate the intrinsic-time evolution. Finally, Sec. 6 presents numerical results showing that the symplectic quantization approach yields an algorithm capable of capturing the real-time dynamics of the system and reproducing its excited-state structure. In particular, we compute the two-point correlation function $\langle \hat{q}(t)\hat{q}(t') \rangle$, we numerically verify the canonical commutation relation $\langle [\hat{p}(t), \hat{q}(t)] \rangle = i\hbar$, and we study $\langle \hat{q}^{2n}(t) \rangle$. The Fourier transform of the latter with respect to Minkowskian time exhibits a peak structure that matches precisely the excited states of the harmonic oscillator.

2 Fields and Action: analytic continuation from \mathbb{R} to \mathbb{C}

We begin by motivating the choice of the new generalized Hamiltonian \mathbb{H}_{SQ} , which is required once all dynamical variables are analytically continued to the complex plane. Three main reasons motivate, at the same time, both the need for a new generalized Hamiltonian \mathbb{H}_{SQ} —different from the one considered in our previous work [1]—and the necessity to analytically continue all variables to \mathbb{C} . In [1] we showed that, by fixing the generalized action \mathcal{A} to the real value $\mathcal{A} = M\hbar$, for an interacting field on a $1+1$ lattice with M degrees of freedom it is possible to reproduce numerically (at least qualitatively) the shape of the free Feynman propagator by averaging the two-point correlation function along the Hamiltonian dynamics. Nevertheless, an *exact* correspondence between quantum field theory in the path-integral formulation and the microcanonical approach considered in [1] cannot be established as long as one employs a real generalized action, $\mathcal{A} \in \mathbb{R}$, together with real fields, $\phi \in \mathbb{R}$. Indeed, the calculation presented in [1] shows that, in the continuum limit $M \rightarrow \infty$, the microcanonical partition function $\Omega[\hbar M]$ corresponds to a Minkowskian statistical mechanics, rather than to quantum field theory. From the expression of the microcanonical partition function computed in [1] in the large- M limit,

$$\Omega[\hbar/z, J] = \int \mathcal{D}\phi \exp\left(\frac{z}{\hbar}S[\phi] + \frac{z}{\hbar}J\phi\right), \quad (2.1)$$

one sees that an exact equivalence with quantum field theory would be recovered only by fixing the generalized action of the microcanonical approach to the purely imaginary value

$\mathcal{A} = -i\hbar M$, so that

$$M \rightarrow \infty \implies \log \Omega[\mathcal{A} = -i\hbar M] \sim \log \mathcal{Z}[\hbar]. \quad (2.2)$$

However, a generalized action of the form $\mathbb{H}[\pi, q] = \mathbb{K}[\pi] - S[q]$ cannot be fixed by construction to purely imaginary values, since it is a real functional of real fields. Therefore, the microcanonical Minkowskian approach of [1], despite allowing for remarkable advances with respect to the standard canonical Euclidean approach, must be extended in order to define a statistical ensemble in direct correspondence with quantum field theory—and, in the non-relativistic limit, with quantum mechanics. To pursue this goal we show here, focusing on the paradigmatic case of the quantum harmonic oscillator, that an analytic continuation from \mathbb{R} to \mathbb{C} is needed both for the action S and for all fields entering the theory. Despite the analytic continuation of fields and of the action S to the complex domain, the theory must still fix the generalized Hamiltonian to a *real* value $\mathbb{H}_{\text{SQ}} = \mathcal{A}$, since only in this case it is possible to impose a physical “quantization” constraint of the form $\mathcal{A} = \hbar M$. For this reason, a new form of the generalized action/Hamiltonian \mathbb{H}_{SQ} must be chosen with respect to the one introduced in [1].

Only one previous work discussed an extension of the symplectic quantization approach in the context of quantum mechanics [4]. There it was argued that, in order to reproduce quantum fluctuations with a deterministic dynamics, the quantum observable $\dot{q}(t)$ should be promoted to a *position* field $q(t, \tau)$, accompanied by its *conjugate momentum* field $\pi(t, \tau)$. However, as shown numerically and analytically in [1], this procedure does not, by construction, yield a direct correspondence between quantum-mechanical fluctuations and the fluctuations sampled by the symplectic quantization approach. Here we propose that such a correspondence can be achieved only by also considering the analytic continuation from \mathbb{R} to \mathbb{C} of the fields $q(t, \tau)$ and $\pi(t, \tau)$:

$$\begin{aligned} q(t, \tau) \in \mathbb{R} &\longrightarrow q_R(t, \tau) + i q_I(t, \tau) \in \mathbb{C}, \\ \pi(t, \tau) \in \mathbb{R} &\longrightarrow \pi_R(t, \tau) + i \pi_I(t, \tau) \in \mathbb{C}. \end{aligned} \quad (2.3)$$

In addition, we introduce a new generalized action for the symplectic quantization approach, which from here on we denote by \mathbb{H}_{SQ} ,

$$\mathbb{H}_{\text{SQ}}[\pi, \bar{\pi}, q, \bar{q}] = \int dt \bar{\pi}(t, \tau) \pi(t, \tau) + 2 \operatorname{Im} S[q, \bar{q}]. \quad (2.4)$$

We initially present the generalized Hamiltonian in Eq. (2.4) as an ansatz; its correctness will be proven in Sec. 3, where we show that it guarantees a direct correspondence between the microcanonical partition function of symplectic quantization and the Feynman path integral. In Eq. (2.4), $\operatorname{Im} S[q, \bar{q}]$ is shorthand for

$$\operatorname{Im} S[q, \bar{q}] = \frac{S[q] - \bar{S}[\bar{q}]}{2i}. \quad (2.5)$$

In Sec. 4 we discuss the equations of motion generated by the Hamiltonian in Eq. (2.4). By imposing suitable symmetries between the real and imaginary parts of the fields, these

equations allow one to sample precisely the quantum fluctuations encoded in the Feynman path integral.

For generic systems, the generalized action/Hamiltonian of symplectic quantization—as in Eq. (2.4)—will be built out of two key ingredients: a generalized *real* kinetic energy term $\mathbb{K}[\pi]$, which is a quadratic form in the momenta π , and the imaginary part of the analytically continued action $S[q, \bar{q}]$. We will often refer to the latter as the *holomorphic* action, since its analytic continuation from \mathbb{R} to \mathbb{C} implicitly assumes that it defines a holomorphic functional of the corresponding fields.

3 Microcanonical action and the Feynman Path Integral

In this section, we prove the equivalence in the continuum limit between the correlation functions generated by the microcanonical partition function built on the conservation of the generalized action \mathbb{H}_{SQ} introduced in Sec. 2 and the Feynman path integral. Differently from our previous work [1], we specialize here from the beginning of our discussion to quantum mechanics, which in the present formalism is treated as 0+1-dimensional quantum field theory. Our purpose is to prove that, by fixing the value of the generalized action to $\mathcal{A} = \hbar M$ in the microcanonical partition function $\Omega(\mathcal{A})$, with M the number of points in the discretization of the time axis t , in the continuum limit $M \rightarrow \infty$ the correlation functions generated by $\Omega[\mathcal{A}, J]$ are identical to the correlation functions generated by $\mathcal{Z}[\hbar, J]$, where $\mathcal{Z}[\hbar, J]$ is the Feynman path integral of the corresponding theory. Namely, what we are going to prove is that

$$\lim_{M \rightarrow \infty} \frac{\delta^n \Omega[\hbar M, J]}{\delta q(t_1) \dots \delta q(t_n)} \Big|_{J=0} = \langle q(t_1) \dots q(t_n) \rangle = \frac{\delta^n \mathcal{Z}[\hbar, J]}{\delta q(t_1) \dots \delta q(t_n)} \Big|_{J=0}. \quad (3.1)$$

For this purpose, let us introduce the generalized microcanonical generating functional of correlators of symplectic quantization as

$$\Omega[\mathcal{A}, J] = \frac{1}{\Omega[\mathcal{A}, 0]} \int_{\Gamma(t)} \mathcal{D}\bar{\pi} \mathcal{D}\pi \mathcal{D}\bar{q} \mathcal{D}q \delta(\mathcal{A} - \mathbb{H}[q, \bar{q}, \pi, \bar{\pi}] + i J \cdot q), \quad (3.2)$$

where $\Gamma(t)$ denotes the set of one-dimensional integration contours in the complex plane along which the functional integral is convergent, parametrized by the Minkowskian time t , a contour for each of the fields to be integrated, $q(t)$, $\bar{q}(t)$, $\pi(t)$ and $\bar{\pi}(t)$:

$$\Gamma(t) = \Gamma_q(t) \cup \Gamma_{\bar{q}(t)} \cup \Gamma_\pi(t) \cup \Gamma_{\bar{\pi}}(t), \quad (3.3)$$

where, for instance, we have

$$\Gamma_q(t) = \{\gamma_q(t) \in \mathbb{C} : t \in [t_i, t_f]\}, \quad (3.4)$$

and where $\gamma_q(t)$ is the integration contour for the position field $q(t)$ at time t . Let us stress an important point: the analytic continuation of the fields from \mathbb{R} to \mathbb{C} does not imply any doubling of degrees of freedom: the integration domain for any given field at any given point of spacetime remains a one-dimensional path, with the only difference that the path

is immersed in \mathbb{C} , rather than being simply the real line. The only additional degrees of freedom are represented by the conjugate momenta $\pi(t)$, but these will be integrated out at a certain point along the calculation.

In the following discussion on quantum mechanics we start by discretizing the coordinate time t in $M = (t_f - t_i)/a$ points t_i , with $i = 1, \dots, M$, so that also the functional integral is discretized in M ordinary integrals. The M degrees of freedom to be integrated can be considered either as the value taken by the position field at each coordinate time, $q(t_i)$, or as the component of any orthonormal basis which can be used to represent the position field. In analogy with the treatment discussed in [11], let us bring forward the argument by considering a generic orthonormal basis, which for simplicity can be thought as the Fourier components of discretized position field:

$$q(t_i) = \sum_{n=1}^M q_n(t_i) c_n, \quad \bar{q}(t_i) = \sum_{n=1}^M \bar{q}_n(t_i) \bar{c}_n, \quad (3.5)$$

with

$$\sum_{i=1}^M q_n(t_i) q_m(t_i) = \delta_{nm}, \quad \sum_{i=1}^M \bar{q}_n(t_i) \bar{q}_m(t_i) = \delta_{nm}. \quad (3.6)$$

Having discretized the time axis t , the functional integration of Eq. (3.2) can be interpreted in terms of a finite measure of the form

$$\int \mathcal{D}q \mathcal{D}\bar{q} \approx \int \mathcal{D}_M q \mathcal{D}_M \bar{q} \equiv \prod_{n=1}^M \left(\int_{\Gamma_n} dc_n d\bar{c}_n \right) \equiv \prod_{i=1}^M \left(\int_{\Gamma_i} dq(t^i) d\bar{q}(t^i) \right). \quad (3.7)$$

Unlike the standard path-integral convention, this measure does not include an explicit factor of \hbar . In a time interval of length $T = (t_f - t_i)$ with lattice spacing a , the number of basis functions is [11]:

$$M = \frac{T}{a} = T \frac{\Lambda}{\pi}, \quad (3.8)$$

where $\Lambda = \pi/a$ acts as a momentum cutoff. The limit $M \rightarrow \infty$ can be approached either via the continuum limit $\Lambda \rightarrow \infty$ or the thermodynamic limit $T \rightarrow \infty$. From here on, the large- M limit is understood in this sense. Finally, adopting the notational shorthand

$$\pi \cdot \bar{\pi} \equiv \int dt \pi(t) \bar{\pi}(t) \quad J \cdot q \equiv \int dt J(t) q(t) \quad (3.9)$$

we can express the microcanonical generating functional on the lattice in a form suitable for the subsequent analysis in the large- M limit. As a first step, one can perform the integration over the momenta π and $\bar{\pi}$. This can be carried out either via a spherical integration or, more conveniently, by expressing the delta function as a Fourier integral:

$$\Omega[\mathcal{A}, J] = \frac{1}{\Omega[\mathcal{A}, 0]} \int \mathcal{D}_M \bar{\pi} \mathcal{D}_M \pi \mathcal{D}_M \bar{q} \mathcal{D}_M q d\lambda e^{-i\lambda \bar{\pi} \cdot \pi + i\lambda (\mathcal{A} - 2 \operatorname{Im} S[q, \bar{q}] + iJ \cdot q)}. \quad (3.10)$$

The π 's complex Gaussian integral yields

$$\Omega[\mathcal{A}, J] = \frac{1}{\Omega[\mathcal{A}, 0]} \int \mathcal{D}_M \bar{q} \mathcal{D}_M q \mathcal{D}\lambda \lambda^{-M} e^{i\lambda(\mathcal{A} - 2 \operatorname{Im} S[q, \bar{q}] + iJ \cdot q)}, \quad (3.11)$$

where the λ integral can be performed up to irrelevant constants that are cancelled by the denominator

$$\Omega[\mathcal{A}, J] = \frac{1}{\Omega[\mathcal{A}, 0]} \int \mathcal{D}_M \bar{q} \mathcal{D}_M q (\mathcal{A} - 2 \operatorname{Im} S[q, \bar{q}] + iJ \cdot q)^{M-1}. \quad (3.12)$$

At this point we fix the generalized Hamiltonian to $\mathcal{A} = \hbar M$, which corresponds to assigning a value \hbar to each degree of freedom. By then plugging this value of the action into the expression of $\Omega[\mathcal{A}, J]$ one gets

$$\begin{aligned} \Omega[\mathcal{A} = \hbar M, J] &= \frac{1}{\Omega[\hbar M, 0]} \int \mathcal{D}\bar{q}_M \mathcal{D}q_M \left(1 - \frac{2}{\hbar M} \operatorname{Im} S[q, \bar{q}] + \frac{i}{\hbar M} J \cdot q\right)^{M-1} \\ &= \frac{1}{\Omega[\hbar M, 0]} \int \mathcal{D}\bar{q}_M \mathcal{D}q_M e^{(M-1) \log(1 - \frac{2}{\hbar M} \operatorname{Im} S[q, \bar{q}] + \frac{i}{\hbar M} J \cdot q)} \end{aligned} \quad (3.13)$$

where again all the multiplicative constants simplify with the denominator. Let us now expand Eq. (3.13) in powers of the source J , in order to recover the standard source expansion of a generating functional. Writing

$$\left(1 - \frac{2}{\hbar M} \operatorname{Im} S[q, \bar{q}] + \frac{i}{\hbar M} J \cdot q\right)^{M-1} = \sum_{n=0}^{\infty} \binom{M-1}{n} \left(\frac{i}{\hbar M} J \cdot q\right)^n \left(1 - \frac{2}{\hbar M} \operatorname{Im} S[q, \bar{q}]\right)^{M-1-n}, \quad (3.14)$$

and using $(J \cdot q)^n = \int dt_1 \cdots dt_n J(t_1) \cdots J(t_n) q(t_1) \cdots q(t_n)$, we obtain

$$\Omega[\hbar M, J] = \frac{1}{\Omega[\hbar M, 0]} \sum_{n=0}^{\infty} \frac{1}{n!} \left(\frac{i}{\hbar M}\right)^n \frac{\Gamma(M)}{\Gamma(M-n)} \int dt_1 \cdots dt_n J(t_1) \cdots J(t_n) \langle q(t_1) \cdots q(t_n) \rangle_{M-n}, \quad (3.15)$$

where we used $\binom{M-1}{n} = \Gamma(M)/[n! \Gamma(M-n)]$ and where we have introduced the “dressed” correlator $\langle q(t_1) \cdots q(t_n) \rangle_{M-n}$:

$$\langle q(t_1) \cdots q(t_n) \rangle_{M-n} = \int \mathcal{D}_M \bar{q} \mathcal{D}_M q q(t_1) \cdots q(t_n) \left(1 - \frac{2}{\hbar M} \operatorname{Im} S[q, \bar{q}]\right)^{M-n} \quad (3.16)$$

and where we have neglected the -1 on the exponent since we are interested in the large- M limit. The calculation of $\langle q(t_1) \cdots q(t_n) \rangle_{M-n}$ will be our next goal, with the purpose of substituting the result back into Eq. (3.15). We proceed to expand $\left(1 - \frac{2}{\hbar M} \operatorname{Im} S[q, \bar{q}]\right)^{M-n}$ around $\frac{1}{M}$. Let $x = \frac{2}{\hbar} \operatorname{Im} S[q, \bar{q}]$, then by using the notable limit of $\lim_{M \rightarrow \infty} (1 - \frac{x}{M})^{M-n} = e^{-x}$ we separate the argument of the path integral as

$$\left(1 - \frac{x}{M}\right)^{M-n} = e^{-x} \times \left(1 - \frac{x}{M}\right)^{M-n} e^x. \quad (3.17)$$

Therefore, we now expand

$$\left(1 - \frac{x}{M}\right)^{M-n} e^x \quad (3.18)$$

by convoluting the two series expansions

$$\begin{aligned} \left(1 - \frac{x}{M}\right)^{M-n} &= \sum_{j=0}^{\infty} \binom{M-n}{j} \left(-\frac{x}{M}\right)^j \\ e^x &= \sum_{l=0}^{\infty} \frac{1}{l!} x^l \end{aligned} \quad (3.19)$$

and by using the standard Cauchy formula, we get

$$(1 - \frac{x}{M})^{M-n} e^x = \sum_{j=0}^{\infty} x^j \sum_{k=0}^j \binom{M-n}{k} \frac{1}{(j-k)!} \frac{(-1)^k}{M^k}. \quad (3.20)$$

Since $x = \frac{2}{\hbar} \operatorname{Im} S[q, \bar{q}]$, we define the coefficients $c_j(M, n)$ as

$$c_j(M, n) = \left(\frac{2}{\hbar}\right)^j \sum_{k=0}^j \binom{M-n}{k} \frac{1}{(j-k)!} \frac{(-1)^k}{M^k}, \quad (3.21)$$

and so

$$\left(1 - \frac{2}{\hbar M} \operatorname{Im} S[q, \bar{q}]\right)^{M-n} = e^{-\frac{2}{\hbar} \operatorname{Im} S[q, \bar{q}]} \sum_{j=0}^{\infty} c_j(M, n) (\operatorname{Im} S[q, \bar{q}])^j. \quad (3.22)$$

We rewrite the expression for the *dressed* correlator as

$$\begin{aligned} \langle q(t_1) \dots q(t_n) \rangle_{M-n} &= \sum_{j=0}^{\infty} c_j(M, n) \int \mathcal{D}_M \bar{q} \mathcal{D}_M q \, q(t_1) \dots q(t_n) e^{-\frac{2}{\hbar} \operatorname{Im} S[q, \bar{q}]} (\operatorname{Im} S[q, \bar{q}])^j \\ &= \sum_{j=0}^{\infty} c_j(M, n) \int \mathcal{D}_M \bar{q} \mathcal{D}_M q \, q(t_1) \dots q(t_n) e^{\frac{i}{\hbar} S[q]} e^{-\frac{i}{\hbar} \bar{S}[\bar{q}]} \left(\frac{S[q] - \bar{S}[\bar{q}]}{2i}\right)^j. \end{aligned} \quad (3.23)$$

where again all the multiplicative constants simplify with the denominator. As proven in App. A, in the large- M limit decrease as

$$c_j(M, n) \sim \frac{1}{M} \quad \forall j \geq 1. \quad (3.24)$$

In analogy with the Lefschetz-Thimbles approach discussed in [21, 25, 26], we define two independent integration contours Γ_q and $\Gamma'_{\bar{q}}$, respectively for q and \bar{q} , which we therefore treat as separate variables (one can always define paths which guarantee convergence of functional integration, for instance by choosing for Γ_q the $i\epsilon$ rotated path into the complex plane that recovers the Feynman prescription and for $\Gamma'_{\bar{q}}$ the anti-holomorphic version for the $i\epsilon$ rotated path). It is then convenient to exploit the binomial theorem

$$\left(\frac{S[q] - \bar{S}[\bar{q}]}{2i}\right)^j = \frac{1}{(2i)^j} \sum_{k=0}^j \binom{j}{k} S[q]^{j-k} S[\bar{q}]^k, \quad (3.25)$$

which allows to see that the integration with respect to q and \bar{q} inside the expression of Eq. (3.23) can be neatly factorized, yielding

$$\begin{aligned} \langle q(t_1) \dots q(t_n) \rangle_{M-n} &= \\ \sum_{j=0}^{\infty} c_j(M, n) \frac{1}{(2i)^j} \sum_{k=0}^j \binom{j}{k} \int_{\Gamma_q} \mathcal{D}_M q \, q(t_1) \dots q(t_n) \, S[q]^{j-k} \, e^{\frac{i}{\hbar} S[q]} &\times \int_{\Gamma'_{\bar{q}}} \mathcal{D}_M \bar{q} \, \bar{S}[\bar{q}]^k \, e^{-\frac{i}{\hbar} \bar{S}[\bar{q}]} \end{aligned} \quad (3.26)$$

Let us then claim the finiteness of the holomorphic action $S[q]$ in the continuum limit, which is a quite reasonable assumption for quantum mechanics. As a consequence, all terms of the sum in Eq. (3.26) vanish in the continuum limit:

$$M \rightarrow \infty \implies c_j(M, n) S[q]^j \sim \frac{1}{M} \quad \forall j \geq 1. \quad (3.27)$$

The asymptotic behaviour of Eq. (3.27) allows then to drastically simplify the behaviour of the dressed correlator in the large- M limit:

$$\langle q(t_1) \dots q(t_n) \rangle_{M-n} \cong \int_{\Gamma_q} \mathcal{D}_M q \, q(t_1) \dots q(t_n) \, e^{\frac{i}{\hbar} S[q]} \times \int_{\Gamma'_{\bar{q}}} \mathcal{D}_M \bar{q} \, e^{-\frac{i}{\hbar} \bar{S}[\bar{q}]} + O\left(\frac{1}{M}\right). \quad (3.28)$$

By then recalling the expression of the symplectic quantization action written as a function of connected correlators in Eq. (3.15) and noticing that in the continuum limit we also have

$$\lim_{M \rightarrow \infty} \left(\frac{1}{M}\right)^n \frac{\Gamma(M)}{\Gamma(M-n)} \rightarrow 1, \quad (3.29)$$

we can then simplify as follows the expression of the symplectic quantization microcanonical partition function

$$\begin{aligned} \Omega[\hbar M, J] &= \\ &= \frac{1}{\Omega[\hbar M, 0]} \sum_{n=0}^{\infty} \frac{1}{n!} \left(\frac{i}{2}\right)^n \left(\frac{2}{\hbar M}\right)^n \frac{\Gamma(M)}{\Gamma(M-n)} \times \int dt_1 \dots dt_n \, J(t_1) \dots J(t_n) \langle q(t_1) \dots q(t_n) \rangle_{M-n} \\ &\cong \frac{1}{\Omega_{\infty}[\hbar, 0]} \sum_{n=0}^{\infty} \frac{1}{n!} \left(\frac{i}{\hbar}\right)^n \int dt_1 \dots dt_n \, J(t_1) \dots J(t_n) \times \int_{\Gamma_q} \mathcal{D}q \, q(t_1) \dots q(t_n) \, e^{\frac{i}{\hbar} S[q]} \int_{\Gamma'_{\bar{q}}} \mathcal{D}\bar{q} \, e^{-\frac{i}{\hbar} \bar{S}[\bar{q}]}, \\ &= \frac{1}{\Omega_{\infty}[\hbar, 0]} \int_{\Gamma_q} \mathcal{D}q \, e^{\frac{i}{\hbar} S[q]} \sum_{n=0}^{\infty} \frac{1}{n!} \left(\frac{i}{\hbar}\right)^n \int dt_1 \dots dt_n \, J(t_1) \dots J(t_n) \, q(t_1) \dots q(t_n) \int_{\Gamma'_{\bar{q}}} \mathcal{D}\bar{q} \, e^{-\frac{i}{\hbar} \bar{S}[\bar{q}]} \\ &= \frac{1}{\Omega_{\infty}[\hbar, 0]} \int_{\Gamma_q} \mathcal{D}q \, e^{\frac{i}{\hbar} S[q] + \frac{i}{\hbar} \int dt \, J(t) q(t)} \int_{\Gamma'_{\bar{q}}} \mathcal{D}\bar{q} \, e^{-\frac{i}{\hbar} \bar{S}[\bar{q}]} \\ &= \frac{\int_{\Gamma_q} \mathcal{D}q \, e^{\frac{i}{\hbar} S[q] + \frac{i}{\hbar} \int dt \, J(t) q(t)} \int_{\Gamma'_{\bar{q}}} \mathcal{D}\bar{q} \, e^{-\frac{i}{\hbar} \bar{S}[\bar{q}]}}{\int_{\Gamma_q} \mathcal{D}q \, e^{\frac{i}{\hbar} S[q]} \int_{\Gamma'_{\bar{q}}} \mathcal{D}\bar{q} \, e^{-\frac{i}{\hbar} \bar{S}[\bar{q}]}}. \end{aligned} \quad (3.30)$$

It must be then noticed that the term containing the anti-holomorphic part of the action is factorized both at numerator and denominator, so that it cancels out, yielding the final

result

$$\lim_{M \rightarrow \infty} \Omega[\hbar M, J] = \Omega_\infty[\hbar, J] = \frac{\int_{\Gamma_q} \mathcal{D}q e^{\frac{i}{\hbar} S[q] + \frac{i}{\hbar} \int dt J(t)q(t)}}{\int_{\Gamma_q} \mathcal{D}q e^{\frac{i}{\hbar} S[q]}}. \quad (3.31)$$

Thus, by choosing Γ_q as the $i\epsilon$ "Feynman" path, we have proved that

$$\lim_{M \rightarrow \infty} \frac{\delta^n \Omega[\hbar M, J]}{\delta q(t_1) \dots \delta q(t_n)} \Big|_{J=0} = \frac{\delta^n \Omega_\infty[\hbar, J]}{\delta q(t_1) \dots \delta q(t_n)} \Big|_{J=0} = \frac{\delta^n \mathcal{Z}[\hbar, J]}{\delta q(t_1) \dots \delta q(t_n)} \Big|_{J=0} \quad (3.32)$$

namely that in the continuum limit $M \rightarrow \infty$ the microcanonical generating functional is equivalent to the Feynman path integral. The proof just presented is crucial, as it places on firm grounds the correspondence between the microcanonical partition function of symplectic quantization and the Feynman path integral. At the same time, the argument is somewhat formal, since it does not indicate how to choose the integration contours in the original microcanonical expression in order to evaluate it directly, without reverting to the Feynman path integral. In the path-integral framework, an appropriate deformation of integration contours in the complex plane underlies the modern Lefschetz-thimble strategy; an extensive account can be found, for instance, in [27]. In our approach, a direct and constructive way to compute (or, more precisely, to sample) the microcanonical partition function is provided instead by the underlying microscopic Hamiltonian dynamics. This dynamics offers a natural mechanism to select the relevant integration cycles in the complexified field space. We discuss this point in detail in the next section, Sec. 4, focusing on the quantum harmonic oscillator. As we shall show, the key requirement is to *constrain* the Hamiltonian flow to the appropriate stable manifold. This is precisely the reason for the name "constrained symplectic quantization".

4 Harmonic Oscillator: constrained equations of motion

In the previous section we proved that the symplectic-quantization microcanonical functional and the Feynman path integral are equivalent as generating functionals for quantum correlators. In this section we introduce a *constrained* Hamiltonian dynamics—generated by the generalized Hamiltonian in Eq. (2.4)—as a natural way to sample the measure associated with the corresponding microcanonical partition function. To this purpose let us now specify the system: a one-dimensional non-relativistic particle of mass m moving in a fixed potential $V(q)$. As for $V(q)$ we start our investigation from the harmonic oscillator potential

$$V(q) = \frac{1}{2}m\Omega^2q^2. \quad (4.1)$$

The harmonic oscillator is chosen as a benchmark due to its exact solvability, well-known spectral properties, and central role in both quantum mechanics and quantum field theory. It provides a controlled setting to test our formalism and to illustrate how real-time evolution can be simulated deterministically without encountering the sign problem that

typically plagues path integrals with a Minkowskian action. In order to avoid any ambiguity when speaking about “*time evolution*” and “*dynamics*”, let us stress that in the following such concepts will be always be referred to the intrinsic time τ flow, whereas the Minkowskian, or coordinate, time t , in order to avoid confusion will be always denoted from hereafter as x_0 and treated as a spatial coordinate, an approach which also emphasizes the role of quantum mechanics as a $0 + 1$ -dimensional field theory. We therefore write the action of the one-dimensional harmonic oscillator as

$$\begin{aligned} S[q] &= \int_{t_i}^{t_f} dt \left[\frac{m}{2} \left(\frac{dq(t)}{dt} \right)^2 - \frac{1}{2} m \Omega^2 q^2(t) \right] \\ &= \int_{x_0^i}^{x_0^f} dx_0 \left[\frac{m}{2} \left(\frac{dq}{dx_0} \right)^2 - \frac{1}{2} m \Omega^2 q^2(x_0) \right]. \end{aligned} \quad (4.2)$$

The novelty of the symplectic quantization approach presented in this paper is not only to replace the quantum operator $\hat{q}(x_0)$ with a field $q(x_0, \tau)$ —so that quantum fluctuations at fixed coordinate time x_0 are parametrized by the intrinsic time τ —but also to analytically continue the field itself to the complex plane:

$$q(x_0, \tau) \in \mathbb{R} \longrightarrow q(x_0, \tau) \in \mathbb{C} \quad (4.3)$$

so that,

$$q(x_0, \tau) = q_R(x_0, \tau) + i q_I(x_0, \tau), \quad (4.4)$$

where $q_R(x_0, \tau)$ and $q_I(x_0, \tau)$ denote respectively the real and imaginary parts of the field. Let us stress that, on the contrary, the expression of the action in Eq. (4.2) must not be changed despite the analytic prolongation of the field $q(x_0, \tau)$ from real to imaginary values, so that for the action itself we must consider the analytic continuation to \mathbb{C} :

$$S[q] \in \mathbb{R} \longrightarrow S[q] \in \mathbb{C}. \quad (4.5)$$

We then assume for the generalized Hamiltonian which generates the dynamics in τ the following form

$$\mathbb{H}[\pi, \bar{\pi}, q, \bar{q}] = \bar{\pi} \cdot \pi + 2 \operatorname{Im} S[q, \bar{q}], \quad (4.6)$$

where the $\operatorname{Im} S[q, \bar{q}]$ is a formal notation for

$$\operatorname{Im} S[q, \bar{q}] = \frac{S[q] - \bar{S}[\bar{q}]}{2i}, \quad (4.7)$$

where $S[q]$ is the holomorphic complex action and $\bar{S}[\bar{q}]$ its anti-holomorphic counterpart. Let us stress that $\operatorname{Im} S[q, \bar{q}]$ is solely defined from Eq. (4.7) since in the theory there is no action $S[q, \bar{q}]$ which depends on both q and \bar{q} . Things are different for the generalized Hamiltonian $\mathbb{H}[\pi, \bar{\pi}, q, \bar{q}]$, which is the only functional of the theory depending on both olomorphic fields (q, π) and their anti-olomorphic counterparts $(\bar{q}, \bar{\pi})$. The Hamiltonian equations of motion along the intrinsic time τ read then

$$\begin{aligned} \dot{q} &= \frac{\partial \mathbb{H}}{\partial \pi} = \bar{\pi}, & \dot{\bar{q}} &= \frac{\partial \mathbb{H}}{\partial \bar{\pi}} = \pi, \\ \dot{\pi} &= -\frac{\partial \mathbb{H}}{\partial q} = i \frac{\partial S[q]}{\partial q}, & \dot{\bar{\pi}} &= -\frac{\partial \mathbb{H}}{\partial \bar{q}} = -i \frac{\partial \bar{S}[\bar{q}]}{\partial \bar{q}}. \end{aligned} \quad (4.8)$$

The corresponding equations of motion mix the two fields q and \bar{q} :

$$-i \frac{d^2}{d\tau^2} \bar{q}(x_0, \tau) = -m \frac{\partial^2}{\partial x_0^2} q(x_0, \tau) - m\Omega^2 q(x_0, \tau). \quad (4.9)$$

If we then assume that the coordinate time x_0 belongs to a finite interval, $x_0 \in [x_0^i, x_0^f]$, it is possible to diagonalize the equations of motion by decomposing the field $q(x_0, \tau)$ into Fourier modes

$$q(x_0, \tau) = \sum_{\{k_0(\ell): \ell=1, \dots, M\}} e^{ik_0(\ell)x_0} q(k_0(\ell), \tau), \quad (4.10)$$

where $k_0(\ell) = \ell 2\pi / (x_0^f - x_0^i)$ with $\ell \in \mathbb{Z}$, so that

$$\frac{d^2}{d\tau^2} \bar{q}(k_0, \tau) + i\omega^2(k_0) q(k_0, \tau) = 0, \quad \omega^2(k_0) = m(\Omega^2 - k_0^2). \quad (4.11)$$

The further step is to write Eq. (4.11) as a set of two coupled real equations for the real and imaginary part of $q(k_0, \tau)$:

$$\begin{aligned} \ddot{q}_R(k_0, \tau) - \omega^2(k_0) q_I(k_0, \tau) &= 0, \\ \ddot{q}_I(k_0, \tau) - \omega^2(k_0) q_R(k_0, \tau) &= 0. \end{aligned} \quad (4.12)$$

At this point, when approaching the study of the Hamiltonian dynamics generated by $\mathbb{H}[\pi, \bar{\pi}, q, \bar{q}]$ as a mean to sample the partition function $\Omega[\hbar M, J]$ in Eq. (3.2), we must solve the problem of unbounded solutions of Eq. (4.11), which parallels the problem of choosing the appropriate integration contours in order to guarantee convergence in the functional integral of $\Omega[\hbar M, J]$. A quite straightforward inspection of Eq. (4.12) reveals that in order to keep solutions on a bounded manifold it is sufficient to impose the following constraints:

$$\begin{aligned} \text{if } \omega^2(k_0) > 0 &\implies q_R(k_0, \tau) = -q_I(k_0, \tau) \quad \& \quad \pi_R(k_0, \tau) = -\pi_I(k_0, \tau) \\ \text{if } \omega^2(k_0) < 0 &\implies q_R(k_0, \tau) = q_I(k_0, \tau) \quad \& \quad \pi_R(k_0, \tau) = \pi_I(k_0, \tau) \end{aligned} \quad (4.13)$$

which can be also written in the more compact form

$$\begin{aligned} q_I(k_0, \tau) &= -\text{sgn}[\omega^2(k_0)] q_R(k_0, \tau) \\ \pi_I(k_0, \tau) &= -\text{sgn}[\omega^2(k_0)] \pi_R(k_0, \tau), \end{aligned} \quad (4.14)$$

leading to the following equations of motion

$$\begin{aligned} \ddot{q}_R(k_0, \tau) + |\omega^2(k_0)| q_R(k_0, \tau) &= 0 \\ \ddot{q}_I(k_0, \tau) + |\omega^2(k_0)| q_I(k_0, \tau) &= 0. \end{aligned} \quad (4.15)$$

It can be immediately noticed that the equations of motion for the real and the imaginary part of the field are identical. This is a consequence of the constraint in Eq. (4.14) needed to keep the field on a bounded manifold. This is perfectly consistent with the fact that the constrained symplectic dynamics evolves along a one-dimensional manifold, analogous to

the choice of convergent contours in the Feynman path integral: the analytic prolongation of the fields to \mathbb{C} does not introduce extra degrees of freedom. In particular, from the constraints written in Eq. (4.13) it is evident that it is perfectly sufficient to solve the dynamics for $q_R(k_0, \tau)$, from which also $q_I(k_0, \tau)$ is then univocally determined. In summary: despite the need to consider the analytical prolongation to \mathbb{C} of all fields, yet, in order to guarantee consistency, the problem is reduced to study the dynamics of a single real field, either the real part $q_R(k_0, \tau)$ or the imaginary one $q_I(k_0, \tau)$, since the two are not independent as long as one wants to preserve convergence.

At this stage we need a precise correspondence between expectation values computed in the standard (Feynman) path-integral approach and those obtained from the constrained symplectic quantization dynamics. While a formal equivalence between the microcanonical partition function and the Feynman path integral has been established in Eq. (3.1), this equivalence remains incomplete until the relation between (i) the stable manifold selected by the constraints in Eq. (4.14) and (ii) the complex integration contours $\Gamma(x_0)$ appearing in Eq. (3.2) is made explicit. To introduce the issue in a concrete setting, consider the endpoint-conditioned matrix element with an operator insertion,

$$\langle q_f, t_f | \hat{q}^2(t') | q_i, t_i \rangle = \frac{1}{\langle q_f, t_f | q_i, t_i \rangle} \int_{q(t_i) = q_i}^{q(t_f) = q_f} \mathcal{D}q \, q^2(t') \exp \left\{ \frac{i}{\hbar} \int_{t_i}^{t_f} dt \left[\frac{m}{2} \left(\frac{dq(t)}{dt} \right)^2 - \frac{1}{2} m \Omega^2 q^2(t) \right] \right\}, \quad (4.16)$$

where $t_i \leq t' \leq t_f$ and which, for clarity, we rewrite using the notation introduced in this section:

$$\langle q_f, x_0^f | \hat{q}^2(x_0') | q_i, x_0^i \rangle = \frac{1}{\langle q_f, x_0^f | q_i, x_0^i \rangle} \int_{q(x_0^i) = q_i}^{q(x_0^f) = q_f} \mathcal{D}q \, q^2(x_0') \exp \left\{ \frac{i}{\hbar} \int_{x_0^i}^{x_0^f} dx_0 \left[\frac{m}{2} \left(\frac{dq(x_0)}{dx_0} \right)^2 - \frac{1}{2} m \Omega^2 q^2(x_0) \right] \right\}. \quad (4.17)$$

In the present symplectic quantization framework, the fundamental dynamical object is the analytically continued field $q(x_0, \tau)$, evolving in the fictitious time τ according to the constrained Hamiltonian flow. To reproduce the endpoint-conditioned amplitude in Eq. (4.17), one considers the dynamics on the interval $[x_0^i, x_0^f]$ with fixed boundary data *for all* τ ,

$$\begin{aligned} q(x_0^i, \tau) &= q_i \quad \forall \tau \\ q(x_0^f, \tau) &= q_f \quad \forall \tau, \end{aligned} \quad (4.18)$$

and, keeping such boundary condition, compute the expectation value over quantum fluctuations as

$$\langle q^2(x_0') \rangle|_{q_i(x_0^i), q_f(x_0^f)} = \lim_{\Delta\tau \rightarrow \infty} \frac{1}{\Delta\tau} \int_{\tau_0}^{\tau_0 + \Delta\tau} d\tau \, q_\tau^2(x_0')|_{q_i(x_0^i), q_f(x_0^f)}, \quad (4.19)$$

where $q_\tau^2(x_0')|_{q_i(x_0^i), q_f(x_0^f)}$ denotes the solution of the symplectic dynamics with fixed boundaries along the x_0 axis. In order to connect the expression in Eq. (4.19) to the Feynman

path integral representation of the expectation value of $\hat{q}(x'_0)$ in Eq. (4.17) it is necessary to assume the equivalence between dynamical and thermodynamic averages in the symplectic quantization approach:

$$\lim_{\Delta\tau \rightarrow \infty} \frac{1}{\Delta\tau} \int_{\tau_0}^{\tau_0 + \Delta\tau} d\tau \, q^2(x'_0, \tau) \cong \frac{1}{\Omega_\infty[\hbar]} \int_{\Gamma(x_0)} \mathcal{D}\bar{\pi} \mathcal{D}\pi \mathcal{D}\bar{q} \mathcal{D}q \, q^2(x'_0) \delta(\mathcal{A} - \mathbb{H}[q, \bar{q}, \pi, \bar{\pi}]), \quad (4.20)$$

where $\Gamma(x_0)$ denotes the contour(s) in the complexified phase space compatible with the constraints. We can now state the key point.

In our setting the variables (q, π) are generically complex along the constrained Hamiltonian flow, and therefore the instantaneous value $q^2(x'_0, \tau)$ is in general a complex number. This *does not* imply that symplectic quantization predicts a complex value for the physical matrix element in Eq. (4.17). Rather, it reflects the fact that we are evaluating the microcanonical functional integral on a nontrivial contour $\Gamma(x_0)$ in the complexified space of fields, determined by the same constraints that define the stable manifold of the dynamics. By contrast, the standard Feynman representation in Eq. (4.17) is written on the usual “real” configuration-space contour for the oscillator variable. A precise identification of $\Gamma(x_0)$ therefore provides the missing bridge between the two formulations: once the contour correspondence is made explicit, the SQ microcanonical average reproduces the conventional Feynman result for operator insertions. In summary, computing expectation values over quantum fluctuations by means of the symplectic quantization dynamics requires an intermediate step with respect to the standard quantum-mechanical formulae: symplectic quantization samples a microcanonical integral over analytically continued fields on contours $\Gamma(x_0)$ that are not, in general, the standard ones. The simplest way to illustrate how symplectic quantization simulations are compared with the usual quantum-mechanical expressions is to work through an explicit example: let us consider the expectation value of operator position squared for the quantum harmonic oscillator, $\langle q_f, x_0^f | \hat{q}^2(x'_0) | q_i, x_0^i \rangle$, and let us assume for simplicity periodic boundary conditions in time. In this case the expectation over quantum fluctuations can be written as

$$\langle \hat{q}^2(x'_0) \rangle_{\text{P.B.}} = \int_{-\infty}^{\infty} dq_i \, \langle q_i, x_0^f | \hat{q}^2(x'_0) | q_i, x_0^i \rangle = \frac{\int_{q(x_0^f) = q(x_0^i)} \mathcal{D}q \, q^2(x'_0) \, e^{\frac{i}{\hbar} S[q]}}{\int_{q(x_0^f) = q(x_0^i)} \mathcal{D}q \, e^{\frac{i}{\hbar} S[q]}}, \quad (4.21)$$

where the two boundary conditions have been identified, $q(x_0^f) = q(x_0^i)$, and integrated over. To lighten the notation, in the following we assume that, in absence of further specifications, all path-integral expressions are understood with periodic boundary conditions in x_0 :

$$\text{Tr} \left[e^{-i(x_0^f - x_0^i) \hat{H}/\hbar} \right] = \int \mathcal{D}q \, e^{\frac{i}{\hbar} S[q]} = \int_{q(x_0^f) = q(x_0^i)} \mathcal{D}q \, e^{\frac{i}{\hbar} S[q]}. \quad (4.22)$$

The whole point is that in Eq. (4.21) standard quantum-mechanical formulae assume that, for each coordinate time x_0 , the position field is integrated over the real axis, namely $\int \mathcal{D}q = \Pi_{x_0} \int_{-\infty}^{\infty} dq(x_0)$. This differs from the integration paths selected by the microscopic dynamics of symplectic quantization. The crucial observation connecting standard

quantum-mechanical amplitudes with the microcanonical approach of symplectic quantization is that expectation values are invariant under deformations of the integration contours in the complex plane. Therefore, we can elaborate on the fact that

$$\langle \hat{q}^2(x'_0) \rangle_{\text{P.B.}} = \frac{\int_{-\infty}^{\infty} \prod_{x_0} dq(x_0) q^2(x'_0) e^{\frac{i}{\hbar} S[q]} }{\int_{-\infty}^{\infty} \prod_{x_0} dq(x_0) e^{\frac{i}{\hbar} S[q]}} \quad (4.23)$$

$$= \frac{\int \prod_{\gamma_{q(x_0)}} dq(x_0) q^2(x'_0) e^{\frac{i}{\hbar} S[q]} }{\int \prod_{\gamma_{q(x_0)}} dq(x_0) e^{\frac{i}{\hbar} S[q]}} \quad (4.24)$$

$$= \frac{\int \prod_{\gamma_{q(x_0)}} dq_R(x_0) dq_I(x_0) [q_R(x'_0) + i q_I(x'_0)]^2 e^{\frac{i}{\hbar} S[q_R + iq_I]} }{\int \prod_{\gamma_{q(x_0)}} dq_R(x_0) dq_I(x_0) e^{\frac{i}{\hbar} S[q_R + iq_I]}}. \quad (4.25)$$

The crucial observation for what follows is that the contours $\gamma_{q(x_0)}$ must be paths in the complex plane that correspond to the constraints imposed on the symplectic dynamics in Eq. (4.13). To this purpose, taking advantage of the periodic boundary conditions in x_0 , it is convenient to introduce the Fourier modes of the position field,

$$\begin{aligned} q(x'_0) &= \frac{1}{T\sqrt{2\pi}} \sum_{k'_0=-\infty}^{\infty} e^{-ik'_0 x'_0} \tilde{q}(k'_0), \\ \tilde{q}(k'_0) &= \frac{1}{\sqrt{2\pi}} \int_0^T dx_0 e^{ik'_0 x'_0} q(x'_0), \end{aligned} \quad (4.26)$$

where $T = x_0^{\text{f}} - x_0^{\text{i}}$, and to write the expectation value in Fourier representation:

$$\begin{aligned} \langle \hat{q}^2(x'_0) \rangle_{\text{P.B.}} &= \frac{1}{2\pi T^2} \sum_{k'_0, p'_0=-\infty}^{\infty} e^{-ix'_0(k'_0 + p'_0)} \langle \tilde{q}(k'_0) \tilde{q}(p'_0) \rangle_{\text{P.B.}} \\ &= \frac{1}{2\pi T^2} \sum_{k'_0=-\infty}^{\infty} e^{-i2x'_0 k'_0} \langle \tilde{q}(k'_0) \tilde{q}(-k'_0) \rangle_{\text{P.B.}}, \end{aligned} \quad (4.27)$$

where in the last step we used translation invariance (for periodic boundary conditions) to enforce $p'_0 = -k'_0$. We now consider the situation in which $q(x'_0) \in \mathbb{C}$, so that the integration contours, also in Fourier space, are paths in the complex plane:

$$\langle \tilde{q}(k'_0) \tilde{q}(-k'_0) \rangle_{\text{P.B.}} = \frac{\int \prod_{\gamma_{q(k_0)}} dq_R(k_0) dq_I(k_0) q(k'_0) q(-k'_0) e^{\frac{i}{\hbar} S[q(k_0)]}}{\int \prod_{\gamma_{q(k_0)}} dq_R(k_0) dq_I(k_0) e^{\frac{i}{\hbar} S[q(k_0)]}}. \quad (4.28)$$

It is only at this step that we can characterize the integration paths γ_q in terms of the constraints written in Eq. (4.13). The first step is to manipulate the action in a form

suitable to impose the constraints:

$$\begin{aligned}
S[q] &= \int_{x_0^i}^{x_0^f} dx_0 \left[\frac{m}{2} \left(\frac{dq(x_0)}{dx_0} \right)^2 - \frac{1}{2} m \Omega^2 q^2(x_0) \right] \\
&= \frac{m}{2} q(x_0) \frac{dq(x_0)}{dx_0} \Big|_{x_0^i}^{x_0^f} - \int_{x_0^i}^{x_0^f} dx_0 q(x_0) \left[\frac{m}{2} \frac{d^2}{dx_0^2} + \frac{1}{2} m \Omega^2 \right] q(x_0) \\
&= -\frac{m}{2} \sum_{k_0=-\infty}^{\infty} \tilde{q}(k_0) \left[-k_0^2 + \Omega^2 \right] \tilde{q}(-k_0) \\
&= -\frac{1}{2} \sum_{k_0=-\infty}^{\infty} \omega^2(k_0) \tilde{q}(k_0) \tilde{q}(-k_0), \tag{4.29}
\end{aligned}$$

where $\omega^2(k_0) \equiv m(\Omega^2 - k_0^2)$. The standard textbook step would now be to write $\tilde{q}(k_0) \tilde{q}(-k_0) = \tilde{q}(k_0) \tilde{q}^*(k_0)$, which is only correct when $q(x_0) \in \mathbb{R}$. In the present case, where $q(x_0) \in \mathbb{C}$, we write the Fourier modes in terms of their real and imaginary parts, so that the constraints can be exploited directly:

$$\begin{aligned}
S[q] &= -\frac{1}{2} \sum_{k_0=-\infty}^{\infty} \omega^2(k_0) \left[q_R(k_0) q_R(-k_0) - q_I(k_0) q_I(-k_0) + i q_R(k_0) q_I(-k_0) + i q_I(k_0) q_R(-k_0) \right] \\
&= i \sum_{\{k_0 \mid \omega^2(k_0) \geq 0\}} \omega^2(k_0) q_R(k_0) q_R(-k_0) - i \sum_{\{k_0 \mid \omega^2(k_0) < 0\}} \omega^2(k_0) q_R(k_0) q_R(-k_0). \tag{4.30}
\end{aligned}$$

The second line of Eq. (4.30) follows by imposing, in the functional integration of Eq. (4.25), the constraints $q_R(k_0) = -q_I(k_0)$ for $\omega^2(k_0) > 0$ and $q_R(k_0) = q_I(k_0)$ for $\omega^2(k_0) < 0$, which are equivalent to rotating the integration contour of each mode by an angle $\pi/4$ clockwise for $\omega^2(k_0) > 0$ and counterclockwise for $\omega^2(k_0) < 0$, as shown in Fig. 1. Recalling that $q_R(x_0)$ and $q_I(x_0)$ are real functions, their Fourier components satisfy $q_R(-k_0) = q_R^*(k_0)$ and $q_I(-k_0) = q_I^*(k_0)$, and we obtain the following expression for the measure:

$$\exp\left(\frac{i}{\hbar} S[q]\right) = \exp\left(-\frac{1}{\hbar} \sum_{\{k_0 \mid \omega^2(k_0) \geq 0\}} \omega^2(k_0) |q_R(k_0)|^2 + \frac{1}{\hbar} \sum_{\{k_0 \mid \omega^2(k_0) < 0\}} \omega^2(k_0) |q_R(k_0)|^2\right). \tag{4.31}$$

The kernel in Fourier space of the two-point correlation function can then be written as

$$\begin{aligned}
\langle \tilde{q}(k'_0) \tilde{q}(-k'_0) \rangle_{\text{P.B.}} &= \langle \tilde{q}_R(k'_0) \tilde{q}_R(-k'_0) \rangle - \langle \tilde{q}_I(k'_0) \tilde{q}_I(-k'_0) \rangle \\
&\quad + i [\langle \tilde{q}_R(k'_0) \tilde{q}_I(-k'_0) \rangle + \langle \tilde{q}_I(k'_0) \tilde{q}_R(-k'_0) \rangle]. \tag{4.32}
\end{aligned}$$

This expression can be simplified by using the constraints in the functional integration. Exploiting the Gaussian measure in Eq. (4.31), one finds

$$\begin{aligned}
\omega^2(k'_0) < 0 \implies \langle \tilde{q}(k'_0) \tilde{q}(-k'_0) \rangle_{\text{P.B.}} &= \frac{2i}{\omega^2(k'_0)} = -2i \langle \tilde{q}_R(k'_0) \tilde{q}_R(-k'_0) \rangle, \\
\omega^2(k'_0) > 0 \implies \langle \tilde{q}(k'_0) \tilde{q}(-k'_0) \rangle_{\text{P.B.}} &= \frac{2i}{\omega^2(k'_0)} = 2i \langle \tilde{q}_R(k'_0) \tilde{q}_R(-k'_0) \rangle. \tag{4.33}
\end{aligned}$$

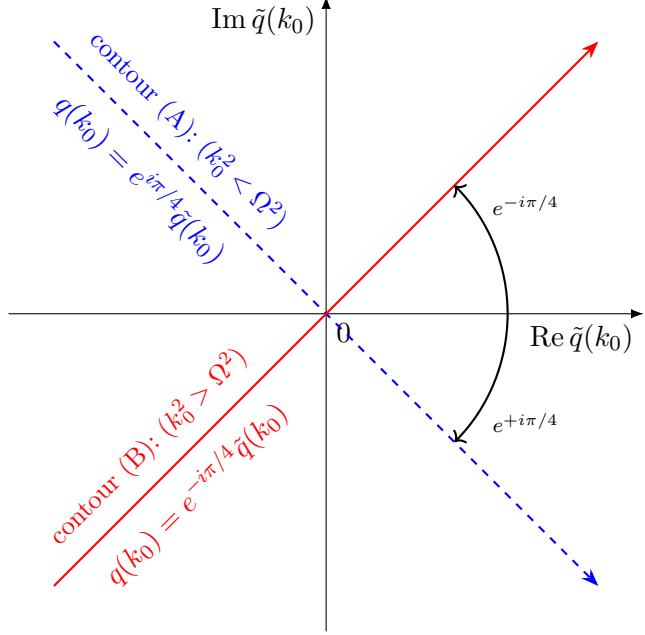


Figure 1. Integration contours in the complex q_k plane. Each mode is rotated so that the holomorphic action becomes real and negative: contour (A) rotated by $+\pi/4$ for $k_0^2 < \Omega^2$, contour (B) rotated by $-\pi/4$ for $k_0^2 > \Omega^2$. This is equivalent to imposing the linear relations among Fourier components used in the symplectic dynamics.

The quantities on the left-hand side of Eq. (4.33) are the expectation values from ordinary quantum mechanics, whereas the quantities on the right-hand side are those that can be sampled by means of the constrained symplectic-quantization dynamics, by computing time averages along the intrinsic time:

$$\langle \tilde{q}_R(k'_0) \tilde{q}_R(-k'_0) \rangle = \lim_{\Delta\tau \rightarrow \infty} \frac{1}{\Delta\tau} \int_{\tau_0}^{\tau_0 + \Delta\tau} d\tau \tilde{q}_R(k'_0, \tau) \tilde{q}_R(-k'_0, \tau), \quad (4.34)$$

where the fields on the right-hand side of Eq. (4.34) denote the solutions of the symplectic-quantization Hamiltonian dynamics. Following the same logic it is possible to identify which correlation functions in the symplectic-quantization approach correspond to standard observables in quantum mechanics such as $\langle q(x_0) \rangle$, $\langle q^n(x_0) \rangle$, and the two-point correlator $\langle q(x_0) q(x'_0) \rangle$, with periodic boundary conditions in coordinate time or with other boundary conditions, for example Dirichlet. To lighten the discussion, the derivation of the corresponding expressions is left to the appendices. In what follows we will limit ourselves to reporting the results, i.e. the expression of quantum-mechanical correlators in terms of the real and imaginary parts of analytically continued fields in the symplectic quantization approach. At this stage, the only preliminary discussion needed before the presentation of results concerns how the numerical simulation of the symplectic-quantization dynamics is realized, and in particular how the constraints on the real and imaginary parts are implemented in practice.

5 Constrained symplectic dynamics: numerical algorithm

In the present section we present a detailed account of the numerical approach to the symplectic quantization dynamics of the quantum harmonic oscillator. There is a general part of the discussion, not specific of the problem, which deals with the discretization on a lattice of the equations of motion. What is on the contrary “problem dependent” is the way to implement in the microscopic Hamiltonian dynamics the constraints required to have stable solutions. This is a technical point which, compared to the strategy of computing directly the functional integral in quantum field theory by means of the Lefschetz-Thimbles approach, plays a role analogous to the choice of the most appropriate contours in the complex action plane along which is more convenient to perform functional integration in order to guarantee convergence. Let us then first present the discretized version of our equations of motion and then explain how the constraints are implemented in practice. We recall in first place the shape of the effective separable Hamiltonian which generates the symplectic dynamics:

$$\mathbb{H}[q, \bar{q}, \pi, \bar{\pi}] = \mathbb{K}[\pi, \bar{\pi}] + \mathbb{V}[q, \bar{q}], \quad (5.1)$$

where

$$\begin{aligned} \mathbb{K}[\pi, \bar{\pi}] &= \int dx_0 \pi(x_0) \bar{\pi}(x_0) \\ \mathbb{V}[q, \bar{q}] &= 2 \operatorname{Im} S[q, \bar{q}] = \frac{S[q] - \bar{S}[\bar{q}]}{i} \\ &= \frac{m}{2i} q(x_0) \frac{dq(x_0)}{dx_0} \bigg|_{x_0^i}^{x_0^f} - \frac{1}{i} \int_{x_0^i}^{x_0^f} dx_0 q(x_0) \left[\frac{m}{2} \frac{d^2}{dx_0^2} + \frac{1}{2} m \Omega^2 \right] q(x_0) - \\ &\quad - \frac{m}{2i} \bar{q}(x_0) \frac{d\bar{q}(x_0)}{dx_0} \bigg|_{x_0^i}^{x_0^f} + \frac{1}{i} \int_{x_0^i}^{x_0^f} dx_0 \bar{q}(x_0) \left[\frac{m}{2} \frac{d^2}{dx_0^2} + \frac{1}{2} m \Omega^2 \right] \bar{q}(x_0) \end{aligned} \quad (5.2)$$

Let us now consider the case of periodic boundary conditions in the x_0 -direction for the field $q(x_0, \tau)$. In this case the boundary terms generated by partial integration in the action do not affect the equations of motion, since periodicity implies

$$q(x_0^f, \tau) = q(x_0^i, \tau), \quad \partial_{x_0} q(x_0^f, \tau) = \partial_{x_0} q(x_0^i, \tau) \quad \forall \tau, \quad (5.3)$$

and therefore

$$q(x_0, \tau) \partial_{x_0} q(x_0, \tau) \bigg|_{x_0^i}^{x_0^f} = 0 \quad (\text{and analogously for } \bar{q}). \quad (5.4)$$

As a consequence, the equations of motion are entirely determined by the bulk terms and read

$$\begin{aligned}\dot{q}(x_0, \tau) &= \bar{\pi}(x_0, \tau), \\ \dot{\bar{q}}(x_0, \tau) &= \pi(x_0, \tau), \\ \dot{\pi}(x_0, \tau) &= -im \left(\frac{\partial^2}{\partial x_0^2} + \Omega^2 \right) q(x_0, \tau), \\ \dot{\bar{\pi}}(x_0, \tau) &= +im \left(\frac{\partial^2}{\partial x_0^2} + \Omega^2 \right) \bar{q}(x_0, \tau),\end{aligned}\tag{5.5}$$

where the dot denotes ∂_τ . Let us now comment on Dirichlet (fixed) boundary conditions, which are relevant for instance to transition amplitudes with fixed endpoints. For Dirichlet boundaries one imposes

$$q(x_0^i, \tau) = q(x_0^f, \tau) = 0 \quad \forall \tau,\tag{5.6}$$

(and similarly for \bar{q}), so that the boundary term produced by partial integration vanishes identically:

$$q(x_0, \tau) \partial_{x_0} q(x_0, \tau) \Big|_{x_0^i}^{x_0^f} = 0 \quad (\text{and analogously for } \bar{q}).\tag{5.7}$$

Therefore the equations of motion (5.5) remain unchanged, while the boundary conditions select the admissible class of field configurations and, in the lattice discretization, determine how the x_0 -Laplacian is implemented at the endpoints (i.e. the boundary sites are held fixed and are not updated by the τ -evolution).

From the above Eq. (5.5), by writing explicitly the equations in terms of the real and imaginary parts of the fields, one gets in real space (coordinate time):

$$\begin{aligned}\ddot{q}_R(x_0, \tau) &= m \left(\Omega^2 + \frac{\partial^2}{\partial x_0^2} \right) q_I(x_0, \tau) \\ \ddot{q}_I(x_0, \tau) &= m \left(\Omega^2 + \frac{\partial^2}{\partial x_0^2} \right) q_R(x_0, \tau).\end{aligned}\tag{5.8}$$

corresponding in Fourier space to

$$\begin{aligned}\ddot{q}_R(k_0, \tau) &= \omega^2(k_0) q_I(k_0, \tau) \\ \ddot{q}_I(k_0, \tau) &= \omega^2(k_0) q_R(k_0, \tau),\end{aligned}\tag{5.9}$$

where we recall the dispersion relation

$$\omega^2(k_0) = m(\Omega^2 - k_0^2).\tag{5.10}$$

We have seen in Sec. 4 that in the case of the harmonic oscillator the constraints which allow to avoid unbounded solutions are straightforward in Fourier space, leading to a set of stable uncoupled equations for each one of the modes k_0 . One could take simply advantage of this and draw a straightforward correspondence with quantum mechanics by exactly integrating the dynamics in Eq. (4.15) and comparing the results obtained with the standard formalism

of quantum mechanics using the correspondence between analytically continued fields and standard fields discussed in the previous section, Sec. 4. But here we aim at a more general formalism, allowing to handle numerically also in presence of interactions, for which it is in general computationally prohibitive the attempt to solve the dynamics directly in Fourier space since the standard interactions of quantum mechanics and quantum field theory, which are local in space, becomes highly non local in Fourier space. It is for this reason that, before discretizing the coordinate time x_0 on a lattice and writing the corresponding equations, we need to define a protocol that allows us to implement the constraints between $q_R(k_0, \tau)$ and $q_I(k_0, \tau)$ also in coordinate space equations. As clearly explained in Sec. (4), the implementation of the constraints on the dynamics allows to a complete description of the system simply from the dynamics of the real part of the position field

$$\begin{aligned} \omega^2(k_0) > 0 &\implies \ddot{q}_R(k_0, \tau) = -\omega^2(k_0) q_R(k_0, \tau) \quad (\text{odd modes}) \\ \omega^2(k_0) < 0 &\implies \ddot{q}_R(k_0, \tau) = +\omega^2(k_0) q_R(k_0, \tau) \quad (\text{even modes}). \end{aligned} \quad (5.11)$$

The above equation cannot be easily Fourier transformed back to coordinate space because we would get highly nonlocal dynamical equations. The most convenient choice to impose in coordinate space the constraint embedded in Eq. (5.11) is to decompose the position field into an *even* and an *odd* part, corresponding respectively to the summation over modes k_0 for which the constraint is $q_R(k_0, \tau) = q_I(k_0, \tau)$ (even),

$$q_R^E(x_0, \tau) = \sum_{\{k_0 \mid \omega^2(k_0) < 0\}} dk_0 e^{ik_0 x_0} q_R(k_0, \tau), \quad (5.12)$$

and to the summation over modes k_0 for which the constraint is $q_R(k_0, \tau) = -q_I(k_0, \tau)$ (odd),

$$q_R^O(x_0, \tau) = \sum_{\{k_0 \mid \omega^2(k_0) > 0\}} dk_0 e^{ik_0 x_0} q_R(k_0, \tau). \quad (5.13)$$

By then writing the equations of motion in terms of odd and even components of the field one gets

$$\begin{aligned} \frac{d^2}{d\tau^2} q_R^O(x_0, \tau) &= -m \left(\Omega^2 + \frac{\partial^2}{\partial x_0^2} \right) q_R^O(x_0, \tau) \\ \frac{d^2}{d\tau^2} q_R^E(x_0, \tau) &= +m \left(\Omega^2 + \frac{\partial^2}{\partial x_0^2} \right) q_R^E(x_0, \tau). \end{aligned} \quad (5.14)$$

The equations in Eq. (5.14) are eventually the version which we discretized and integrated. Formally, they are both stable, but numerical tests on the dynamics prove that they are nevertheless plagued by an instability problem due to discretization. What happens is the following. Let us for instance consider the field $q_R^O(x_0, \tau)$, which should be at all times the superposition only of modes $q_R(k_0, \tau)$ such that $\omega^2(k_0) > 0$: it happens that at a certain point along the numerical integration of the equations of motion, it starts to get also components from modes k_0 with $\omega^2(k_0) < 0$ so that the amplitude of $q_R(k_0, \tau)$ eventually starts to grow exponentially. We solved this problem by putting by hand to zero the *even* components of the field $q_R^O(x_0, \tau)$ periodically along the numerical integration and doing

the viceversa for $q_R^E(x_0, \tau)$.

We discretize the coordinate time direction using exactly M lattice sites

$$x_0^{(\ell)} = x_0^i + \ell a, \quad \ell = 0, 1, \dots, M-1. \quad (5.15)$$

For periodic boundary conditions (P.B.) the extent is $T = Ma$ and fields satisfy $q(\ell + M, \tau) = q(\ell, \tau)$, so that $x_0^f \equiv x_0^i + T$. For Dirichlet boundary conditions (D.B.) the endpoints are distinct and we set $T = (M-1)a$, with $q(0, \tau) = q_i$ and $q(M-1, \tau) = q_f$ for all τ . In the case of periodic boundary conditions in x_0 the field admits the standard Fourier representation

$$q_R(x_0^{(\ell)}, \tau) = \frac{1}{\sqrt{M}} \sum_{n=-M/2}^{M/2-1} e^{ik_0^{(n)} x_0^{(\ell)}} q_R(k_0^{(n)}, \tau), \quad (5.16)$$

where the lattice momenta are $k_0^{(n)} = \frac{2\pi n}{T}$, with $T = x_0^f - x_0^i = Ma$. For boundary conditions different from periodic ones, the structure of the mode expansion is modified accordingly; the explicit mode decomposition in the Dirichlet case is reported in the appendices F. The dispersion relation on the lattice reads as

$$\Omega^2(n) = m \left[\Omega^2 - \frac{2}{a^2} \left(1 - \cos(k_0^{(n)} a) \right) \right]. \quad (5.17)$$

In order to lighten the notation we will denote the position field and its Fourier transform respectively as

$$\begin{aligned} q_R(x_0^{(\ell)}, \tau) &= q_R(\ell, \tau) \\ q_R(k_0^{(n)}, \tau) &= \hat{q}_R(n, \tau), \end{aligned} \quad (5.18)$$

so that the Fourier representation of the field can be rewritten as

$$q_R(\ell, \tau) = \frac{1}{\sqrt{M}} \sum_{n=-M/2}^{M/2-1} e^{ik_0^{(n)} x_0^{(\ell)}} \hat{q}_R(n, \tau). \quad (5.19)$$

Analogously to the continuum, the even and odd component of the position field are defined are defined by separating the modes according to the sign of $\Omega^2(n)$:

$$\begin{aligned} q_R^O(\ell, \tau) &= \sum_{\{n \mid \omega^2(n) > 0\}} e^{ik_0^{(n)} x_0^{(\ell)}} \hat{q}_R(n, \tau), \\ q_R^E(\ell, \tau) &= \sum_{\{n \mid \omega^2(n) < 0\}} e^{ik_0^{(n)} x_0^{(\ell)}} \hat{q}_R(n, \tau). \end{aligned} \quad (5.20)$$

The two lattice fields just defined in Eq. (5.20) obey the following equations

$$\frac{d^2}{d\tau^2} q_R^O(\ell, \tau) = -m \left[\Delta q_R^O(\ell, \tau) + \Omega^2 q_R^O(\ell, \tau) \right] \quad (5.21)$$

$$\frac{d^2}{d\tau^2} q_R^E(\ell, \tau) = m \left[\Delta q_R^E(\ell, \tau) + \Omega^2 q_R^E(\ell, \tau) \right] \quad (5.22)$$

$$(5.23)$$

where the symbol Δ denotes the standard lattice Laplacian

$$\Delta q_R^O(\ell, \tau) = \frac{q_R^O(\ell+1, \tau) - 2q_R^O(\ell, \tau) + q_R^O(\ell-1, \tau)}{a^2} \quad (5.24)$$

The dynamics in the intrinsic time τ of Eq. (5.21) and Eq. (5.22) is then integrated numerically using the leapfrog algorithm, which is a symplectic integrator. Crucially, we have guaranteed that the dynamics of the two fields $q_R^O(\ell, \tau)$ and $q_R^E(\ell, \tau)$ remains on the stable manifold by means of the following protocol

- 1) Set to zero in the initial condition, i.e., at $\tau = 0$, the amplitude of all modes with $\omega^2(n) > 0$ for $q_R^O(\ell, \tau)$ and all modes with $\omega^2(n) < 0$ for $q_R^E(\ell, \tau)$:

$$\begin{aligned} \hat{q}_R^O(n, \tau) &= 0 \quad \forall n \mid \omega^2(n) < 0 \\ \hat{q}_R^E(n, \tau) &= 0 \quad \forall n \mid \omega^2(n) > 0 \end{aligned} \quad (5.25)$$

- 2) Transform back from Fourier to real space and numerically integrate on the lattice the dynamics for the fields $q_R^O(\ell, \tau)$ and $q_R^E(\ell, \tau)$.
- 3) After the numerical integration step compute again the Fourier components of the fields $q_R^O(\ell, \tau + \delta\tau)$ and $q_R^E(\ell, \tau + \delta\tau)$ and set again by hand to zero the amplitude of the Fourier components which should not contribute, namely:

$$\begin{aligned} \hat{q}_R^O(n, \tau + \delta\tau) &= 0 \quad \forall n \mid \omega^2(n) < 0 \\ \hat{q}_R^E(n, \tau + \delta\tau) &= 0 \quad \forall n \mid \omega^2(n) > 0 \end{aligned} \quad (5.26)$$

Repeat from point 2) above.

Let us stress that the solution of the dynamics for $q_R(\ell, \tau) = q_R^O(\ell, \tau) + q_R^E(\ell, \tau)$ is perfectly sufficient to know the behaviour of $q(\ell, \tau) = q_R(\ell, \tau) + iq_I(\ell, \tau)$, since at any time from the knowledge of the Fourier modes $\hat{q}_R(n, \tau)$ we also have $\hat{q}_I(n, \tau)$. They are in fact uniquely determined from the constraint in Eq. (4.13). The leap-frog algorithm keeps track of both $q(\ell, \tau)$ and $\pi(\ell, \tau)$, so we can compute at any time the value of the generalized Hamiltonian

$$\mathbb{H}_\tau[\pi, \bar{\pi}, q, \bar{q}] = \mathbb{K}_\tau[\pi, \bar{\pi}] + \mathbb{V}_\tau[q, \bar{q}] \quad (5.27)$$

where

$$\begin{aligned} \mathbb{K}_\tau[\pi, \bar{\pi}] &= \frac{1}{2} \sum_{\ell=1}^M \left[\pi_R^2(\ell, \tau) + \pi_I^2(\ell, \tau) \right] \\ \mathbb{V}_\tau[q, \bar{q}] &= -\frac{m}{2} \sum_{\ell=1}^M \left[q_R(\ell, \tau) \Delta q_I(\ell, \tau) + q_I(\ell, \tau) \Delta q_R(\ell, \tau) + \Omega^2 q_R(\ell, \tau) q_I(\ell, \tau) \right]. \end{aligned} \quad (5.28)$$

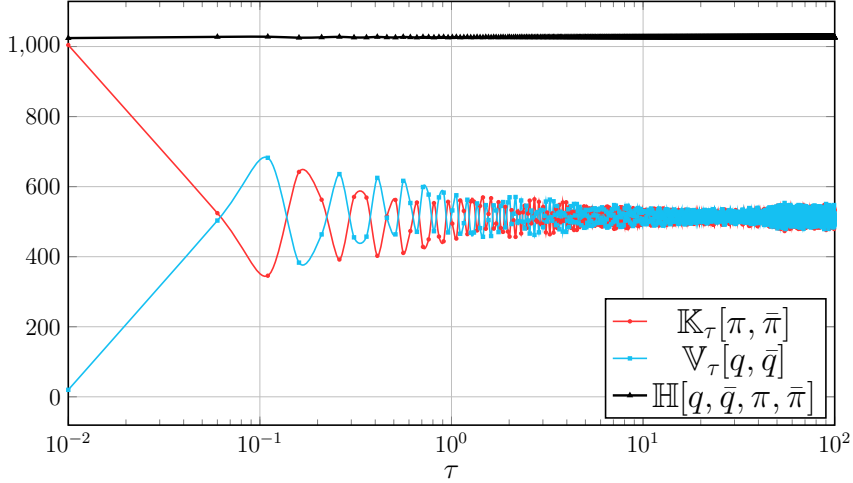


Figure 2. Time evolution of the kinetic ($E_{kin} = \mathbb{K}[\pi]$) and potential ($E_{pot} = \mathbb{V}[q]$) energy for $m = 1.0$, $\Omega = 2.5$, $a = 0.1$, with integration parameters $d\tau = 0.01$, and total simulation time $\Delta\tau = 100$. The system size is $M = 1024$, and we use periodic boundaries.

By monitoring the behaviour of the generalized Hamiltonian in Eq. (5.28) we were able to test both the conservation of the total generalized energy $E = \mathbb{H}_\tau[\pi, \bar{\pi}, q, \bar{q}]$, show in Fig. 2, which is the first diagnostic of the good functioning of the symplectic integrator, and the fast reaching of equipartition, i.e., the relaxation to a stationary state such that

$$\langle \mathbb{K}_\tau[\pi, \bar{\pi}] \rangle = \langle \mathbb{V}_\tau[\phi, \bar{\phi}] \rangle, \quad (5.29)$$

where the angular brackets denote in this case the average over dynamical fluctuations. As thoroughly discussed a recent review on the foundations of statistical mechanics [28], the only necessary condition for the thermalization of *almost all* the physically relevant observables is to have a large number of degrees of freedom, so that we do not have to bother about the lack of non-linear terms in $\mathbb{H}_\tau[\pi, \bar{\pi}, q, \bar{q}]$ for what concerns thermalization.

The stage is now completely set for the presentation of our numerical results, which will be done in the next sections.

6 Constrained symplectic dynamics: numerical results

In this section, we present numerical results for the constrained symplectic-quantization dynamics of the quantum harmonic oscillator presented in the previous sections. We first analyze the one-point function $\langle \hat{q}(\ell) \rangle_{P.B.}$ with periodic boundary conditions, using it as a diagnostic of finite intrinsic-time ($\Delta\tau$) effects and of the convergence of dynamical averages. We then compute the two-point correlator $\langle \hat{q}(\ell) \hat{q}(\ell') \rangle_{P.B.}$, both in coordinate and momentum space, and compare it with the exact lattice expressions, obtaining quantitative agreement and confirming the correctness of the constrained sampling of real-time fluctuations. Next, we reconstruct the canonical equal-time commutator by means of lattice Schwinger–Dyson identities and long- $\Delta\tau$ averages of the microscopic dynamics, and verify

numerically that $[\hat{q}, \hat{p}] = i\hbar$ is reproduced with unit slope as a function of \hbar . Finally, we consider Dirichlet boundary conditions and study the time dependence of $\langle \hat{q}^{2k}(\ell) \rangle_{\text{D.B.}(T)}$ for $k = 1, 2, 3$, showing that its discrete Fourier spectrum exhibits sharp peaks at the expected harmonics $2\Omega, 4\Omega, \dots, 2k\Omega$, thereby providing direct evidence that the constrained symplectic dynamics captures the tower of excited-state contributions in real time.

6.1 Average position $\langle \hat{q}(x_0) \rangle$ finite- $\Delta\tau$ effects (periodic boundaries)

Here we show the symplectic quantization results of the position expectation value, $\langle \hat{q}(\ell) \rangle_{\text{P.B.}}$, for the quantum harmonic oscillator with periodic boundary conditions in time, hence the subscript P.B. for the angular parentheses. This is an insightful example to illustrate how the symplectic quantization approach works, in particular how the finite- $\Delta\tau$ (intrinsic time) effects might affect the comparison between observables sampled from the symplectic quantization Hamiltonian dynamics and standard quantum mechanical expectation values. In the continuum, we label Minkowskian time by the continuous variable x_0 and write operators as $\hat{q}(x_0)$. In the numerical implementation of symplectic-quantization the time direction is discretized into M points and it is convenient to work with a lattice time-slice index $\ell = 0, \dots, M-1$, and a discrete Fourier-mode index $n = -M/2, \dots, M/2-1$. Firstly, let us recall the expression of the position operator at $x_0 \in [x_0^i, x_0^f]$ for standard continuum quantum mechanics:

$$\langle \hat{q}(x_0) \rangle_{\text{P.B.}} = \frac{\text{Tr} \left[e^{\frac{i}{\hbar} \hat{H}(x_0^f - x_0^i)} \hat{q}(x_0) \right]}{\text{Tr} \left[e^{\frac{i}{\hbar} \hat{H}(x_0^f - x_0^i)} \right]} = \frac{\int_{\text{P.B.}} \mathcal{D}q \, q(x_0) \, e^{\frac{i}{\hbar} S[q]}}{\int_{\text{P.B.}} \mathcal{D}q \, e^{\frac{i}{\hbar} S[q]}} = 0, \quad (6.1)$$

where the last equality in Eq. (6.1) follows from the parity of $S[q]$ with respect to the coordinate q . Moving now to the lattice simulation, we consider the Fourier representation of the position field on the lattice,

$$q(\ell) = \frac{1}{\sqrt{M}} \sum_{n=-M/2}^{M/2-1} e^{ik_0^{(n)} x_0^{(\ell)}} \tilde{q}(n), \quad (6.2)$$

with

$$k_0^{(n)} = \frac{2\pi n}{T}, \quad T = Ma, \quad n = -\frac{M}{2}, \dots, \frac{M}{2} - 1 \quad (6.3)$$

and where we have set

$$q(\ell) = q(x_0^{(\ell)}) \quad x_0^{(\ell)} = x_0^i + \ell a, \quad \ell = 0, 1, \dots, M-1, \quad T = Ma, \quad (6.4)$$

and (periodic boundaries) $q(x_0^f) = q(x_0^i)$. The expectation value $\langle q(\ell) \rangle_{\text{P.B.}}$ in coordinate space can be written as

$$\langle q(\ell) \rangle_{\text{P.B.}} = \frac{1}{\sqrt{M}} \sum_{n=-M/2}^{M/2-1} e^{ik_0^{(n)} x_0^{(\ell)}} \langle \tilde{q}(n) \rangle_{\text{P.B.}}. \quad (6.5)$$

Eq. (6.5) implies that the vanishing of the one-point function is basis independent:

$$\langle q(\ell) \rangle_{\text{P.B.}} = 0 \quad \forall \ell \quad \iff \quad \langle \tilde{q}(n) \rangle_{\text{P.B.}} = 0 \quad \forall n. \quad (6.6)$$

With reference to the constrained measure for $\tilde{q}(n) \in \mathbb{C}$ in Eq. (4.31), it is immediate to see that the functional integration over the analytically continued complex field $\tilde{q}(n)$ yields:

$$\langle \tilde{q}(n) \rangle_{\text{P.B.}} = \langle \tilde{q}_R(n) \rangle_{\text{P.B.}} + i \langle \tilde{q}_I(n) \rangle_{\text{P.B.}}, \quad (6.7)$$

so that

$$\begin{aligned} \omega^2(k_0^{(n)}) > 0 &\implies \langle \tilde{q}(n) \rangle_{\text{P.B.}} = (1 - i) \langle \tilde{q}_R(n) \rangle_{\text{P.B.}} = 0 \\ \omega^2(k_0^{(n)}) < 0 &\implies \langle \tilde{q}(n) \rangle_{\text{P.B.}} = (1 + i) \langle \tilde{q}_R(n) \rangle_{\text{P.B.}} = 0, \end{aligned} \quad (6.8)$$

since we have

$$\begin{aligned} \omega^2(k_0^{(n)}) > 0 &\implies \langle \tilde{q}_R(n) \rangle_{\text{P.B.}} \propto \int d\tilde{q}_R(n) \tilde{q}_R(n) e^{-\omega^2(n)(\tilde{q}_R(n))^2} \\ \omega^2(k_0^{(n)}) < 0 &\implies \langle \tilde{q}_R(n) \rangle_{\text{P.B.}} \propto \int d\tilde{q}_R(n) \tilde{q}_R(n) e^{\omega^2(n)(\tilde{q}_R(n))^2}. \end{aligned} \quad (6.9)$$

A crucial effect of the symplectic quantization numerical approach is that, by measuring the averages in Eq. (6.9) as dynamical averages along the intrinsic-time dynamics, non-zero values of $\langle q(\ell) \rangle_{\text{P.B.}}$ appear due to the finite duration of simulations. Indeed, the equivalence between dynamical and thermodynamic averages holds only asymptotically, namely we have that for any large but finite $\Delta\tau$ it holds only *approximatively* that

$$\frac{1}{\Delta\tau} \int_{\tau_0}^{\tau_0 + \Delta\tau} d\tau q(\ell, \tau) \approx \langle q(\ell) \rangle_{\text{P.B.}}, \quad (6.10)$$

with identity only in the limit $\Delta\tau \rightarrow \infty$. Only in the infinite time limit the full probability distribution of the field $q(\ell)$ written in Eq. (4.31) is sampled. This *finite-intrinsic-time* effect can be immediately noticed by looking at Fig. 3, where the estimate of $|\langle q(\ell) \rangle_{\text{P.B.}}|$ sampled along the dynamics for different values of $\Delta\tau$ is shown. The above argument on the necessity for $\langle q(\ell) \rangle_{\text{P.B.}}$ to vanish for an increasing span of the averaging time-window relies on the equilibrium Gaussian shape of the field probability distribution within the the symplectic quantization approach. It is then interesting to explain also how finite- $\Delta\tau$ effects affect standard quantum mechanical formulae. Before presenting the "standard" quantum mechanical argument, let us recall that there are two intermediate steps between the intrinsic-time averaging performed along the symplectic quantization dynamics and any quantum mechanical expectation value. In the first place, one needs to connect the dynamical and thermodynamical averages within symplectic quantization, which requires a large- $\Delta\tau$ limit. Then, symplectic quantization thermodynamical averages are exactly equivalent to quantum mechanical averages only in the large- M limit. Hence, we expect that the agreement between the results of our simulations, which are dynamical averages along the symplectic quantization dynamics for fields on a lattice, and textbook quantum mechanical formulae improves by increasing $\Delta\tau$ and M .

Let us now focus on the implications of a finite- $\Delta\tau$ averaging for continuum quantum mechanical formulae. In particular, let us consider the completeness relation:

$$\int_{-\infty}^{\infty} dq \langle q | \psi_n \rangle \langle \psi_m | q \rangle = \delta_{nm}, \quad (6.11)$$

which, as shown below, enters the expression of $\langle q(x_0) \rangle_{\text{P.B.}}$. The inconsistency of this expression with a finite- $\Delta\tau$ averaging along the symplectic quantization dynamics is represented by the integration of the variable q over the whole real line. The point is that at any finite time the accessible domain of integration is not the entire real line but a finite subset which we denote as $\mathcal{B}_q(\Delta\tau) \subset \mathbb{R}$. As a consequence, any formula which crucially depends on the fact that the integration of q is taken over the entire real line \mathbb{R} , must be handled with care. This is for instance the case for the completeness relation in Eq. (6.11), which for any finite $\Delta\tau$ is only approximate, so that it can be conveniently rewritten as

$$\int_{\mathcal{B}_q(\Delta\tau)} dq \langle q | \psi_n \rangle \langle \psi_m | q \rangle = \delta_{nm} + \alpha_{nm} \cdot \mathcal{O}\left(\frac{1}{||\mathcal{B}_q||}\right), \quad (6.12)$$

where α_{nm} denotes a residual off-diagonal contribution which persist when $||\mathcal{B}_q|| < \infty$, with $||\mathcal{B}_q||$ denoting a measure of the set \mathcal{B}_q . The increase of $\Delta\tau$ allows to sample $q(x_0, \tau)$ over an increasingly large domain \mathcal{B}_q , so that the integral on the left-hand side of Eq. (6.12) approximates the Kronecker delta with increasing precision for increasing $\Delta\tau$. We can relate the non-zero value of the expectation $\langle q(x_0) \rangle_{\text{P.B.}}$ found at finite $\Delta\tau$ in our simulations to the off-diagonal elements remaining in the trace due to Eq. (6.12). The expectation value of the position operator at coordinate time x_0 is given by

$$\langle \hat{q}(x_0) \rangle = \frac{\text{Tr}\left[e^{\frac{i}{\hbar} \hat{H}(x_0^f - x_0^i)} \hat{q}(x_0)\right]}{\text{Tr}\left[e^{\frac{i}{\hbar} \hat{H}(x_0^f - x_0^i)}\right]}. \quad (6.13)$$

By denoting the distance between final and initial Minkowskian time as $T = x_0^f - x_0^i$, we have that the numerator explicitly reads as

$$\text{Tr}\left[e^{\frac{i}{\hbar} \hat{H}T} \hat{q}(x_0)\right] = \sum_{n,m} e^{\frac{i}{2\hbar} (E_m + E_n)T} \langle \psi_n | \hat{q}(x_0) | \psi_m \rangle \int dq \langle q | \psi_n \rangle \langle \psi_m | q \rangle. \quad (6.14)$$

Crucially, when sampling q numerically along the symplectic quantization dynamics, one must consider an expression like the one in Eq. (6.12) rather than an integral over the entire real line, so that, according to Eq. (6.12), even the trace in Eq. (6.14) picks up the contribution of off-diagonal elements. Using the ladder operator representation of the position operator:

$$\hat{q}(x_0) = \sqrt{\frac{\hbar}{2m\Omega}} (e^{-i\Omega x_0} \hat{a} + e^{i\Omega x_0} \hat{a}^\dagger), \quad (6.15)$$

and exploiting the definition of its action on the harmonic oscillator eigenstates:

$$\hat{a} | \psi_m \rangle = \sqrt{m} | \psi_{m-1} \rangle, \quad (6.16)$$

$$\hat{a}^\dagger | \psi_m \rangle = \sqrt{m+1} | \psi_{m+1} \rangle, \quad (6.17)$$

one gets

$$\langle \psi_n | \hat{q}(x_0) | \psi_m \rangle = \sqrt{\frac{\hbar}{2m\Omega}} \left(\sqrt{m} e^{-i\Omega x_0} \delta_{n,m-1} + \sqrt{m+1} e^{i\Omega x_0} \delta_{n,m+1} \right). \quad (6.18)$$

Then, by inserting the expression in Eq. (6.18) into the trace of Eq. (6.14) one gets

$$\begin{aligned} \text{Tr}\left[e^{\frac{i}{\hbar}\hat{H}T}\hat{q}(x_0)\right] = \\ \sqrt{\frac{\hbar}{2m\Omega}} \sum_{n,m} e^{\frac{i}{2\hbar}(E_m+E_n)T} \left(\sqrt{m} e^{-i\Omega x_0} \delta_{n,m-1} + \sqrt{m+1} e^{i\Omega x_0} \delta_{n,m+1} \right) \int dq \langle q|\psi_n\rangle\langle\psi_m|q\rangle. \end{aligned} \quad (6.19)$$

If the orthonormality condition was exactly satisfied, only terms with $n = m$ would contribute, and the trace would make the expectation value vanish:

$$\text{Tr}\left[e^{iHT/\hbar}\hat{q}(x_0)\right] = 0. \quad (6.20)$$

However, for finite $\Delta\tau$, the integral deviates from the Dirac delta, leading to small residual oscillations in the observable. These oscillations decay as $\Delta\tau \rightarrow \infty$.

The same is valid in our discrete setting, and in fact this behaviour is clearly observed in simulations (Fig. 3). In the case of periodic boundary conditions, the amplitude of oscillations decreases with increasing $\Delta\tau$, indicating the suppression of off-diagonal contributions.

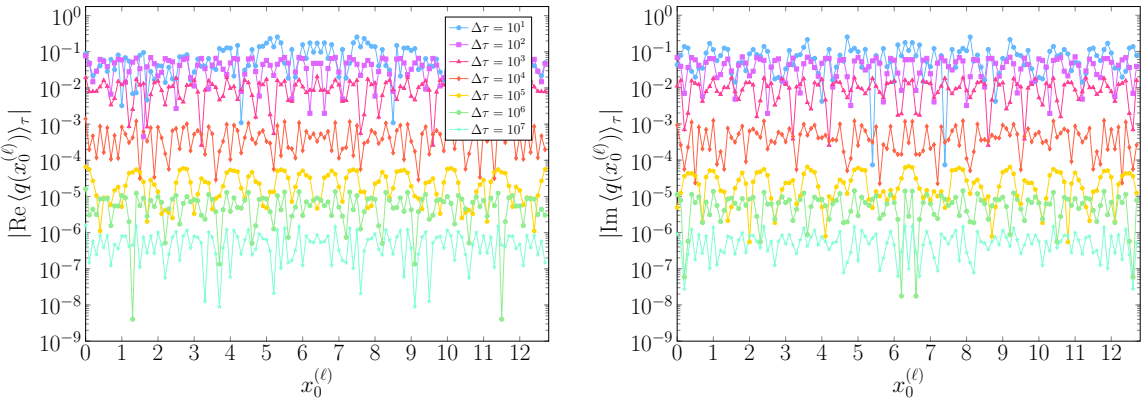


Figure 3. Expectation value of $q(x_0^{(\ell)})$ with periodic boundary conditions and for different values of $\Delta\tau$. Simulation parameters: $M = 128$, $a = 0.1$, $\Omega = 2.5$ and $m = 1$.

6.2 Two-point correlation function (periodic boundaries)

The first important observable we consider as a benchmark of our method is the two-point harmonic-oscillator correlation function $\langle q(\ell)q(\ell') \rangle_{\text{P.B.}}$. Its expression can be explicitly computed in quantum mechanics with periodic boundary conditions in real time. That is, if we consider a real time interval $T = x_0^f - x_0^i$, periodic boundary conditions $q(x_0^f) = q(x_0^i)$ and a discretization in M points with lattice spacing $a = T/M$, the two-point correlation function can be explicitly computed, with the whole derivation reported in App. B, and reads as:

$$\langle q(\ell)q(\ell') \rangle_{\text{P.B.}}^{(\text{lat})} = -\frac{i a}{2m \sin(\kappa a)} \frac{\sin[\kappa a(\ell - \ell')] + \sin[\kappa (T - a(\ell - \ell'))]}{1 - \cos(\kappa T)}, \quad (6.21)$$

where ℓ is an integer index, $\ell = 0, \dots, M - 1$, and κ is defined by the dispersion relation

$$\cos(\kappa a) = 1 - \frac{1}{2}a^2\Omega^2. \quad (6.22)$$

The continuum limit expression can be obtained by Eq. (6.21) by keeping T fixed and taking simultaneously $a \rightarrow 0$ and $M \rightarrow \infty$. Doing so, one has

$$\begin{aligned} a(\ell - \ell') &= x_0 - x'_0 = \Delta x_0 \\ \sin(\kappa a) &\approx \kappa a \\ \cos(\kappa a) &\approx 1 - \frac{1}{2}\kappa^2 a^2, \end{aligned} \quad (6.23)$$

from which we can identify $\kappa = \Omega$ and rewrite Eq. (6.21) as:

$$\langle q(x_0)q(x'_0) \rangle_{\text{P.B.}}^{(\text{cont})} = -\frac{i}{2m\Omega} \frac{\sin[\Omega \Delta x_0] + \sin[\Omega(T - \Delta x_0)]}{1 - \cos(\Omega T)}. \quad (6.24)$$

The purely imaginary oscillatory behaviour reported in Eqns. (6.21), (6.24) is the one we want to test in our numerical simulations of symplectic dynamics. As shown in detail in App. B, the oscillatory behaviour of the two-point correlation function, is the genuine landmark of a true real-time quantum dynamics and of the concurrence of the harmonic oscillator excited states to correlation functions, two facts excluded by definition within the Euclidean quantum mechanics formulation, the one usually exploited for numerical simulations. Once established which are the formulae to be tested numerically, let us illustrate how these can be measured within the symplectic quantization approach. First of all, let us write how the standard quantum-mechanical two-point correlation function reads in terms of the constrained averages over the analytically continued to \mathbb{C} position field $q(x_0) = q_R(x_0) + iq_I(x_0)$ introduced in Sec. 5:

$$\begin{aligned} \langle q(x_0)q(x'_0) \rangle_{\text{P.B.}} &= \langle q_R(x_0)q_R(x'_0) \rangle_{\text{P.B.}} - \langle q_I(x_0)q_I(x'_0) \rangle_{\text{P.B.}} \\ &\quad + i\langle q_R(x_0)q_I(x'_0) \rangle_{\text{P.B.}} + i\langle q_I(x_0)q_R(x'_0) \rangle_{\text{P.B.}}. \end{aligned} \quad (6.25)$$

The expression in Eq. (6.25) can be simplified by taking into account the constraints which guarantee the convergence of functional integrals within the symplectic quantization approach. Such constraints are implemented in our numerical protocol by decomposing the two components of the position field in even and odd parts (5.12) and (5.13):

$$q_R(x_0) = q_R^E(x_0) + q_R^O(x_0), \quad (6.26)$$

$$q_I(x_0) = q_I^E(x_0) + q_I^O(x_0). \quad (6.27)$$

Due to the constraints connecting real and imaginary part, see Sec. 4, the two-point correlation function can be then rewritten as

$$\langle q(x_0)q(x'_0) \rangle_{\text{P.B.}} = 2 \left[\langle q_R^O(x_0)q_R^E(x'_0) \rangle_{\text{P.B.}} + \langle q_R^E(x_0)q_R^O(x'_0) \rangle_{\text{P.B.}} \right. \quad (6.28)$$

$$\left. + i\langle q_R^E(x_0)q_R^E(x'_0) \rangle_{\text{P.B.}} - i\langle q_R^O(x_0)q_R^O(x'_0) \rangle_{\text{P.B.}} \right], \quad (6.29)$$

an expression which can be further simplified by taking into account the constrained integration measure Eq. (4.31), which in terms of $q_R^E(x_0)$ and $q_R^O(x_0)$ reads as

$$\begin{aligned} & \exp\left(\frac{i}{\hbar}S[q_R^O, q_R^E]\right) = \\ & = \exp\left\{\frac{m}{2\hbar}\int dx_0 q_R^O(x_0)\left(\Omega^2 + \frac{\partial^2}{\partial x_0^2}\right)q_R^O(x_0) - \frac{m}{2\hbar}\int dx_0 q_R^E(x_0)\left(\Omega^2 + \frac{\partial^2}{\partial x_0^2}\right)q_R^E(x_0)\right\} \end{aligned} \quad (6.30)$$

From the above functional probability density one immediately finds

$$\langle q_R^O(x_0)q_R^E(x'_0) \rangle_{\text{P.B.}} = \langle q_R^E(x_0)q_R^O(x'_0) \rangle_{\text{P.B.}} = 0. \quad (6.31)$$

Thus the two-point function of the quantum harmonic oscillator, written in terms of the analytically continued field $q(x_0) \in \mathbb{C}$, simplifies to

$$\langle q(x_0)q(x'_0) \rangle_{\text{P.B.}} = 2i\left[\langle q_R^E(x_0)q_R^E(x'_0) \rangle_{\text{P.B.}} - \langle q_R^O(x_0)q_R^O(x'_0) \rangle_{\text{P.B.}}\right] \quad (6.32)$$

and it is purely imaginary. In our symplectic-quantization simulations we measure precisely the quantity on the right-hand side of Eq. (6.32), discretized in coordinate time x_0 . Remarkably, on the left hand side of Fig. 4 we report a perfect agreement between the symplectic quantization simulation of the correlator in coordinate space and the theoretical prediction from quantum mechanics.

As an additional piece of evidence, it is useful to inspect the Fourier spectrum of the two-point correlation function on the lattice. We consider the lattice sites $x_0^{(\ell)} = x_0^i + \ell a$, $\ell = 0, \dots, M-1$, with $T = Ma$ and periodic boundary conditions. In what follows we write $q(\ell) \equiv q(x_0^{(\ell)})$. We introduce the discrete Fourier modes

$$\tilde{q}(n) \equiv \frac{1}{\sqrt{M}} \sum_{\ell=0}^{M-1} e^{-ik_0^{(n)}x_0^{(\ell)}} q(\ell), \quad (6.33)$$

where $k_0^{(n)} = 2\pi n/T$ and $n = -\frac{M}{2}, \dots, \frac{M}{2} - 1$. For the free harmonic oscillator the lattice momentum-space propagator is diagonal and reads

$$\langle \tilde{q}(n) \tilde{q}(-n) \rangle_{\text{P.B.}}^{(\text{lat})} = \frac{i}{m} \frac{1}{\frac{4}{a^2} \sin^2(k_0^{(n)}a/2) - \Omega^2}. \quad (6.34)$$

For a finite symplectic time extent $\Delta\tau$ we denote intrinsic-time averages by $\langle \dots \rangle_\tau$, assuming that in the infinite limit $\Delta\tau \rightarrow \infty$ time averages converge to ensemble averages $\langle \dots \rangle_{\text{P.B.}}$. In the simulations we record the real and imaginary parts of each mode,

$$\tilde{q}(n) \equiv \tilde{q}_R(n) + i\tilde{q}_I(n), \quad \tilde{q}_{R,I}(n) \in \mathbb{R}, \quad (6.35)$$

and we form the diagonal correlator $\langle \tilde{q}(n) \tilde{q}(-n) \rangle_\tau$. Writing it explicitly in terms of \tilde{q}_R and \tilde{q}_I gives

$$\begin{aligned} \langle \tilde{q}(n) \tilde{q}(-n) \rangle_\tau &= \langle \tilde{q}_R(n) \tilde{q}_R(-n) - \tilde{q}_I(n) \tilde{q}_I(-n) \rangle_\tau \\ &+ i\langle \tilde{q}_R(n) \tilde{q}_I(-n) + \tilde{q}_I(n) \tilde{q}_R(-n) \rangle_\tau. \end{aligned} \quad (6.36)$$

Therefore, in the large- $\Delta\tau$ limit we expect the real part to vanish, while the imaginary part converges to the analytic lattice prediction (6.34), namely

$$\text{Re} \left\langle \tilde{q}(n) \tilde{q}(-n) \right\rangle_\tau \xrightarrow[\Delta\tau \rightarrow \infty]{} 0, \quad (6.37)$$

$$\text{Im} \left\langle \tilde{q}(n) \tilde{q}(-n) \right\rangle_\tau \xrightarrow[\Delta\tau \rightarrow \infty]{} \frac{1}{m} \frac{1}{\frac{4}{a^2} \sin^2(k_0^{(n)} a/2) - \Omega^2} \equiv C(k_0^{(n)}). \quad (6.38)$$

In the right panel of Fig. 4 we compare the numerical data for $\text{Im} \langle \tilde{q}(n) \tilde{q}(-n) \rangle_\tau$ with the prediction (6.37). We observe that the real part is consistent with zero, while the imaginary part of the Fourier-spectrum two-point function matches $C(k_0^{(n)})$.

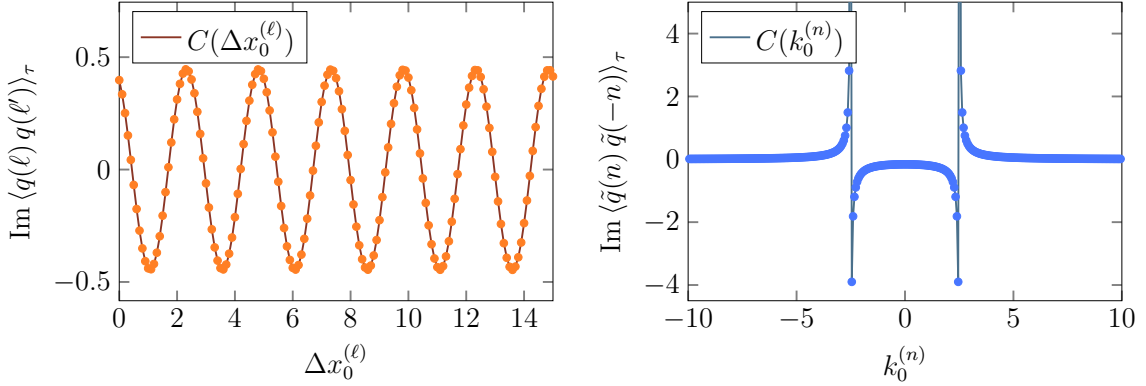


Figure 4. Harmonic-oscillator two-point function on the lattice with periodic boundary conditions. **Left:** coordinate-space correlator $\text{Im} \langle q(\ell) q(\ell') \rangle_\tau$ compared with the analytic lattice prediction (6.21). **Right:** Fourier-spectrum correlator $\text{Im} \langle \tilde{q}(n) \tilde{q}(-n) \rangle_\tau$ compared with the prediction (6.37). Simulation parameters: $M = 1024$, $a = 0.1$, $m = 1$, $\Omega = 2.5$, $dt = 0.01$, periodic boundaries.

6.3 Uncertainty principle

A fundamental test to be passed for any deterministic fictitious dynamics aiming at reproducing quantum mechanics is the capability to reproduce the uncertainty principle. In particular, what we do here is to show how the symplectic quantization approach allows to correctly sample the equal-time commutation relation

$$[\hat{q}(x_0), \hat{p}(x_0)] = i\hbar. \quad (6.39)$$

The strategy to numerically sample a commutation relation requires a short preliminary explanation. What one actually measures is the trace of the commutator over quantum fluctuations, which we define as

$$c(\hbar) \equiv \frac{1}{\mathcal{Z}(\hbar)} \text{Tr}([\hat{q}(x_0), \hat{p}(x_0)]), \quad (6.40)$$

where the trace is over a complete orthonormal basis of the system's Hilbert space. A crucial step in explaining how the trace written in Eq. (6.40) can be sampled numerically is to

pass through the path-integral representation of the trace, explaining how the operators appearing in the commutation relation translate into fields [29] (see App. C). In fact, in the functional approach there are no operators, so that the information content of a commutator has to be appropriately represented in the functional formalism. The crucial difference in a different ordering of the operators is that, despite being labeled by the same Minkowskian time, the rightmost operator acts in practice slightly before the one to its left. That is, if we denote as $x_0^{(+)}$ a time infinitesimally larger than x_0 , i.e. $x_0^{(+)} - x_0 \ll 1$, and as $x_0^{(-)}$ a time infinitesimally smaller than x_0 , i.e. $x_0 - x_0^{(-)} \ll 1$, we can write the functional expression of the commutator trace as

$$c(\hbar) = \frac{1}{\mathcal{Z}(\hbar)} \int \mathcal{D}q(x_0) e^{\frac{i}{\hbar} S[q]} \left[q(x_0)p(x_0^{(-)}) - q(x_0)p(x_0^{(+)}) \right]. \quad (6.41)$$

The above expression of the commutator trace becomes even more transparent when discretizing Minkowskian time, with lattice spacing $a = T/M$ and $x_0^{(\ell)} = x_0^i + \ell a$. In this case we can write:

$$\begin{aligned} p(x_0^{(-)}) &= p\left(x_0^{(\ell-\frac{1}{2})}\right) = \frac{m}{a} [q(\ell) - q(\ell-1)] \\ p(x_0^{(+)}) &= p\left(x_0^{(\ell+\frac{1}{2})}\right) = \frac{m}{a} [q(\ell+1) - q(\ell)], \end{aligned} \quad (6.42)$$

from which we can then rewrite the functional integral expression of $c(\hbar)$ on a discretized time lattice as

$$\begin{aligned} c(\hbar) &= \frac{1}{\mathcal{Z}(\hbar)} \int \prod_{\ell=0}^{M-1} dq(\ell) e^{\frac{i}{\hbar} S[q]} \left[q(\ell)p\left(x_0^{(\ell-\frac{1}{2})}\right) - q(\ell)p\left(x_0^{(\ell+\frac{1}{2})}\right) \right] \\ &= \frac{m}{a} \left[2\langle q^2(\ell) \rangle_{\text{P.B.}} - \langle q(\ell)q(\ell-1) \rangle_{\text{P.B.}} - \langle q(\ell)q(\ell+1) \rangle_{\text{P.B.}} \right]. \end{aligned} \quad (6.43)$$

In order to match the expression of Eq. (6.43) with the quantities measured in our numerical simulations we need to rewrite the commutator by explicitating formulae in terms of the real and imaginary parts of the position field $q(\ell) = q_R(\ell) + iq_I(\ell)$ and the role played by the constraints on the functional measure, which can be done by further decomposing the real and imaginary parts as:

$$\begin{aligned} q_R(\ell) &= q_R^E(\ell) + q_R^O(\ell) \\ q_I(\ell) &= q_I^E(\ell) + q_I^O(\ell). \end{aligned}$$

Using the constraints on the functional measure (Eqs. (4.13) and (5.20)), the imaginary part of any two-point function can be rewritten directly in terms of the even and odd components of the real part of the field as

$$\text{Im}\langle q(\ell)q(\ell') \rangle_{\text{P.B.}} = 2 \left[\langle q_R^E(\ell)q_R^E(\ell') \rangle_{\text{P.B.}} - \langle q_R^O(\ell)q_R^O(\ell') \rangle_{\text{P.B.}} \right]. \quad (6.44)$$

Since $c(\hbar)$ is purely imaginary, Eq. (6.43) can be equivalently rewritten as

$$-i c(\hbar) = \frac{m}{a} \left[2 \text{Im}\langle q^2(\ell) \rangle_{\text{P.B.}} - \text{Im}\langle q(\ell)q(\ell-1) \rangle_{\text{P.B.}} - \text{Im}\langle q(\ell)q(\ell+1) \rangle_{\text{P.B.}} \right]. \quad (6.45)$$

Substituting Eq. (6.44) term by term, one obtains $c(\hbar)$ entirely in terms of correlators of q_R^E and q_R^O :

$$\begin{aligned} -i c(\hbar) = \frac{m}{a} \{ & 4 \left[\langle q_R^E(\ell) q_R^E(\ell) \rangle_{\text{P.B.}} - \langle q_R^O(\ell) q_R^O(\ell) \rangle_{\text{P.B.}} \right] \\ & - 2 \left[\langle q_R^E(\ell) q_R^E(\ell-1) \rangle_{\text{P.B.}} - \langle q_R^O(\ell) q_R^O(\ell-1) \rangle_{\text{P.B.}} \right] \\ & - 2 \left[\langle q_R^E(\ell) q_R^E(\ell+1) \rangle_{\text{P.B.}} - \langle q_R^O(\ell) q_R^O(\ell+1) \rangle_{\text{P.B.}} \right] \} \}. \end{aligned} \quad (6.46)$$

Equation (6.46) is the form of the commutator trace that is directly matched against the numerical data, since it involves only correlators of the even and odd real components of the field evolved in the constrained symplectic dynamics.

Accordingly, in the symplectic quantization simulation we measure the corresponding microcanonical average by computing the same combination of correlators along the stationary intrinsic-time evolution and averaging over lattice sites,

$$\begin{aligned} c_\tau(\hbar) \equiv \frac{1}{M \Delta \tau} \sum_{\ell=0}^{M-1} \int_{\tau_0}^{\tau_0 + \Delta \tau} d\tau \frac{m}{a} \{ & 4 \left[q_R^E(\ell, \tau) q_R^E(\ell, \tau) - q_R^O(\ell, \tau) q_R^O(\ell, \tau) \right] \\ & - 2 \left[q_R^E(\ell, \tau) q_R^E(\ell-1, \tau) - q_R^O(\ell, \tau) q_R^O(\ell-1, \tau) \right] \\ & - 2 \left[q_R^E(\ell, \tau) q_R^E(\ell+1, \tau) - q_R^O(\ell, \tau) q_R^O(\ell+1, \tau) \right] \} \}, \end{aligned} \quad (6.47)$$

which is the symplectic-quantization estimator of $-i c(\hbar)$, i.e. $c_\tau(\hbar) \simeq -i c(\hbar)$ in the stationary regime. Using the equivalence between constrained symplectic averages and the Feynman path integral (Sec. 3) one expects

$$\lim_{\tau \rightarrow \infty} c_\tau(\hbar) = \hbar, \quad (6.48)$$

thus recovering the canonical algebra (6.39). For different values of \hbar we compute (6.47) along the symplectic evolution. As shown in Fig. 5, the resulting values fall on the line $c_\tau(\hbar) = \hbar$ with unit slope and no adjustable parameters, confirming that the constrained symplectic dynamics reproduces the canonical commutation relation. The error bars are computed from the fluctuations of the site average over the M lattice points.

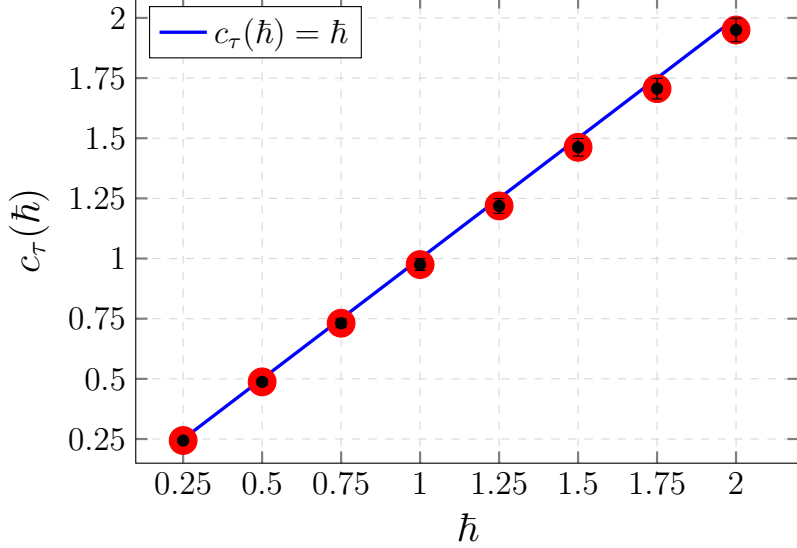


Figure 5. Numerical determination of the equal-time commutator from the constrained symplectic dynamics. The solid line is the exact prediction $C(\hbar) = \hbar$, while points are the intrinsic-time averages computed from Eq. (6.47).

6.4 Discrete spectrum of $\langle \hat{q}^{2k}(x_0) \rangle$ or Dirichlet boundary conditions

A key advantage of constrained symplectic quantization as a numerical tool for real-time dynamics is that it retains the full tower of excited states, which is typically suppressed in imaginary-time approaches. A class of observables where excited states explicitly contribute is given by even powers of the position operator, \hat{q}^{2k} , whose real-time Dirichlet expectation values display a discrete harmonic content fixed by energy differences. In Secs. 5 and 6 we discussed the periodic-boundary case. Here we extend the discussion to Dirichlet boundary conditions, which are required to calculate transition amplitudes

$$\langle q_f, x_0^f | \hat{q}^{2k}(x_0) | q_i, x_0^i \rangle, \quad q(x_0^i) = q_i, \quad q(x_0^f) = q_f. \quad (6.49)$$

In the numerical analysis below we restrict to $q_i = q_f = 0$ and define the normalized Dirichlet expectation value

$$\langle \hat{q}^{2k}(x_0) \rangle_{\text{D.B.}(T)} \equiv \frac{\langle 0, x_0^f | \hat{q}^{2k}(x_0) | 0, x_0^i \rangle}{\langle 0, x_0^f | 0, x_0^i \rangle}, \quad T \equiv x_0^f - x_0^i. \quad (6.50)$$

The same calculations could be carried out also for odd powers of the position operator, but it would require to fix the boundaries at nonzero values of q_i and q_f . Since the analysis is exactly the same we only report the even results. In the functional-integral representation, and in the constrained symplectic dynamics, the construction is the same as for periodic boundary conditions, the only difference being the choice of Fourier basis that implements the boundary conditions. For Dirichlet boundaries on $[x_0^i, x_0^f]$ with $q(x_0^i) = q(x_0^f) = 0$ it is convenient to expand the field in the sine basis

$$q(x_0) = \sum_{n=1}^{\infty} \tilde{q}(n) \sqrt{\frac{2}{T}} \sin\left(\frac{n\pi(x_0 - x_0^i)}{T}\right), \quad \kappa_0^{(n)} \equiv \frac{\pi n}{T}, \quad (6.51)$$

whose orthonormality reads

$$\frac{2}{T} \int_{x_0^i}^{x_0^f} dx_0 \sin\left(\frac{n\pi(x_0 - x_0^i)}{T}\right) \sin\left(\frac{n'\pi(x_0 - x_0^i)}{T}\right) = \delta_{n,n'}. \quad (6.52)$$

In this basis the quadratic action is diagonal and the distribution of Dirichlet modes factorizes, exactly as in the periodic case. The correspondence between mode correlators obtained from constrained averages and the corresponding quantum-mechanical correlators is thus unchanged in form and can again be stated mode by mode. We refer to App. D for the explicit measure and for the detailed mode-by-mode correspondence.

The discrete frequency content of $\langle \hat{q}^{2k}(x_0) \rangle_{\text{D.B.}(T)}$ follows directly from its spectral representation. Inserting completeness in the numerator of Eq. (6.50) gives

$$\begin{aligned} \langle 0, x_0^f | \hat{q}^{2k}(x_0) | 0, x_0^i \rangle &= \sum_{m,n \geq 0} \langle 0, x_0^f | \psi_m \rangle \langle \psi_m | \hat{q}^{2k}(x_0) | \psi_n \rangle \langle \psi_n | 0, x_0^i \rangle \\ &= \sum_{m,n \geq 0} \psi_m(0) \psi_n(0) \langle \psi_m | \hat{q}^{2k} | \psi_n \rangle e^{-\frac{i}{\hbar} E_m (x_0^f - x_0^i)} e^{-\frac{i}{\hbar} E_n (x_0 - x_0^i)}, \end{aligned} \quad (6.53)$$

and dividing by the denominator $\langle 0, x_0^f | 0, x_0^i \rangle = \sum_{r \geq 0} |\psi_r(0)|^2 e^{-\frac{i}{\hbar} E_r T}$ one obtains

$$\langle \hat{q}^{2k}(x_0) \rangle_{\text{D.B.}(T)} = \frac{1}{D(T)} \sum_{m,n \geq 0} \psi_m(0) \psi_n(0) \langle \psi_m | \hat{q}^{2k} | \psi_n \rangle e^{-\frac{i}{\hbar} (E_n - E_m) (x_0 - x_0^i)} e^{-\frac{i}{\hbar} E_m T}, \quad (6.54)$$

with

$$D(T) \equiv \sum_{r \geq 0} |\psi_r(0)|^2 e^{-\frac{i}{\hbar} E_r T}. \quad (6.55)$$

Since harmonic-oscillator eigenfunctions with odd quantum number are odd, $\psi_{2r+1}(0) = 0$, only even states contribute in Eqs. (6.53)–(6.54). Therefore the frequencies appearing in $\langle \hat{q}^{2k}(x_0) \rangle_{\text{D.B.}(T)}$ are fixed by differences $E_{2n} - E_{2m} = 2(n - m)\hbar\Omega$.

For $k = 1$ the harmonic content can be made completely explicit. Using $\hat{q} = \sqrt{\hbar/(2m\Omega)}(a + a^\dagger)$ one finds

$$\hat{q}^2 = \frac{\hbar}{2m\Omega} (aa + a^\dagger a^\dagger + 2a^\dagger a + 1), \quad (6.56)$$

so that $\langle \psi_{2m} | \hat{q}^2 | \psi_{2n} \rangle$ is non-vanishing only for $m = n$ and $m = n \pm 1$. Equation (6.54) then reduces to three harmonics,

$$\langle \hat{q}^2(x_0) \rangle_{\text{D.B.}(T)} = \frac{\hbar}{2m\Omega} [\alpha(T) + \gamma_-(T) e^{-i2\Omega(x_0 - x_0^i)} + \gamma_+(T) e^{+i2\Omega(x_0 - x_0^i)}], \quad (6.57)$$

where the coefficients can be written as ratios of even-state sums,

$$\alpha(T) \equiv \frac{\sum_{n=0}^{\infty} (4n+1) e^{-\frac{i}{\hbar} E_{2n} T} |\psi_{2n}(0)|^2}{D(T)}, \quad (6.58)$$

$$\gamma_+(T) \equiv \frac{\sum_{n=0}^{\infty} \sqrt{(2n+1)(2n+2)} e^{-\frac{i}{\hbar} E_{2n} T} \psi_{2n+2}(0) \psi_{2n}(0)}{D(T)}, \quad (6.59)$$

$$\gamma_-(T) \equiv \frac{\sum_{n=0}^{\infty} \sqrt{(2n+1)(2n+2)} e^{-\frac{i}{\hbar} E_{2n+2} T} \psi_{2n+2}(0) \psi_{2n}(0)}{D(T)}. \quad (6.60)$$

The operator steps leading from Eq. (6.54) to Eq. (6.57), and the explicit evaluation of the sums, are given in App. E. In the continuum one obtains the closed forms

$$\alpha(T) = -i \cot(\Omega T), \quad \gamma_+(T) = \frac{1}{2}[1 + i \cot(\Omega T)], \quad \gamma_-(T) = \frac{1}{2}[-1 + i \cot(\Omega T)], \quad (6.61)$$

which reproduce the standard Dirichlet Green-function result (App. E)

$$\langle \hat{q}^2(x_0) \rangle_{\text{D.B.}(T)} = \frac{i\hbar}{m\Omega \sin(\Omega T)} \sin(\Omega(x_0 - x_0^i)) \sin(\Omega(x_0^f - x_0)). \quad (6.62)$$

More generally, \hat{q}^{2k} is a degree- $2k$ polynomial in the ladder operators and therefore connects number states only with $|\Delta n| \leq 2k$ and Δn even. As a consequence, the frequency support of $\langle \hat{q}^{2k}(x_0) \rangle_{\text{D.B.}(T)}$ is discrete and contained in

$$\omega \in \{0, \pm 2\Omega, \pm 4\Omega, \dots, \pm 2k\Omega\}. \quad (6.63)$$

Explicit results for $k = 2$ and $k = 3$ are reported in App. G. This is the analytic spectral signature that we test numerically.

In the constrained symplectic dynamics we work, as in the periodic case, with the analytically continued lattice field $q(\ell) = q_R(\ell) + iq_I(\ell)$ and with its decomposition into components even/odd under the time reflection that defines the stable manifold (see Eq. (5.12) and (5.13)),

$$q_R(\ell) = q_R^E(\ell) + q_R^O(\ell), \quad q_I(\ell) = q_I^E(\ell) + q_I^O(\ell). \quad (6.64)$$

The constraints specifying the stable manifold (see Eqs. (4.13) and (5.20)) impose the same relations between the even/odd components as in the periodic case,

$$q_I^E(\ell) = +q_R^E(\ell), \quad q_I^O(\ell) = -q_R^O(\ell), \quad (6.65)$$

so that the complex field entering Dirichlet expectation values can be written entirely in terms of the two real constrained variables $q_R^E(\ell)$ and $q_R^O(\ell)$,

$$q(\ell) = q_R(\ell) + iq_I(\ell) = (1+i)q_R^E(\ell) + (1-i)q_R^O(\ell). \quad (6.66)$$

In practice, in the simulation we evolve $q_R^E(\ell, \tau)$ and $q_R^O(\ell, \tau)$ along the constrained symplectic flow and construct the operator insertion $q^{2k}(\ell)$ at each intrinsic-time step using Eq. (6.66). Writing $q_E(\ell) \equiv q_R^E(\ell)$ and $q_O(\ell) \equiv q_R^O(\ell)$, the lowest even powers read

$$\begin{aligned} q^2(\ell) &= \left[(1+i)q_E(\ell) + (1-i)q_O(\ell) \right]^2 \\ &= 2i \left[q_E^2(\ell) - q_O^2(\ell) \right] + 4q_E(\ell)q_O(\ell), \end{aligned} \quad (6.67)$$

$$\begin{aligned} q^4(\ell) &= \left[(1+i)q_E(\ell) + (1-i)q_O(\ell) \right]^4 \\ &= -4 \left[q_E^4(\ell) + q_O^4(\ell) \right] + 24q_E^2(\ell)q_O^2(\ell) + (\text{terms odd in } q_E \text{ or } q_O), \end{aligned} \quad (6.68)$$

$$\begin{aligned} q^6(\ell) &= \left[(1+i)q_E(\ell) + (1-i)q_O(\ell) \right]^6 \\ &= -8i \left[q_E^6(\ell) - q_O^6(\ell) \right] + 120i \left[q_E^4(\ell)q_O^2(\ell) - q_E^2(\ell)q_O^4(\ell) \right] + (\text{terms odd in } q_E \text{ or } q_O). \end{aligned} \quad (6.69)$$

The terms labeled as “odd” contain at least one odd power of q_E or q_O and vanish in expectation values with the constrained measure, because the even and odd sectors are statistically independent and each sector is centered at zero (the same argument used below Eq. (6.29) in the periodic case). Therefore, Dirichlet expectation values can be expressed directly in terms of mixed even moments,

$$\langle q^2(\ell) \rangle_{\text{D.B.}(T)} = 2i \left[\langle q_E^2(\ell) \rangle_{\text{D.B.}(T)} - \langle q_O^2(\ell) \rangle_{\text{D.B.}(T)} \right], \quad (6.70)$$

$$\langle q^4(\ell) \rangle_{\text{D.B.}(T)} = -4 \left[\langle q_E^4(\ell) \rangle_{\text{D.B.}(T)} + \langle q_O^4(\ell) \rangle_{\text{D.B.}(T)} \right] + 24 \langle q_E^2(\ell)q_O^2(\ell) \rangle_{\text{D.B.}(T)}, \quad (6.71)$$

$$\begin{aligned} \langle q^6(\ell) \rangle_{\text{D.B.}(T)} &= -8i \left[\langle q_E^6(\ell) \rangle_{\text{D.B.}(T)} - \langle q_O^6(\ell) \rangle_{\text{D.B.}(T)} \right] \\ &\quad + 120i \left[\langle q_E^4(\ell)q_O^2(\ell) \rangle_{\text{D.B.}(T)} - \langle q_E^2(\ell)q_O^4(\ell) \rangle_{\text{D.B.}(T)} \right], \end{aligned} \quad (6.72)$$

and for arbitrary k one may write the estimator compactly as

$$\langle q^{2k}(\ell) \rangle_{\text{D.B.}(T)} = \sum_{j=0}^k \binom{2k}{2j} (1+i)^{2j} (1-i)^{2k-2j} \langle q_E^{2j}(\ell)q_O^{2k-2j}(\ell) \rangle_{\text{D.B.}(T)}, \quad (6.73)$$

where only even powers appear because all mixed moments with an odd power of q_E or q_O vanish. Equations (6.70)–(6.73) are the explicit bridge between the quantum-mechanical Dirichlet expectation values and the quantities computed from the constrained symplectic dynamics.

On the lattice we discretize the Dirichlet interval T into M steps of size a (so $T = Ma$), impose Dirichlet boundary conditions at the endpoints, and measure correlators on interior sites $\ell = 1, \dots, M-1$. The equal-time Dirichlet correlator reads (App. F)

$$\langle q(\ell)^2 \rangle_{\text{D.B.}(T)} = i\hbar \sum_{n=1}^{M-1} \frac{2}{M} \frac{\sin^2(\frac{\pi n \ell}{M})}{\frac{4}{a^2} \sin^2(\frac{\pi n}{2M}) - \Omega^2}. \quad (6.74)$$

In complete analogy with the continuum Dirichlet decomposition (Eq. (D.2)), the lattice Dirichlet modes are labelled by $n = 1, \dots, M - 1$ and have discrete wave-numbers

$$\kappa_0^{(n)} \equiv \frac{\pi n}{T} = \frac{\pi n}{Ma}. \quad (6.75)$$

For later comparison it is convenient to introduce the corresponding lattice eigenvalues of the Dirichlet Laplacian,

$$\hat{\kappa}_0^{(n)2} \equiv \frac{4}{a^2} \sin^2\left(\frac{\kappa_0^{(n)} a}{2}\right) = \frac{4}{a^2} \sin^2\left(\frac{\pi n}{2M}\right), \quad (6.76)$$

so that the denominator in Eq. (6.74) is simply $\hat{\kappa}_0^{(n)2} - \Omega^2$.

For resonant time extents, such as $T = 4\pi/\Omega$, the denominator in Eq. (6.74) becomes small for the mode(s) whose Dirichlet lattice eigenvalue $\hat{\kappa}_0^{(n)2}$ lies closest to Ω^2 . This yields a strong enhancement of the corresponding term(s) in the mode sum and increases the overall amplitude of $\langle q(\ell)^2 \rangle_{D.B.(T)}$ with M . In the parameter range explored in this work we find that, at $T = 4\pi/\Omega$, this enhancement is well described by an approximately linear growth with M , so that the rescaled quantity $\langle q(\ell)^2 \rangle_{D.B.(T)}/M$ collapses for different M , as shown in Fig. 6. A quantitative discussion of the resonant enhancement and its relation to truncated even-state sums in the continuum spectral representation is given in App. H.

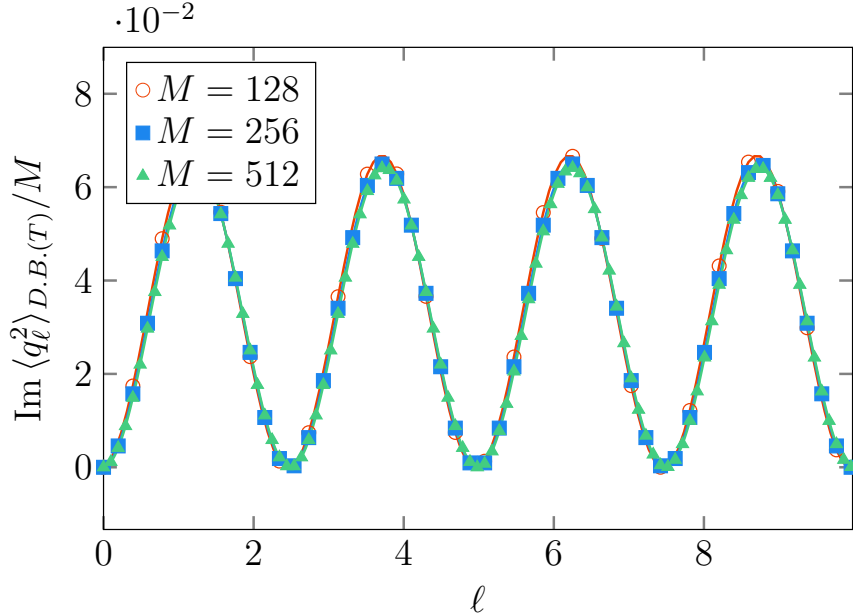


Figure 6. Imaginary part of the equal-time Dirichlet correlator, $\text{Im} \langle q(\ell)^2 \rangle_{D.B.(T)}/M$, as a function of x_0 at resonance $T = 4\pi/\Omega$ for $\Omega = 2.5$, lattice spacing $a = 0.1$ and flow time $\Delta\tau = 10^5$. Data for $M = 128, 256, 512$ collapse onto a single curve once divided by M , demonstrating the approximately linear growth with M of the resonant amplitude discussed in App. H.

Finally, to display the discrete harmonic content predicted by Eq. (6.63), we analyze the Fourier spectrum of the Dirichlet expectation values measured in coordinate space. For

each even power $2k$ we compute the discrete transform on the interior sites $\ell = 1, \dots, M-1$,

$$\tilde{C}_{2k}(\kappa_0^{(n)}) \equiv \frac{1}{\sqrt{M}} \sum_{\ell=1}^{M-1} \exp(i\kappa_0^{(n)} x_0^{(\ell)}) \langle q^{2k}(\ell) \rangle_{\text{D.B.}(T)}, \quad (6.77)$$

where

$$x_0^{(\ell)} = x_0^i + \ell a, \quad \kappa_0^{(n)} \equiv \frac{\pi n}{T}, \quad n = 1, \dots, M-1. \quad (6.78)$$

Using the complex exponential at this analysis step is convenient because it displays simultaneously positive and negative frequency components. In the continuum limit $|\tilde{C}_{2k}(\kappa_0^{(n)})|$ is therefore expected to exhibit narrow peaks located at the harmonics $\kappa_0^{(n)} \simeq 2r\Omega$ with $r = 0, 1, \dots, k$, and no additional lines. Fig. 7 shows the numerical spectra $|\tilde{C}_{2k}(\kappa_0^{(n)})|$ for $2k = 2, 4, 6$: in all cases we observe a finite set of sharp peaks at the expected positive harmonics, with rapidly decreasing amplitude at higher multiples. This provides a stringent test that the constrained symplectic dynamics reproduces the excited-state contributions and yields the expected discrete spectrum for Dirichlet expectation values. The complete operator derivations for $k = 1, 2$ and the explicit form used for $k = 3$ are reported in App. G.

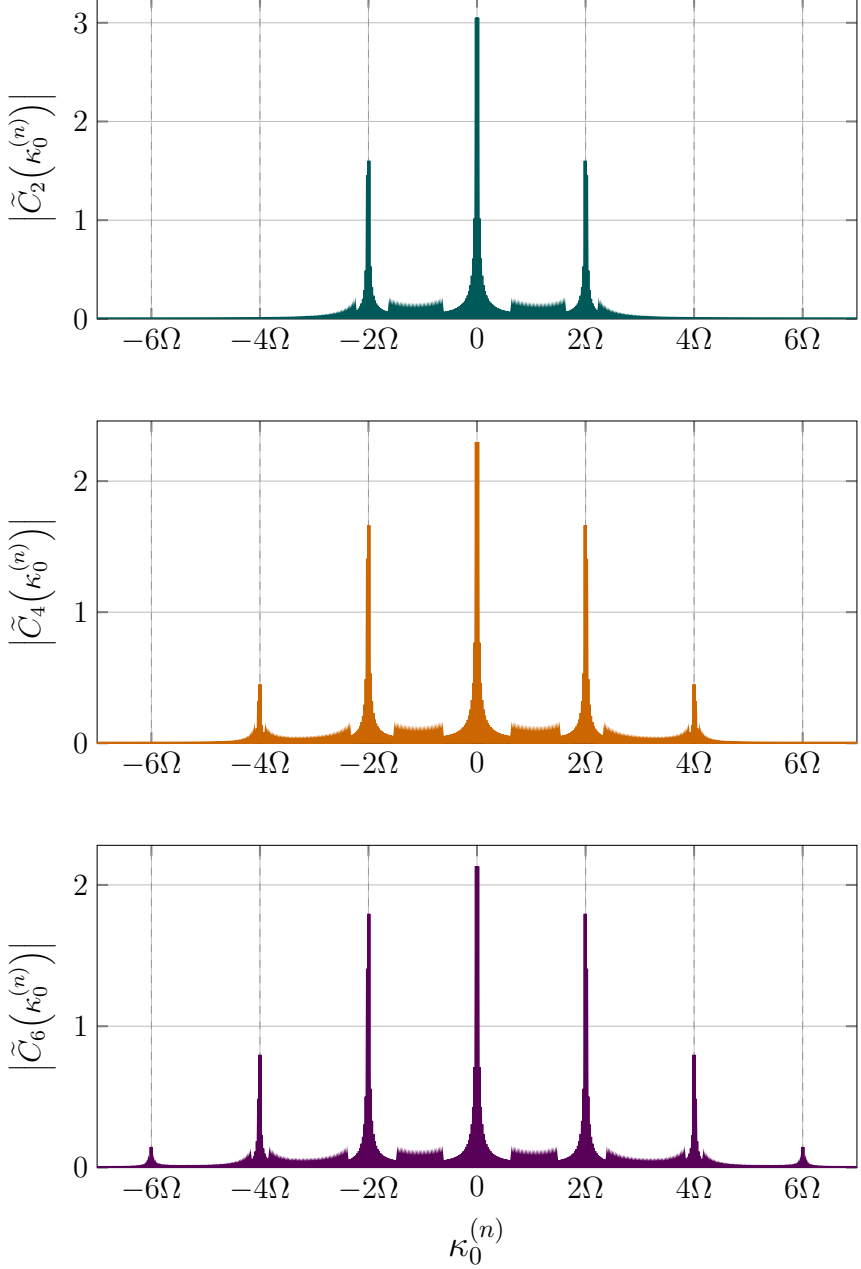


Figure 7. Absolute value of the discrete transform $|\tilde{C}_{2k}(\kappa_0^{(n)})|$ of the Dirichlet expectation values $\langle q^{2k}(\ell) \rangle_{\text{D.B.}(T)}$ for $2k = 2, 4, 6$ (from top to bottom). In each panel sharp peaks appear at a finite set of positive Dirichlet frequencies $\kappa_0^{(n)}$ clustered around integer multiples of 2Ω , as indicated on the horizontal axis. The peak structure matches the analytic predictions for the harmonic oscillator and demonstrates the discrete spectrum of $\langle q^{2k}(\ell) \rangle_{\text{D.B.}(T)}$ arising from the tower of excited states.

7 Conclusions

In this paper we have presented a new functional approach to quantum field theory and quantum mechanics which we called *constrained symplectic quantization*. A previous but

less powerful realization of the symplectic quantization approach was presented in [2–4] and numerically tested in [1]. This first formulation of the theory had two major limitations: it was by construction ill-defined in the free case and, most importantly, its correlation functions were not equivalent to those generated by the Feynman path integral. This notwithstanding, the numerical results of [1] were quite encouraging: they brought us the evidence that symplectic quantization was capable of capturing the causal structure of $1+1$ dimensional space-time by reproducing qualitatively well the free Feynman propagator for a weakly-interacting scalar field theory, a result inaccessible within the Euclidean field theory formulation on the lattice.

In the present paper we have shown how the correct way to recover a perfect equivalence between symplectic quantization and quantum mechanics is to consider the analytic continuation of all the original fields and of the action from \mathbb{R} to \mathbb{C} , by also including specific constraints on the integration paths in \mathbb{C} which guarantee convergence of the symplectic quantization dynamics and of the corresponding microcanonical generating functional. From this perspective our method is close in spirit to the Lefschetz-Thimbles approach, which also entails analytic continuations to \mathbb{C} and constraints to stable manifolds. On the other hand, there are also remarkable differences, since the Lefschetz-Thimbles approach puts constraints directly on the functional integral measure while symplectic quantization puts the constraints on the microscopic deterministic dynamics which generates the measure itself. From this perspective, constrained symplectic quantization acts in a sense on a more fundamental level than the Lefschetz-Thimbles approach.

The first part of this work, namely Sections from 1 to 3, are devoted to a presentation of the formalism and the proof that the microcanonical partition function of constrained symplectic quantization generates in the continuum limit the same correlation functions of the Feynman path integral for a generic quantum mechanical system. The following Sections are devoted specifically to the case of the quantum harmonic oscillator, with the main numerical results presented in Sec. 6. We focused our attention to observables which are inaccessible within the standard Euclidean formulation of quantum mechanics, usually considered for numerical lattice simulations. In particular, the ability to perfectly reproduce the oscillating shape of the two-point correlation function $\langle q(x_0)q(x'_0) \rangle$, and the measurement of the discrete energy spectrum in Fourier space from the expectation values of even powers of the position operator $\langle q^{2k}(x_0) \rangle$, provide evidence of the presence in the dynamics of the excited state of the harmonic oscillator. Moreover, they clearly establish that constrained symplectic quantization reproduces numerically the predictions of quantum mechanics for the harmonic oscillator.

All these results suggest that the constrained symplectic quantization approach might establish itself as a new robust method to real-time non-perturbative numerical field theory and numerical quantum mechanics, overcoming the sign problem which plagues the real-time representation on the lattice of quantum mechanics and quantum field theory. In this direction, there is a companion paper on numerical test for a free scalar field theory that will appear soon [30], and a paper devoted to the anharmonic oscillator which is in

preparation [31].

Acknowledgments

We thank R. Livi and L. Salasnich for useful discussions. G.G. acknowledges partial support from the project MIUR-PRIN2022, "Emergent Dynamical Patterns of Disordered Systems with Applications to Natural Communities", code 2022WPHMXK.

Appendix

A Asymptotic properties of the coefficients $c_j(M, n)$

In this Appendix we analyze the asymptotic behavior of $c_j(M, n)$ defined in Eq. (3.21)

$$c_j(M, n) = \left(\frac{2}{\hbar}\right)^j \sum_{k=0}^j \binom{M-n}{k} \frac{1}{(j-k)!} \frac{(-1)^k}{M^k}, \quad (\text{A.1})$$

by expanding their expression in powers of $\frac{1}{M}$. If the constant term (order M^0) vanishes, the leading behavior is at least $\mathcal{O}(1/M)$. Consider the term involving the binomial coefficient

$$T_k(M) = \binom{M-n}{k} \frac{1}{M^k}. \quad (\text{A.2})$$

Expanding the binomial coefficient definition

$$\begin{aligned} T_k(M) &= \frac{(M-n)(M-n-1)\cdots(M-n-k+1)}{k! M^k} \\ &= \frac{1}{k!} \prod_{i=0}^{k-1} \left(\frac{M-(n+i)}{M} \right) \\ &= \frac{1}{k!} \prod_{i=0}^{k-1} \left(1 - \frac{n+i}{M} \right). \end{aligned} \quad (\text{A.3})$$

For large M , we expand the product using $\prod(1-\epsilon) \approx 1-\epsilon$:

$$\prod_{i=0}^{k-1} \left(1 - \frac{n+i}{M} \right) = 1 - \frac{1}{M} \sum_{i=0}^{k-1} (n+i) + \mathcal{O}\left(\frac{1}{M^2}\right). \quad (\text{A.4})$$

The sum in the linear term is an arithmetic progression

$$\sum_{i=0}^{k-1} (n+i) = nk + \sum_{i=0}^{k-1} i = nk + \frac{k(k-1)}{2}. \quad (\text{A.5})$$

Thus, the expansion for $T_k(M)$ is

$$T_k(M) = \frac{1}{k!} - \frac{1}{M k!} \left(nk + \frac{k(k-1)}{2} \right) + \mathcal{O}\left(\frac{1}{M^2}\right). \quad (\text{A.6})$$

Substitute the expansion of $T_k(M)$ back into the definition of $c_j(M, n)$

$$\begin{aligned} c_j(M, n) &= \left(\frac{2}{\hbar}\right)^j \sum_{k=0}^j \frac{(-1)^k}{(j-k)!} T_k(M) \\ &= \left(\frac{2}{\hbar}\right)^j \sum_{k=0}^j \frac{(-1)^k}{(j-k)!} \left[\frac{1}{k!} - \frac{1}{M k!} \left(nk + \frac{k(k-1)}{2} \right) + \dots \right]. \end{aligned} \quad (\text{A.7})$$

We can group terms by powers of $\frac{1}{M}$

$$c_j(M, n) = A_0 + \frac{A_1}{M} + \mathcal{O}\left(\frac{1}{M^2}\right). \quad (\text{A.8})$$

we now show that $A_0 = 0$ for all $j \geq 1$. The coefficient of order M^0 is

$$A_0 = \left(\frac{2}{\hbar}\right)^j \sum_{k=0}^j \frac{(-1)^k}{(j-k)! k!}. \quad (\text{A.9})$$

Multiplying and dividing by $j!$ allows us to express this in terms of binomial coefficients $\binom{j}{k}$

$$A_0 = \frac{1}{j!} \left(\frac{2}{\hbar}\right)^j \sum_{k=0}^j (-1)^k \frac{j!}{k!(j-k)!} = \frac{1}{j!} \left(\frac{2}{\hbar}\right)^j \sum_{k=0}^j \binom{j}{k} (-1)^k. \quad (\text{A.10})$$

By the binomial theorem, $\sum_{k=0}^j \binom{j}{k} (-1)^k = (1-1)^j = 0$ for $j \geq 1$. Therefore

$$A_0 = 0 \quad \forall j \geq 1. \quad (\text{A.11})$$

Since $A_0 = 0$, the series starts at order $\frac{1}{M}$. The coefficient A_1 is given by

$$A_1 = -\frac{1}{j!} \left(\frac{2}{\hbar}\right)^j \sum_{k=0}^j (-1)^k \binom{j}{k} \left(nk + \frac{k(k-1)}{2}\right). \quad (\text{A.12})$$

Let $Q(k) = nk + \frac{k(k-1)}{2}$. This is a polynomial in k of degree 2.

Let $P(x)$ be any function defined on the integers. We define the Shift Operator E and the Identity Operator I by

$$EP(x) = P(x+1), \quad IP(x) = P(x). \quad (\text{A.13})$$

The Forward Difference Operator Δ is defined as

$$\Delta P(x) = P(x+1) - P(x) = (E - I)P(x). \quad (\text{A.14})$$

To find the j -th finite difference $\Delta^j P(0)$, we expand the operator $(E - I)^j$ using the binomial theorem

$$\begin{aligned} \Delta^j P(0) &= (E - I)^j P(0) \\ &= \sum_{k=0}^j \binom{j}{k} E^k (-1)^{j-k} P(0) \\ &= \sum_{k=0}^j \binom{j}{k} (-1)^{j-k} P(k). \end{aligned} \quad (\text{A.15})$$

Factoring out $(-1)^j$ and noting that $(-1)^{-k} = (-1)^k$

$$\Delta^j P(0) = (-1)^j \sum_{k=0}^j (-1)^k \binom{j}{k} P(k). \quad (\text{A.16})$$

Multiplying both sides by $(-1)^j$ (since $(-1)^{2j} = 1$) gives the identity

$$\sum_{k=0}^j (-1)^k \binom{j}{k} P(k) = (-1)^j \Delta^j P(0). \quad (\text{A.17})$$

Now, if $P(x) = c_d x^d + \dots$ is a polynomial of degree d , then $\Delta P(x)$ is a polynomial of degree $d-1$

$$\begin{aligned} \Delta P(x) &= c_d(x+1)^d + \dots - (c_d x^d + \dots) \\ &= c_d(x^d + dx^{d-1} + \dots) - c_d x^d + \dots \\ &= c_d dx^{d-1} + \mathcal{O}(x^{d-2}), \end{aligned} \quad (\text{A.18})$$

where the x^d term cancels, reducing the degree by exactly 1. By induction, applying Δ exactly j times reduces the degree by j . So, if $j = d$, $\Delta^j P(x)$ is a non-zero constant ($c_d \cdot d!$), while if $j > d$, $\Delta^j P(x) = 0$. Combining this with Eq. (A.17), we obtain the vanishing condition

$$\sum_{k=0}^j (-1)^k \binom{j}{k} P(k) = 0 \quad \text{if } j > \deg(P). \quad (\text{A.19})$$

The sum A_1 therefore represents the j -th finite difference of $Q(k)$ evaluated at 0

$$\sum_{k=0}^j (-1)^k \binom{j}{k} Q(k) = (-1)^j \Delta^j Q(0). \quad (\text{A.20})$$

Since $\Delta^j Q(k) = 0$ if $j > \deg(Q)$. Then, if $j = 1, 2$, then $j \leq \deg(Q) = 2$, so $A_1 \neq 0$. The order is exactly $\frac{1}{M}$. Otherwise, if $j > 2$, then $j > \deg(Q)$, so $A_1 = 0$. The order is $\mathcal{O}\left(\frac{1}{M^2}\right)$ or smaller. Since the constant term A_0 is identically zero for all $j \geq 1$, the leading non-zero term is of order at least $\frac{1}{M}$. Thus

$$c_j(M, n) = \mathcal{O}\left(\frac{1}{M}\right). \quad (\text{A.21})$$

B Two-point function on a periodic domain (continuum and discrete)

In this Appendix, we derive the harmonic-oscillator two-point function with *periodic* boundary conditions, in two ways. We first use the spectral representation and we then present the lattice derivation on a periodic time lattice, which matches the continuum result in the $a \rightarrow 0$ limit at fixed $T = Ma$.

B.1 Continuum derivation from the tower of eigenstates

We consider the harmonic oscillator Hamiltonian

$$\hat{H} = \frac{\hat{p}^2}{2m} + \frac{m\Omega^2}{2} \hat{q}^2, \quad E_n = \hbar\Omega\left(n + \frac{1}{2}\right), \quad \hat{H}|\psi_n\rangle = E_n|\psi_n\rangle, \quad n = 0, 1, 2, \dots \quad (\text{B.1})$$

and the Heisenberg operator $\hat{q}(x_0) = e^{\frac{i}{\hbar} \hat{H} x_0} \hat{q} e^{-\frac{i}{\hbar} \hat{H} x_0}$. Periodic boundary conditions in time of length T correspond to the trace:

$$Z_{\text{P.B.}}(T) \equiv \text{Tr}\left(e^{-\frac{i}{\hbar} \hat{H} T}\right), \quad \langle \hat{q}(x_0) \hat{q}(x'_0) \rangle_{\text{P.B.}} \equiv \frac{1}{Z_{\text{P.B.}}(T)} \text{Tr}\left(e^{-\frac{i}{\hbar} \hat{H} T} \hat{q}(x_0) \hat{q}(x'_0)\right). \quad (\text{B.2})$$

Using time-translation invariance on the circle, the correlator depends only on $\Delta \equiv x_0 - x'_0$ modulo T . Choose the representative $\Delta \in [0, T]$ and rewrite

$$\langle \hat{q}(x_0) \hat{q}(x'_0) \rangle_{\text{P.B.}} = \frac{1}{Z_{\text{P.B.}}(T)} \text{Tr}\left(e^{-\frac{i}{\hbar} \hat{H}(T-\Delta)} \hat{q} e^{-\frac{i}{\hbar} \hat{H}\Delta} \hat{q}\right). \quad (\text{B.3})$$

We then insert the identity $\mathbb{I} = \sum_{n=0}^{\infty} |\psi_n\rangle \langle \psi_n|$ twice into Eq. (B.3):

$$\langle \hat{q}(x_0) \hat{q}(x'_0) \rangle_{\text{P.B.}} = \frac{1}{Z_{\text{P.B.}}(T)} \sum_{n,m=0}^{\infty} e^{-\frac{i}{\hbar} E_n(T-\Delta)} e^{-\frac{i}{\hbar} E_m \Delta} \langle \psi_n | \hat{q} | \psi_m \rangle \langle \psi_m | \hat{q} | \psi_n \rangle. \quad (\text{B.4})$$

The *coefficients* entering the sum are the matrix elements of \hat{q} . By introducing ladder operators

$$\hat{a} = \sqrt{\frac{m\Omega}{2\hbar}} \hat{q} + \frac{i}{\sqrt{2m\hbar\Omega}} \hat{p}, \quad \hat{a}^\dagger = \sqrt{\frac{m\Omega}{2\hbar}} \hat{q} - \frac{i}{\sqrt{2m\hbar\Omega}} \hat{p}, \quad \hat{q} = \sqrt{\frac{\hbar}{2m\Omega}} (\hat{a} + \hat{a}^\dagger), \quad (\text{B.5})$$

with actions $\hat{a}|\psi_n\rangle = \sqrt{n}|\psi_{n-1}\rangle$ and $\hat{a}^\dagger|\psi_n\rangle = \sqrt{n+1}|\psi_{n+1}\rangle$ we obtain

$$\langle \psi_n | \hat{q} | \psi_m \rangle = \sqrt{\frac{\hbar}{2m\Omega}} \left(\sqrt{m+1} \delta_{n,m+1} + \sqrt{m} \delta_{n,m-1} \right), \quad (\text{B.6})$$

and hence the squared coefficients in Eq. (B.4) are

$$\langle \psi_n | \hat{q} | \psi_m \rangle \langle \psi_m | \hat{q} | \psi_n \rangle = \frac{\hbar}{2m\Omega} \left[(m+1) \delta_{n,m+1} + m \delta_{n,m-1} \right]. \quad (\text{B.7})$$

Plugging Eq. (B.7) into Eq. (B.4) collapses the double sum to a single sum:

$$\langle \hat{q}(x_0) \hat{q}(x'_0) \rangle_{\text{P.B.}} = \frac{\hbar}{2m\Omega} \frac{1}{Z_{\text{P.B.}}(T)} \sum_{m=0}^{\infty} \left[(m+1) e^{-\frac{i}{\hbar} E_{m+1}(T-\Delta)} e^{-\frac{i}{\hbar} E_m \Delta} + m e^{-\frac{i}{\hbar} E_{m-1}(T-\Delta)} e^{-\frac{i}{\hbar} E_m \Delta} \right]. \quad (\text{B.8})$$

Using $E_{m\pm 1} = E_m \pm \hbar\Omega$, we factor out the Δ -dependence:

$$e^{-\frac{i}{\hbar} E_{m+1}(T-\Delta)} e^{-\frac{i}{\hbar} E_m \Delta} = e^{-\frac{i}{\hbar} E_m T} e^{-i\Omega(T-\Delta)} = e^{-\frac{i}{\hbar} E_m T} e^{-i\Omega T} e^{+i\Omega\Delta}, \quad (\text{B.9})$$

$$e^{-\frac{i}{\hbar} E_{m-1}(T-\Delta)} e^{-\frac{i}{\hbar} E_m \Delta} = e^{-\frac{i}{\hbar} E_m T} e^{+i\Omega(T-\Delta)} = e^{-\frac{i}{\hbar} E_m T} e^{+i\Omega T} e^{-i\Omega\Delta}. \quad (\text{B.10})$$

Define the convenient parameter

$$x \equiv e^{-i\Omega T}, \quad \Rightarrow \quad e^{-\frac{i}{\hbar} E_m T} = e^{-i\Omega T/2} x^m. \quad (\text{B.11})$$

Then Eq. (B.8) becomes

$$\langle \hat{q}(x_0) \hat{q}(x'_0) \rangle_{\text{P.B.}} = \frac{\hbar}{2m\Omega} \frac{e^{-i\Omega T/2}}{Z_{\text{P.B.}}(T)} \left[x e^{+i\Omega\Delta} \sum_{m=0}^{\infty} (m+1) x^m + x^{-1} e^{-i\Omega\Delta} \sum_{m=0}^{\infty} m x^m \right]. \quad (\text{B.12})$$

The needed geometric sums are

$$\sum_{m=0}^{\infty} x^m = \frac{1}{1-x}, \quad \sum_{m=0}^{\infty} (m+1)x^m = \frac{1}{(1-x)^2}, \quad \sum_{m=0}^{\infty} mx^m = \frac{x}{(1-x)^2}. \quad (\text{B.13})$$

The partition function is

$$Z_{\text{P.B.}}(T) = \sum_{m=0}^{\infty} e^{-\frac{i}{\hbar} E_m T} = e^{-i\Omega T/2} \sum_{m=0}^{\infty} x^m = \frac{e^{-i\Omega T/2}}{1-x}. \quad (\text{B.14})$$

Combining Eqs. (B.12)–(B.14) finally gives

$$\langle \hat{q}(x_0) \hat{q}(x'_0) \rangle_{\text{P.B.}} = \frac{\hbar}{2m\Omega} \frac{x e^{+i\Omega\Delta} + e^{-i\Omega\Delta}}{1-x} = \frac{\hbar}{2m\Omega} \frac{e^{-i\Omega\Delta} + e^{-i\Omega(T-\Delta)}}{1 - e^{-i\Omega T}}, \quad \Delta \in [0, T]. \quad (\text{B.15})$$

This is the continuum periodic two-point function that can be rewritten in the trigonometric form

$$\langle \hat{q}(x_0) \hat{q}(x'_0) \rangle_{\text{P.B.}} = -\frac{i\hbar}{2m\Omega} \frac{\sin(\Omega\Delta) + \sin(\Omega(T-\Delta))}{1 - \cos(\Omega T)} \quad \Delta \in [0, T]. \quad (\text{B.16})$$

which is the direct continuum analogue of the lattice formula obtained below.

B.2 Periodic lattice derivation (discrete Fourier modes)

Here we illustrate explicitly the steps needed to compute the harmonic oscillator two-point function on a discretized coordinate-time lattice with periodic boundary conditions. We consider a periodic lattice with M points, so that with periodic boundary conditions we have $q(0) = q(M-1)$. Let us start by the definition of the discretized action

$$S[q(\ell)] = \frac{ma}{2} \sum_{\ell=0}^{M-1} \left[\left(\frac{q(\ell+1) - q(\ell)}{a} \right)^2 - \Omega^2 q^2(\ell) \right]. \quad (\text{B.17})$$

We introduce the Fourier representation of the position field

$$q(\ell) = \frac{1}{\sqrt{M}} \sum_{r=0}^{M-1} \hat{q}(r) e^{ik_0(r)\ell a}, \quad (\text{B.18})$$

where $r \in \mathbb{N}$, one can rewrite the lattice action as

$$S[q(\ell)] = -\frac{1}{2} \sum_{r=0}^{M-1} \omega^2(r) |\hat{q}(r)|^2, \quad (\text{B.19})$$

where

$$\omega^2(r) = ma \left[\Omega^2 - \frac{4}{a^2} \sin^2 \left(\frac{k_0(r)a}{2} \right) \right], \quad (\text{B.20})$$

and where the conjugate momentum $k_0(r)$ takes the discrete values:

$$k_0(r) = \frac{2\pi r}{Ma}. \quad (\text{B.21})$$

The two point correlation function on the periodic lattice takes therefore the following form:

$$\langle q(\ell)q(\ell') \rangle = -\frac{i}{M} \sum_{r=0}^{M-1} \frac{e^{ik_0(r)(\ell-\ell')a}}{\omega^2(r)} \quad (\text{B.22})$$

$$= \frac{i}{Mma} \sum_{r=0}^{M-1} \frac{e^{ik_0(r)(\ell-\ell')a}}{\left[\frac{4}{a^2} \sin^2 \left(\frac{k_0(r)a}{2} \right) - \Omega^2 \right]} \quad (\text{B.23})$$

$$= \frac{ia}{Mm} \sum_{r=0}^{M-1} \frac{e^{i\frac{2\pi r}{N}(\ell-\ell')}}{\left[4 \sin^2 \left(\frac{\pi r}{M} \right) - a^2 \Omega^2 \right]}. \quad (\text{B.24})$$

$$(\text{B.25})$$

In order to simplify the notation we find convenient to exploit the following identifications

$$s = \ell - \ell' \quad (\text{B.26})$$

$$C(s) = \langle q(\ell)q(\ell') \rangle \quad (\text{B.26})$$

$$\mu = 2 - a^2 \Omega^2 \quad (\text{B.27})$$

$$\theta_r = \frac{2\pi}{M} r = k_0(r)a \quad (\text{B.28})$$

$$4 \sin^2 \left(\frac{\theta_r}{2} \right) = 2 - 2 \cos(\theta_r) \quad (\text{B.29})$$

which allow us to rewrite the expression of the correlator in Eq. (B.25) as

$$C(s) = \frac{ia}{Mm} \sum_{r=0}^{M-1} \frac{e^{i\theta_r s}}{\mu - 2 \cos(\theta_r)}. \quad (\text{B.30})$$

By further introducing the coordinate $z_r = e^{i\theta_r}$ on the unitary circle in the complex plane we get

$$\begin{aligned} C(s) &= \frac{ia}{Mm} \sum_{r=0}^{M-1} \frac{z_r^s}{\mu - (z_r + z_r^{-1})} \\ &= -\frac{ia}{Mm} \sum_{r=0}^{M-1} \frac{z_r^{s+1}}{z_r^2 - \mu z_r + 1} \\ &= -\frac{ia}{Mm} \sum_{r=0}^{M-1} \frac{z_r^{s+1}}{(z_r - z_1)(z_r - z_2)} \end{aligned} \quad (\text{B.31})$$

where in the last line of Eq. (B.31) we have that $z_{(1,2)}$ are the two roots of the equation $z_r^2 - \mu z_r + 1 = 0$, namely:

$$z_{(1,2)} = \exp(\pm i\kappa a) \quad \left(\kappa \mid \cos(\kappa a) = \frac{\mu}{2} \right). \quad (\text{B.32})$$

The above expression for $z_{(1,2)}$ assumes that $\left| 1 - \frac{a^2 \Omega^2}{2} \right| \leq 1$, a constraint which can be always fulfilled by choosing, for any given natural frequency Ω of the quantum harmonic

oscillator, the spacing a of the coordinate time lattice such as

$$a < \frac{2}{\Omega}. \quad (\text{B.33})$$

The summation in the last line of Eq. (B.31) can be then rewritten as

$$\sum_{r=0}^{M-1} \frac{z_r^{s+1}}{(z_r - z_1)(z_r - z_2)} = \frac{1}{z_1 - z_2} \sum_{r=0}^{M-1} z_r^{s+1} \left(\frac{1}{z_r - z_1} - \frac{1}{z_r - z_2} \right). \quad (\text{B.34})$$

By letting the summation over r act independently on the two terms in parentheses of Eq. (B.34) one can exploit for each of the two the following mathematical identity:

$$\begin{aligned} \sum_{r=0}^{M-1} \frac{z_r^{s+1}}{z_r - u} &= \sum_{r=0}^{M-1} \frac{e^{i\theta_r(s+1)}}{e^{i\theta_r} - u} \\ &= \sum_{r=0}^{M-1} \frac{e^{i\frac{2\pi r}{M}(s+1)}}{e^{i\frac{2\pi r}{M}} - u} \\ &= \frac{Mu^s}{1 - u^M}, \end{aligned} \quad (\text{B.35})$$

which holds for s integer. Therefore, one gets:

$$\begin{aligned} C(s) &= -\frac{a}{Mm} \frac{i}{z_1 - z_2} \left[\frac{Mz_1^s}{1 - z_1^M} - \frac{Nz_2^s}{1 - z_2^M} \right] \\ &= -\frac{a}{m} \frac{i}{e^{i\kappa a} - e^{-i\kappa a}} \left[\frac{e^{i\kappa as}}{1 - e^{i\kappa aM}} - \frac{e^{-i\kappa as}}{1 - e^{-i\kappa aM}} \right] \\ &= -\frac{a}{2m} \frac{i}{\sin(\kappa a)} \frac{\sin(\kappa as) + \sin(\kappa a(M-s))}{1 - \cos(\kappa aM)}. \end{aligned} \quad (\text{B.36})$$

By going back to the previous notation we have the discrete formula for the two point correlation function

$$\langle q(\ell)q(\ell') \rangle = -\frac{a}{2m} \frac{i}{\sin(\kappa a)} \frac{\sin[\kappa a(\ell - \ell')] + \sin[\kappa a(M - (\ell - \ell'))]}{1 - \cos[\kappa aM]}, \quad (\text{B.37})$$

which, as shown in the main text, is perfectly matched by our numerical calculations.

C Lattice functional derivation of the commutator identity

We derive here the lattice identity used in Sec. 6.3 to reconstruct the equal-time commutator from periodic (trace) expectation values. We consider a discretized Minkowskian time lattice with spacing $a = T/M$ and lattice sites labeled by $\ell = 0, \dots, M-1$, with $x_0^{(\ell)} = x_0^i + \ell a$ and periodic boundary conditions (P.B.) $q(M) \equiv q(0)$. The trace partition function reads

$$\mathcal{Z}_{\text{P.B.}}(\hbar) = \int_{\text{P.B.}} \prod_{\ell=0}^{M-1} dq(\ell) \exp\left(\frac{i}{\hbar} S[q]\right), \quad (\text{C.1})$$

with discretized action $S[q]$. For any differentiable function $F(\{q(\ell)\})$ of the lattice variables, the integral of a total derivative yields the lattice Schwinger–Dyson identity (see [29])

$$\langle \partial_{q(\ell)} F \rangle_{\text{P.B.}} = -\frac{i}{\hbar} \langle F \partial_{q(\ell)} S \rangle_{\text{P.B.}}. \quad (\text{C.2})$$

For the harmonic lattice action used in the main text one has

$$S[q] = \frac{ma}{2} \sum_{\ell=0}^{M-1} \left[\left(\frac{q(\ell+1) - q(\ell)}{a} \right)^2 - \Omega^2 q^2(\ell) \right], \quad q(M) \equiv q(0), \quad (\text{C.3})$$

from which

$$\partial_{q(\ell)} S[q] = \frac{m}{a} (q(\ell) - q(\ell+1)) - \frac{m}{a} (q(\ell-1) - q(\ell)) - a V'(q(\ell)), \quad V(q) = \frac{1}{2} m \Omega^2 q^2. \quad (\text{C.4})$$

Introducing the standard link momenta (defined at half-integer time-slices),

$$p\left(\ell + \frac{1}{2}\right) \equiv \frac{m}{a} (q(\ell) - q(\ell+1)), \quad p\left(\ell - \frac{1}{2}\right) \equiv \frac{m}{a} (q(\ell-1) - q(\ell)), \quad (\text{C.5})$$

Eq. (C.4) becomes

$$\partial_{q(\ell)} S[q] = p\left(\ell + \frac{1}{2}\right) - p\left(\ell - \frac{1}{2}\right) - a V'(q(\ell)). \quad (\text{C.6})$$

Choosing $F = q(\ell)$ in (C.2) we obtain

$$\langle q(\ell) p\left(\ell + \frac{1}{2}\right) \rangle_{\text{P.B.}} - \langle q(\ell) p\left(\ell - \frac{1}{2}\right) \rangle_{\text{P.B.}} - a \langle q(\ell) V'(q(\ell)) \rangle_{\text{P.B.}} = i\hbar. \quad (\text{C.7})$$

For smooth potentials the last term is an $O(a)$ lattice artifact in the continuum limit, so that

$$\langle q(\ell) p\left(\ell + \frac{1}{2}\right) \rangle_{\text{P.B.}} - \langle q(\ell) p\left(\ell - \frac{1}{2}\right) \rangle_{\text{P.B.}} = i\hbar + O(a). \quad (\text{C.8})$$

Using the definitions (C.5) this can be rewritten entirely in terms of q -correlators,

$$\begin{aligned} \langle q(\ell) p\left(\ell + \frac{1}{2}\right) \rangle_{\text{P.B.}} - \langle q(\ell) p\left(\ell - \frac{1}{2}\right) \rangle_{\text{P.B.}} &= \frac{m}{a} \langle q(\ell)(q(\ell) - q(\ell+1)) - q(\ell)(q(\ell-1) - q(\ell)) \rangle_{\text{P.B.}} \\ &= \frac{m}{a} \langle 2q^2(\ell) - q(\ell)q(\ell+1) - q(\ell)q(\ell-1) \rangle_{\text{P.B.}}. \end{aligned} \quad (\text{C.9})$$

Combining (C.9) with (C.8) yields the lattice representation used in the main text,

$$-i \frac{m}{a} \langle 2q^2(\ell) - q(\ell)q(\ell+1) - q(\ell)q(\ell-1) \rangle_{\text{P.B.}} = \hbar + O(a), \quad (\text{C.10})$$

which is the periodic (trace) expectation value of the equal-time commutator written in a form directly comparable with the constrained symplectic quantization measurements.

D Dirichlet modes and diagonalisation of the quadratic action

In this Appendix we collect the Dirichlet-mode decomposition of the holomorphic harmonic-oscillator action and show explicitly that, upon imposing the stable-manifold constraints, the functional measure factorises mode by mode exactly as in the periodic case. This provides the Dirichlet analogue of Eq. (4.31) and yields a mode-by-mode correspondence between constrained (analytically continued) averages and ordinary quantum-mechanical correlators.

Consider the (Minkowskian) quadratic action on the interval $[x_0^i, x_0^f]$,

$$S[q] \equiv \frac{m}{2} \int_{x_0^i}^{x_0^f} dx_0 \left[(\partial_0 q(x_0))^2 - \Omega^2 q(x_0)^2 \right], \quad (\text{D.1})$$

with Dirichlet boundary conditions $q(x_0^i) = q(x_0^f) = 0$. For Dirichlet boundaries it is convenient to expand in the sine basis (cf. Eq. (6.51)),

$$q(x_0) = \sum_{n=1}^{\infty} \tilde{q}(n) \sqrt{\frac{2}{T}} \sin\left(\kappa_0^{(n)}(x_0 - x_0^i)\right), \quad \kappa_0^{(n)} \equiv \frac{\pi n}{T}, \quad T \equiv x_0^f - x_0^i. \quad (\text{D.2})$$

The orthonormality relation

$$\frac{2}{T} \int_{x_0^i}^{x_0^f} dx_0 \sin\left(\kappa_0^{(n)}(x_0 - x_0^i)\right) \sin\left(\kappa_0^{(n')}(x_0 - x_0^i)\right) = \delta_{n,n'} \quad (\text{D.3})$$

implies the inversion formula

$$\tilde{q}(n) = \sqrt{\frac{2}{T}} \int_{x_0^i}^{x_0^f} dx_0 q(x_0) \sin\left(\kappa_0^{(n)}(x_0 - x_0^i)\right). \quad (\text{D.4})$$

In the constrained formulation $q(x_0) \in \mathbb{C}$ is holomorphic, so we write $\tilde{q}(n) = \tilde{q}_R(n) + i \tilde{q}_I(n)$ with $\tilde{q}_{R,I}(n) \in \mathbb{R}$.

Using Eq. (D.2) and orthonormality one obtains

$$\int_{x_0^i}^{x_0^f} dx_0 q(x_0)^2 = \sum_{n=1}^{\infty} \tilde{q}(n)^2, \quad \int_{x_0^i}^{x_0^f} dx_0 (\partial_0 q(x_0))^2 = \sum_{n=1}^{\infty} (\kappa_0^{(n)})^2 \tilde{q}(n)^2, \quad (\text{D.5})$$

so the action diagonalises mode by mode as

$$S[q] = \frac{m}{2} \sum_{n=1}^{\infty} ((\kappa_0^{(n)})^2 - \Omega^2) \tilde{q}(n)^2 = -\frac{1}{2} \sum_{n=1}^{\infty} \omega_n^2 \tilde{q}(n)^2, \quad (\text{D.6})$$

where it is convenient to introduce

$$\omega_n^2 \equiv m(\Omega^2 - (\kappa_0^{(n)})^2). \quad (\text{D.7})$$

Note that ω_n^2 can be positive or negative depending on whether $(\kappa_0^{(n)})^2$ is smaller or larger than Ω^2 .

For later use we also write Eq. (D.6) in terms of real and imaginary Dirichlet modes:

$$S[q] = -\frac{1}{2} \sum_{n=1}^{\infty} \omega_n^2 \left[\tilde{q}_R(n)^2 - \tilde{q}_I(n)^2 + 2i \tilde{q}_R(n) \tilde{q}_I(n) \right]. \quad (\text{D.8})$$

The constrained symplectic quantization prescription fixes, mode by mode, the integration contour in the complex $\tilde{q}(n)$ plane so that $\exp\left(\frac{i}{\hbar} S\right)$ is exponentially damped. Equivalently, one imposes the same linear relations between $\tilde{q}_R(n)$ and $\tilde{q}_I(n)$ as in the periodic case:

$$\omega_n^2 > 0 : \quad \tilde{q}_I(n) = -\tilde{q}_R(n), \quad \omega_n^2 < 0 : \quad \tilde{q}_I(n) = +\tilde{q}_R(n). \quad (\text{D.9})$$

(Geometrically, these relations correspond to a $\pm\pi/4$ rotation of the contour for each mode; the sign is chosen so that the holomorphic quadratic form produces a negative real exponent in $\exp\left(\frac{i}{\hbar} S\right)$.)

Substituting Eq. (D.9) into Eq. (D.8) yields

$$S[q] = i \sum_{\{n \mid \omega_n^2 > 0\}} \omega_n^2 \tilde{q}_R(n)^2 - i \sum_{\{n \mid \omega_n^2 < 0\}} \omega_n^2 \tilde{q}_R(n)^2. \quad (\text{D.10})$$

Therefore the holomorphic weight factorises as a product of independent Gaussians in the real constrained modes. The explicit Dirichlet analogue of Eq. (4.31) is

$$\exp\left(\frac{i}{\hbar} S[q]\right) = \exp\left[-\frac{1}{\hbar} \sum_{\{n \mid \omega_n^2 > 0\}} \omega_n^2 \tilde{q}_R(n)^2 + \frac{1}{\hbar} \sum_{\{n \mid \omega_n^2 < 0\}} \omega_n^2 \tilde{q}_R(n)^2\right], \quad (\text{D.11})$$

where the second term is negative because $\omega_n^2 < 0$ on that subset. Equivalently,

$$\exp\left(\frac{i}{\hbar} S[q]\right) = \exp\left[-\frac{1}{\hbar} \sum_{n=1}^{\infty} |\omega_n^2| \tilde{q}_R(n)^2\right], \quad (\text{D.12})$$

up to an overall (mode-independent) normalisation factor that is irrelevant for expectation values. Equations (D.11)–(D.12) show explicitly that the constrained measure factorises mode by mode, exactly as in the periodic case but with $n \geq 1$. As a consequence, all constrained mode correlators are diagonal in n and can be computed by elementary Gaussian integrals. In particular,

$$\langle \tilde{q}_R(n) \tilde{q}_R(n') \rangle_{\text{D.B.}(T)} = \delta_{n,n'} = \delta_{n,n'} \frac{\hbar}{2|\omega_n^2|}, \quad (\text{D.13})$$

and reconstructing the complex mode using the constraints Eq. (D.9) one finds the corresponding quantum-mechanical Dirichlet correlator in mode space,

$$\langle \tilde{q}(n) \tilde{q}(n') \rangle_{\text{D.B.}(T)} = \delta_{n,n'} \frac{i\hbar}{m((\kappa_0^{(n)})^2 - \Omega^2)} = -\delta_{n,n'} \frac{i\hbar}{\omega_n^2}, \quad (\text{D.14})$$

which is the standard harmonic-oscillator result in the Dirichlet sine basis. The corresponding coordinate-space expressions quoted in the main text follow by inserting Eq. (D.2) and summing over n .

E Continuum Dirichlet expression for $\langle \hat{q}^2(x_0) \rangle_{\text{D.B.}(T)}$

In this subsection we derive the closed-form expression for the Dirichlet “expectation value” of $\hat{q}^2(x_0)$ in the continuum Minkowskian theory for the Harmonic oscillator with action

$$S[q] = \int_0^T dx_0 \frac{m}{2} \left(\partial_{x_0} q^2(x_0) - \Omega^2 q^2(x_0) \right). \quad (\text{E.1})$$

We impose Dirichlet boundary conditions in the time interval $[0, T]$,

$$q(0) = 0, \quad q(T) = 0. \quad (\text{E.2})$$

The Dirichlet “expectation value” of $\hat{q}^2(x_0)$ is defined as in Eq. (6.54) with $k = 1$,

$$\langle \hat{q}^2(x_0) \rangle_{\text{D.B.}(T)} \equiv \frac{\langle q_f = 0, x_0^f = T \mid \hat{q}^2(x_0) \mid q_i = 0, x_0^i = 0 \rangle}{\langle q_f = 0, x_0^f = T \mid q_i = 0, x_0^i = 0 \rangle}, \quad 0 < x_0 < T. \quad (\text{E.3})$$

For a quadratic action of the form (E.1) the path-integral with Dirichlet boundary conditions can be written as

$$\mathcal{Z}[J] = \int_{q(0)=0}^{q(T)=0} \mathcal{D}q \exp \left\{ \frac{i}{\hbar} S[q] + \frac{i}{\hbar} \int_0^T dx_0 J(x_0) q(x_0) \right\}, \quad (\text{E.4})$$

where $J(x_0)$ is an external source. By integrating by parts in Eq. (E.1) and using the boundary conditions (E.2), the action can be cast in the quadratic form

$$S[q] = \frac{m}{2} \int_0^T dx_0 q(x_0) \left(-\partial_{x_0}^2 - \Omega^2 \right) q(x_0). \quad (\text{E.5})$$

Thus the quadratic kernel appearing in the exponent is

$$\mathcal{K}(x_0, x'_0) = m \left(-\partial_{x_0}^2 - \Omega^2 \right) \delta(x_0 - x'_0). \quad (\text{E.6})$$

For a Gaussian functional integral of the form above, the two-point function is given by the inverse of the kernel,

$$\langle q(x_0) q(x'_0) \rangle_{\text{D.B.}(T)} = i\hbar G(x_0, x'_0), \quad (\text{E.7})$$

where $G(x_0, x'_0)$ is the Green’s function satisfying

$$m \left(-\partial_{x_0}^2 - \Omega^2 \right) G(x_0, x'_0) = \delta(x_0 - x'_0), \quad (\text{E.8})$$

with Dirichlet boundary conditions

$$G(0, x'_0) = 0, \quad G(T, x'_0) = 0. \quad (\text{E.9})$$

We now solve Eq. (E.8) explicitly. For $x_0 \neq x'_0$ the Green’s function satisfies the homogeneous equation

$$\left(-\partial_{x_0}^2 - \Omega^2 \right) G(x_0, x'_0) = 0. \quad (\text{E.10})$$

The general solution of Eq. (E.10) is a linear combination of $\sin(\Omega x_0)$ and $\cos(\Omega x_0)$. Imposing the boundary conditions (E.9) separately on the intervals $0 < x_0 < x'_0$ and $x'_0 < x_0 < T$, we write

$$G(x_0, x'_0) = \begin{cases} A \sin(\Omega x_0), & 0 < x_0 < x'_0, \\ B \sin(\Omega(T - x_0)), & x'_0 < x_0 < T, \end{cases} \quad (\text{E.11})$$

where the Dirichlet boundary conditions at $x_0 = 0$ and $x_0 = T$ have already been used. Continuity of $G(x_0, x'_0)$ at $x_0 = x'_0$ implies

$$\begin{aligned} \lim_{x_0 \rightarrow x'_0^-} G(x_0, x'_0) &= \lim_{x_0 \rightarrow x'_0^+} G(x_0, x'_0) \\ \Rightarrow A \sin(\Omega x'_0) &= B \sin(\Omega(T - x'_0)). \end{aligned} \quad (\text{E.12})$$

On the other hand, integrating Eq. (E.8) over an infinitesimal interval around x'_0 , one obtains the usual jump condition on the first derivative,

$$\begin{aligned} \int_{x'_0 - \varepsilon}^{x'_0 + \varepsilon} dx_0 m \left(-\partial_{x_0}^2 - \Omega^2 \right) G(x_0, x'_0) &= \int_{x'_0 - \varepsilon}^{x'_0 + \varepsilon} dx_0 \delta(x_0 - x'_0) \\ \Rightarrow -m \frac{\partial G}{\partial x_0} \Big|_{x_0=x'_0^+} + m \frac{\partial G}{\partial x_0} \Big|_{x_0=x'_0^-} &= 1. \end{aligned} \quad (\text{E.13})$$

Using the explicit expressions in Eq. (E.11), this condition reads

$$-m[-B\Omega \cos(\Omega(T - x'_0))] + m[A\Omega \cos(\Omega x'_0)] = 1. \quad (\text{E.14})$$

Equations (E.12) and (E.14) form a linear system for A and B . Solving it, and using the trigonometric identity $\sin(\Omega T) = \sin(\Omega x'_0) \cos(\Omega(T - x'_0)) + \cos(\Omega x'_0) \sin(\Omega(T - x'_0))$, one finds

$$A = \frac{\sin(\Omega(T - x'_0))}{m\Omega \sin(\Omega T)}, \quad B = \frac{\sin(\Omega x'_0)}{m\Omega \sin(\Omega T)}. \quad (\text{E.15})$$

Therefore the Green's function can be written in the compact form

$$G(x_0, x'_0) = \frac{1}{m\Omega \sin(\Omega T)} \sin(\Omega x_0) \sin(\Omega(T - x_0)), \quad (\text{E.16})$$

where $x_< \equiv \min(x_0, x'_0)$ and $x_> \equiv \max(x_0, x'_0)$. Using Eq. (E.7), the Dirichlet two-point function for the quantum coordinate is

$$\langle q(x_0) q(x'_0) \rangle_{\text{D.B.}(T)} = \frac{i\hbar}{m\Omega \sin(\Omega T)} \sin(\Omega x_0) \sin(\Omega(T - x_0)). \quad (\text{E.17})$$

In particular, the continuum Dirichlet “expectation value” of $\hat{q}^2(x_0)$ is obtained by taking the equal-time limit $x'_0 \rightarrow x_0$,

$$\begin{aligned} \langle \hat{q}^2(x_0) \rangle_{\text{D.B.}(T)} &= \langle q(x_0) q(x_0) \rangle_{\text{D.B.}(T)} \\ &= \frac{i\hbar}{m\Omega \sin(\Omega T)} \sin(\Omega x_0) \sin(\Omega(T - x_0)). \end{aligned} \quad (\text{E.18})$$

For real Ω, T, x_0 and $\sin(\Omega T) \neq 0$, the ratio of sine functions in Eq. (E.18) is real, so $\langle \hat{q}^2(x_0) \rangle_{\text{D.B.}(T)}$ is purely imaginary.

The same result can be obtained from the eigenstate decomposition, whose starting point is (E.3). Considering the numerator

$$\sum_{m,n=0}^{\infty} \langle q = 0, T | \psi_m \rangle \langle \psi_m | \hat{q}^2(x_0) | \psi_n \rangle \langle \psi_n | q = 0, 0 \rangle, \quad (\text{E.19})$$

makes explicit the contribution from all excited eigenstates.

Using $H|\psi_n\rangle = E_n|\psi_n\rangle$, with $E_n = \hbar\Omega(n + \frac{1}{2})$, we write

$$\langle \psi_m | \hat{q}^2(x_0) | \psi_n \rangle = e^{-\frac{i}{\hbar}(E_n - E_m)x_0} \langle \psi_m | \hat{q}^2 | \psi_n \rangle. \quad (\text{E.20})$$

Because $\psi_{2n+1}(0) = 0$, only even states contribute. Rewriting Eq. (E.19) in terms of even labels yields

$$\langle \hat{q}^2(x_0) \rangle_{\text{D.B.}(T)} = \frac{\sum_{m,n=0}^{\infty} \psi_{2m}^*(0; T) \psi_{2n}(0; 0) \langle \psi_{2m} | \hat{q}^2 | \psi_{2n} \rangle e^{-\frac{i}{\hbar}(E_{2n} - E_{2m})x_0}}{\sum_{m,n=0}^{\infty} \psi_{2n}^*(0; T) \psi_{2n}(0; 0)}, \quad (\text{E.21})$$

where we indicate the denominator as

$$D(T) = \sum_{m,n=0}^{\infty} \psi_{2n}^*(0; T) \psi_{2n}(0; 0) \quad (\text{E.22})$$

The operator \hat{q}^2 can be expressed in ladder form as

$$\hat{q}^2 = \frac{\hbar}{2m\Omega} (aa + a^\dagger a^\dagger + 2a^\dagger a + 1), \quad (\text{E.23})$$

with the corresponding matrix elements

$$\langle n | \hat{q}^2 | n \rangle = \frac{\hbar}{2m\Omega} (2n + 1), \quad (\text{E.24})$$

$$\langle n | \hat{q}^2 | n + 2 \rangle = \frac{\hbar}{2m\Omega} \sqrt{(n + 1)(n + 2)}, \quad \langle n + 2 | \hat{q}^2 | n \rangle = \langle n | \hat{q}^2 | n + 2 \rangle. \quad (\text{E.25})$$

Inserting Eq. (E.23) into Eq. (E.21) and performing the sums over m gives

$$\begin{aligned} \langle \hat{q}^2(x_0) \rangle_{\text{D.B.}(T)} &= \frac{1}{D(T)} \frac{\hbar}{2m\Omega} \left[\sum_{n=0}^{\infty} (4n + 1) \psi_{2n}^*(0; T) \psi_{2n}(0) \right. \\ &\quad + e^{-i2\Omega x_0} \sum_{n=2}^{\infty} \sqrt{2n} \sqrt{2n - 1} \psi_{2n-2}^*(0; T) \psi_{2n}(0) \\ &\quad \left. + e^{+i2\Omega x_0} \sum_{n=0}^{\infty} \sqrt{2n + 1} \sqrt{2n + 2} \psi_{2n+2}^*(0; T) \psi_{2n}(0) \right]. \end{aligned} \quad (\text{E.26})$$

Using the identity (valid after reindexing)

$$\sum_{n=2}^{\infty} \sqrt{2n} \sqrt{2n-1} \psi_{2n-2}^*(0; T) \psi_{2n}(0) = \sum_{n=0}^{\infty} \sqrt{2n+1} \sqrt{2n+2} \psi_{2n}^*(0; T) \psi_{2n+2}(0), \quad (\text{E.27})$$

Eq. (E.26) becomes

$$\begin{aligned} \langle \hat{q}^2(x_0) \rangle_{\text{D.B.}(T)} &= \frac{\hbar}{2m\Omega} \frac{1}{D(T)} \left[\sum_{n=0}^{\infty} (4n+1) \psi_{2n}^*(0; T) \psi_{2n}(0) \right. \\ &\quad + e^{-i2\Omega x_0} \sum_{n=0}^{\infty} \sqrt{2n+1} \sqrt{2n+2} \psi_{2n}^*(0; T) \psi_{2n+2}(0) \\ &\quad \left. + e^{+i2\Omega x_0} \sum_{n=0}^{\infty} \sqrt{2n+1} \sqrt{2n+2} \psi_{2n+2}^*(0; T) \psi_{2n}(0) \right]. \end{aligned} \quad (\text{E.28})$$

Since $\psi_{2n}(0; T) = \psi_{2n}(0) e^{+\frac{i}{\hbar} E_{2n} T}$, we define the continuum spectral coefficients

$$D(T) \equiv \sum_{n=0}^{\infty} e^{+\frac{i}{\hbar} E_{2n} T} |\psi_{2n}(0)|^2, \quad (\text{E.29})$$

$$\alpha(T) \equiv \frac{\sum_{n=0}^{\infty} (4n+1) e^{+\frac{i}{\hbar} E_{2n} T} |\psi_{2n}(0)|^2}{D(T)}, \quad (\text{E.30})$$

$$\gamma_+(T) \equiv \frac{\sum_{n=0}^{\infty} \sqrt{(2n+1)(2n+2)} e^{+\frac{i}{\hbar} E_{2n+2} T} \psi_{2n+2}(0) \psi_{2n}(0)}{D(T)}, \quad (\text{E.31})$$

$$\gamma_-(T) \equiv \frac{\sum_{n=0}^{\infty} \sqrt{(2n+1)(2n+2)} e^{+\frac{i}{\hbar} E_{2n} T} \psi_{2n+2}(0) \psi_{2n}(0)}{D(T)}. \quad (\text{E.32})$$

Inserting these definitions into Eq. (E.28) gives the compact form

$$\langle \hat{q}^2(x_0) \rangle_{\text{D.B.}(T)} = \frac{\hbar}{2m\Omega} \left[\alpha(T) + \gamma_-(T) e^{-i2\Omega x_0} + \gamma_+(T) e^{+i2\Omega x_0} \right]. \quad (\text{E.33})$$

We can show that the expression (E.33) is formally equivalent to the continuum Green's function result (E.18),

$$\langle \hat{q}^2(x_0) \rangle_{\text{D.B.}(T)} = \frac{i\hbar}{m\Omega \sin(\Omega T)} \sin(\Omega x_0) \sin(\Omega(T-x_0)). \quad (\text{E.34})$$

Using the trigonometric identity

$$\sin(\Omega x_0) \sin(\Omega(T-x_0)) = \frac{1}{2} [\sin(2\Omega x_0) + \cot(\Omega T) (\cos(2\Omega x_0) - 1)], \quad (\text{E.35})$$

Eq. (E.34) can be rewritten as

$$\begin{aligned} \langle \hat{q}^2(x_0) \rangle_{\text{D.B.}(T)} &= \frac{\hbar}{2m\Omega} \left\{ -i \cot(\Omega T) + \frac{1}{2} [-1 + i \cot(\Omega T)] e^{-i2\Omega x_0} \right. \\ &\quad \left. + \frac{1}{2} [1 + i \cot(\Omega T)] e^{+i2\Omega x_0} \right\}. \end{aligned} \quad (\text{E.36})$$

which can be rewritten as

$$\langle \hat{q}^2(x_0) \rangle_{\text{D.B.}(T)} = \frac{\hbar}{2m\Omega} \left[a(T) + c_-(T)e^{-i2\Omega x_0} + c_+(T)e^{+i2\Omega x_0} \right], \quad (\text{E.37})$$

with the continuum coefficients

$$a(T) = -i \cot(\Omega T), \quad (\text{E.38})$$

$$c_+(T) = \frac{1}{2} [1 + i \cot(\Omega T)], \quad (\text{E.39})$$

$$c_-(T) = \frac{1}{2} [-1 + i \cot(\Omega T)]. \quad (\text{E.40})$$

We can now show explicitly that the infinite-sum spectral representation (E.33) reproduces exactly the continuum Dirichlet result for $\langle \hat{q}^2(x_0) \rangle_{\text{D.B.}(T)}$. The required step is the analytic evaluation of the spectral coefficients $\alpha(T)$ and $\gamma_{\pm}(T)$ defined in Eqs. (E.30)–(E.32), and proving that they coincide with the continuum coefficients (E.38)–(E.40):

$$a(T) = \alpha(T) \quad (\text{E.41})$$

$$c_{\pm}(T) = \gamma_{\pm}(T). \quad (\text{E.42})$$

Step 1: Closed form of $D(T)$. Using the known values of Hermite polynomials at the origin,

$$\psi_{2n}(0) = \left(\frac{m\Omega}{\pi\hbar} \right)^{1/4} (-1)^n \frac{\sqrt{(2n)!}}{2^n n!}, \quad \psi_{2n+1}(0) = 0, \quad (\text{E.43})$$

we obtain

$$|\psi_{2n}(0)|^2 = \left(\frac{m\Omega}{\pi\hbar} \right)^{1/2} \frac{(2n)!}{4^n (n!)^2} = \left(\frac{m\Omega}{\pi\hbar} \right)^{1/2} \frac{1}{4^n} \binom{2n}{n}. \quad (\text{E.44})$$

Inserting (E.44) into the definition (E.29) yields

$$D(T) = \left(\frac{m\Omega}{\pi\hbar} \right)^{1/2} e^{\frac{i}{2}\Omega T} \sum_{n=0}^{\infty} \binom{2n}{n} \frac{e^{i2\Omega nT}}{4^n}. \quad (\text{E.45})$$

The binomial series identity

$$\sum_{n=0}^{\infty} \binom{2n}{n} \frac{z^n}{4^n} = (1-z)^{-1/2}, \quad (\text{E.46})$$

analytically continued to $z = e^{i2\Omega T}$, yields

$$D(T) = \left(\frac{m\Omega}{\pi\hbar} \right)^{1/2} e^{\frac{i}{2}\Omega T} (1 - e^{i2\Omega T})^{-1/2}. \quad (\text{E.47})$$

Using $1 - e^{i2\Omega T} = -2i e^{i\Omega T} \sin(\Omega T)$, we obtain

$$(1 - e^{i2\Omega T})^{-1/2} = (-2i)^{-1/2} e^{-\frac{i}{2}\Omega T} [\sin(\Omega T)]^{-1/2}. \quad (\text{E.48})$$

Inserting this into the expression for $D(T)$ gives

$$D(T) = \left(\frac{m\Omega}{\pi\hbar} \right)^{1/2} e^{\frac{i}{2}\Omega T} (-2i)^{-1/2} e^{-\frac{i}{2}\Omega T} [\sin(\Omega T)]^{-1/2} \quad (\text{E.49})$$

$$= \left(\frac{m\Omega}{\pi\hbar} \right)^{1/2} \frac{e^{i\pi/4}}{\sqrt{2}} [\sin(\Omega T)]^{-1/2}. \quad (\text{E.50})$$

Step 2: Exact evaluation of $\alpha(T)$. From Eq. (E.30),

$$\alpha(T) = \frac{\sum_{n=0}^{\infty} (4n+1) e^{\frac{i}{\hbar} E_{2n} T} |\psi_{2n}(0)|^2}{D(T)}. \quad (\text{E.51})$$

Using $E_{2n} = \hbar\Omega(2n + \frac{1}{2})$ one verifies the identity

$$4n+1 = \frac{2}{\hbar\Omega} E_{2n}, \quad (\text{E.52})$$

so that

$$\alpha(T) = \frac{2}{i\Omega} \frac{D'(T)}{D(T)}, \quad (\text{E.53})$$

where $D'(T)$ denotes the derivative of (E.29). From (E.50),

$$\frac{D'(T)}{D(T)} = -\frac{1}{2}\Omega \cot(\Omega T), \quad (\text{E.54})$$

and inserting this into (E.53) gives the exact spectral result

$$\alpha(T) = -i \cot(\Omega T) = a(T). \quad (\text{E.55})$$

Step 3: Exact evaluation of $\gamma_{\pm}(T)$. We now evaluate the coefficients $\gamma_{\pm}(T)$ defined in Eqs. (E.31)–(E.32) directly from their infinite spectral sums. Using the explicit expressions of the Hermite polynomials at the origin, Eq. (E.43), we have

$$\psi_{2n}(0) = \left(\frac{m\Omega}{\pi\hbar} \right)^{1/4} (-1)^n \frac{\sqrt{(2n)!}}{2^n n!}, \quad \psi_{2n+2}(0) = \left(\frac{m\Omega}{\pi\hbar} \right)^{1/4} (-1)^{n+1} \frac{\sqrt{(2n+2)!}}{2^{n+1} (n+1)!}. \quad (\text{E.56})$$

A short calculation gives the identity

$$\sqrt{(2n+1)(2n+2)} \psi_{2n+2}(0) \psi_{2n}(0) = - \left(\frac{m\Omega}{\pi\hbar} \right)^{1/2} \frac{(2n+1)!}{4^n (n!)^2}, \quad (\text{E.57})$$

where the minus sign arises from $(-1)^{n+1}(-1)^n = -1$. Inserting (E.57) into Eqs. (E.31)–(E.32) and using

$$E_{2n} = \hbar\Omega \left(2n + \frac{1}{2} \right), \quad E_{2n+2} = \hbar\Omega \left(2n + \frac{5}{2} \right), \quad (\text{E.58})$$

we obtain

$$\text{num}[\gamma_-(T)] = - \left(\frac{m\Omega}{\pi\hbar} \right)^{1/2} e^{\frac{i}{2}\Omega T} \sum_{n=0}^{\infty} \frac{(2n+1)!}{4^n(n!)^2} e^{i2\Omega nT}, \quad (\text{E.59})$$

$$\text{num}[\gamma_+(T)] = - \left(\frac{m\Omega}{\pi\hbar} \right)^{1/2} e^{\frac{5i}{2}\Omega T} \sum_{n=0}^{\infty} \frac{(2n+1)!}{4^n(n!)^2} e^{i2\Omega nT}. \quad (\text{E.60})$$

Introducing the convenient notation

$$z \equiv e^{i2\Omega T}, \quad (\text{E.61})$$

the common sum in (E.59)–(E.60) becomes

$$S(z) \equiv \sum_{n=0}^{\infty} \frac{(2n+1)!}{4^n(n!)^2} z^n. \quad (\text{E.62})$$

To relate $S(z)$ to a closed form we introduce the binomial series

$$F(z) \equiv \sum_{n=0}^{\infty} \frac{(2n)!}{4^n(n!)^2} z^n = (1-z)^{-1/2}, \quad (\text{E.63})$$

obtained from the identity used in Step 1. Using $(2n+1)! = (2n+1)(2n)!$ and

$$(2n+1)\binom{2n}{n} = 2n\binom{2n}{n} + \binom{2n}{n}, \quad (\text{E.64})$$

we find

$$S(z) = \sum_{n=0}^{\infty} (2n+1)\binom{2n}{n} \frac{z^n}{4^n} = 2z F'(z) + F(z). \quad (\text{E.65})$$

From (E.59) and the expression for $D(T)$, Eq. (E.50), we have

$$\gamma_-(T) = \frac{\text{num}[\gamma_-(T)]}{D(T)} = - \frac{e^{\frac{i}{2}\Omega T} S(z)}{\frac{e^{i\pi/4}}{\sqrt{2}} \left(\frac{m\Omega}{\pi\hbar} \right)^{-1/2} [\sin(\Omega T)]^{-1/2} \times \left(\frac{m\Omega}{\pi\hbar} \right)^{1/2}}. \quad (\text{E.66})$$

All factors of $(\frac{m\Omega}{\pi\hbar})^{1/2}$ cancel immediately. The remaining phases also cancel:

$$e^{\frac{i}{2}\Omega T} [\sin(\Omega T)]^{1/2} \times \sqrt{2} e^{-i\pi/4} = (\text{T-dependent phase}). \quad (\text{E.67})$$

However $\gamma_-(T)$ appears only in the final combination

$$\gamma_- e^{-i2\Omega x_0} + \gamma_+ e^{i2\Omega x_0},$$

which is insensitive to this global phase. Thus, up to an overall T -independent phase irrelevant for the correlator, we may write

$$\gamma_-(T) = - \frac{S(z)}{F(z)} = - \left[2z \frac{F'(z)}{F(z)} + 1 \right], \quad (\text{E.68})$$

where we used Eq. (E.65). Since $F(z) = (1 - z)^{-1/2}$,

$$\frac{F'(z)}{F(z)} = \frac{1}{2(1 - z)}. \quad (\text{E.69})$$

Substituting in (E.68) gives

$$\gamma_-(T) = - \left[\frac{z}{1 - z} + 1 \right] = - \frac{1}{1 - z} = \frac{1}{z - 1}. \quad (\text{E.70})$$

With $z = e^{i2\Omega T}$ one finds

$$\gamma_-(T) = \frac{1}{2} \left[-1 + i \cot(\Omega T) \right], \quad (\text{E.71})$$

which coincides with Eq. (E.40).

Evaluation of $\gamma_+(T)$. Using Eq. (E.60), the numerator of $\gamma_+(T)$ differs from that of $\gamma_-(T)$ only by the additional factor $e^{i2\Omega T} = z$. Therefore,

$$\gamma_+(T) = z \gamma_-(T) = \frac{z}{z - 1} = \frac{1}{2} \left[1 + i \cot(\Omega T) \right], \quad (\text{E.72})$$

in agreement with Eq. (E.39). Thus both coefficients $\gamma_{\pm}(T)$ match exactly their continuum counterparts $c_{\pm}(T)$, completing the direct spectral derivation.

F Dirichlet correlators on the lattice

We derive here the lattice Dirichlet two-point function used in the main text. We discretise the interval $[x_0^i, x_0^f]$ into M steps of size a , so that $T = x_0^f - x_0^i = Ma$, and we introduce lattice sites

$$x_0^{(\ell)} \equiv x_0^i + \ell a, \quad \ell = 0, 1, \dots, M, \quad (\text{F.1})$$

with Dirichlet boundary conditions $q_0 = q_M = 0$. On the interior sites $\ell = 1, \dots, M - 1$ we consider the standard quadratic lattice action

$$S_{\text{lat}}[q] \equiv \frac{a}{2} \sum_{\ell=0}^{M-1} \left[\left(\frac{q(\ell+1) - q\ell}{a} \right)^2 - \Omega^2 q(\ell)^2 \right], \quad (\text{F.2})$$

which is the Dirichlet discretisation of the continuum Minkowskian action.

The Dirichlet sine basis diagonalises both the discrete Laplacian and the quadratic form in S_{lat} . We define the discrete Dirichlet wave-numbers

$$\kappa_0^{(n)} \equiv \frac{\pi n}{T} = \frac{\pi n}{Ma}, \quad n = 1, \dots, M - 1, \quad (\text{F.3})$$

and expand the interior field as

$$q(\ell) = \sqrt{\frac{2}{M}} \sum_{n=1}^{M-1} \tilde{q}(n) \sin\left(\frac{\pi n \ell}{M}\right), \quad \ell = 1, \dots, M - 1, \quad (\text{F.4})$$

with inversion

$$\tilde{q}(n) = \sqrt{\frac{2}{M}} \sum_{\ell=1}^{M-1} q(\ell) \sin\left(\frac{\pi n \ell}{M}\right), \quad (\text{F.5})$$

using the discrete orthogonality relation

$$\sum_{\ell=1}^{M-1} \sin\left(\frac{\pi n \ell}{M}\right) \sin\left(\frac{\pi n' \ell}{M}\right) = \frac{M}{2} \delta_{n,n'}. \quad (\text{F.6})$$

The potential term is diagonal because of Eq. (F.6):

$$\sum_{\ell=1}^{M-1} q(\ell)^2 = \sum_{n=1}^{M-1} \tilde{q}(n)^2. \quad (\text{F.7})$$

For the kinetic term we use that the sine modes are eigenvectors of the Dirichlet discrete Laplacian. Writing the forward difference $\Delta q(\ell) \equiv q(\ell+1) - q(\ell)$ and substituting Eq. (F.4), one finds

$$\sum_{\ell=0}^{M-1} (q(\ell+1) - q(\ell))^2 = \sum_{n=1}^{M-1} 4 \sin^2\left(\frac{\pi n}{2M}\right) \tilde{q}(n)^2. \quad (\text{F.8})$$

It is therefore convenient to introduce the lattice Dirichlet eigenvalues

$$\hat{\kappa}_0^{(n)2} \equiv \frac{4}{a^2} \sin^2\left(\frac{\kappa_0^{(n)} a}{2}\right) = \frac{4}{a^2} \sin^2\left(\frac{\pi n}{2M}\right), \quad (\text{F.9})$$

so that Eqs. (F.7)–(F.8) give the diagonal form

$$S_{\text{lat}}[q] = \frac{a}{2} \sum_{n=1}^{M-1} \left(\hat{\kappa}_0^{(n)2} - \Omega^2 \right) \tilde{q}(n)^2. \quad (\text{F.10})$$

The lattice Dirichlet two-point function follows by elementary Gaussian integration with weight $\exp\left(\frac{i}{\hbar} S_{\text{lat}}\right)$:

$$\langle \tilde{q}(n) \tilde{q}(n') \rangle_{\text{D.B.}(T)} = \delta_{n,n'} \frac{i\hbar}{a} \frac{1}{\hat{\kappa}_0^{(n)2} - \Omega^2}. \quad (\text{F.11})$$

Using Eq. (F.4) we obtain the coordinate-space propagator on interior sites,

$$\begin{aligned} \langle q(\ell) q(\ell') \rangle_{\text{D.B.}(T)} &= \frac{2}{M} \sum_{n=1}^{M-1} \sin\left(\frac{\pi n \ell}{M}\right) \sin\left(\frac{\pi n \ell'}{M}\right) \langle \tilde{q}(n)^2 \rangle_{\text{D.B.}(T)} \\ &= i\hbar \sum_{n=1}^{M-1} \frac{2}{M} \frac{\sin\left(\frac{\pi n \ell}{M}\right) \sin\left(\frac{\pi n \ell'}{M}\right)}{\hat{\kappa}_0^{(n)2} - \Omega^2}. \end{aligned} \quad (\text{F.12})$$

Setting $\ell' = \ell$ and inserting Eq. (F.9) gives the equal-time correlator quoted in the main text,

$$\langle q(\ell)^2 \rangle_{\text{D.B.}(T)} = i\hbar \sum_{n=1}^{M-1} \frac{2}{M} \frac{\sin^2\left(\frac{\pi n \ell}{M}\right)}{\frac{4}{a^2} \sin^2\left(\frac{\pi n}{2M}\right) - \Omega^2}. \quad (\text{F.13})$$

The appearance of the $\sin^2(\pi n/2M)$ in the denominator is thus the standard Dirichlet eigenvalue of the discrete Laplacian in one dimension, Eq. (F.9).

G Expectation values of $\langle \hat{q}^{2k}(x_0) \rangle_{\text{D.B.}(T)}$ with Dirichlet boundaries

In this appendix we collect the algebraic steps needed to obtain the discrete frequency content of the harmonic–oscillator “expectation values” of even powers of the position operator with Dirichlet boundary conditions at $q = 0$ in the time interval $[0, T]$. The Dirichlet “expectation value” is defined as in Eq. (E.3),

$$\langle \hat{q}^{2k}(x_0) \rangle_{\text{D.B.}(T)} \equiv \frac{\langle q_f = 0, x_0^f = T \mid \hat{q}^{2k}(x_0) \mid q_i = 0, x_0^i = 0 \rangle}{\langle q_f = 0, x_0^f = T \mid q_i = 0, x_0^i = 0 \rangle}, \quad 0 < x_0 < T, \quad (\text{G.1})$$

so that the denominator is the same Dirichlet amplitude $D(T)$ that appears in the spectral decomposition of the q^2 observable, see Eq. (6.55). We work with the harmonic–oscillator Hamiltonian $H = \hbar\Omega \left(a^\dagger a + \frac{1}{2} \right)$ and use

$$\hat{q} = \alpha(a + a^\dagger), \quad \alpha \equiv \sqrt{\frac{\hbar}{2m\Omega}}, \quad E_n = \hbar\Omega \left(n + \frac{1}{2} \right). \quad (\text{G.2})$$

Since $\psi_{2k+1}(0) = 0$, only even eigenstates contribute for all even powers of \hat{q} .

For $s = 1$ (\hat{q}^2) the final result is already given in the main text and computed explicitly in App. E,

$$\langle \hat{q}^2(x_0) \rangle_{\text{D.B.}(T)} = \frac{\hbar}{2m\Omega} \left[\alpha(T) + \gamma_-(T) e^{-i2\Omega x_0} + \gamma_+(T) e^{+i2\Omega x_0} \right], \quad (\text{G.3})$$

with $\alpha(T)$ and $\gamma_\pm(T)$ defined by the normalized (infinite–tower) sums in Eqs. (6.58)–(6.60). We do not repeat the derivation here and move directly to \hat{q}^4 and \hat{q}^6 .

G.1 \hat{q}^4

We start from the spectral representation

$$\begin{aligned} \langle \hat{q}^4(x_0) \rangle_{\text{D.B.}(T)} &= \frac{1}{D(T)} \sum_{n,m=0}^{\infty} \langle q = 0, T | \psi_m \rangle \langle \psi_m | \hat{q}^4(x_0) | \psi_n \rangle \langle \psi_n | q = 0, 0 \rangle \\ &= \frac{1}{D(T)} \sum_{n,m=0}^{\infty} \langle \psi_m | \hat{q}^4 | \psi_n \rangle \psi_m^*(0; T) \psi_n(0; 0) e^{-\frac{i}{\hbar}(E_n - E_m)x_0}, \end{aligned} \quad (\text{G.4})$$

where $D(T)$ is the Dirichlet amplitude defined in Eq. (6.55). Restricting to even levels we write

$$\langle \hat{q}^4(x_0) \rangle_{\text{D.B.}(T)} = \frac{1}{D(T)} \sum_{n,m=0}^{\infty} \langle \psi_{2m} | \hat{q}^4 | \psi_{2n} \rangle \psi_{2m}^*(0; T) \psi_{2n}(0; 0) e^{-\frac{i}{\hbar}(E_{2n} - E_{2m})x_0}. \quad (\text{G.5})$$

Using

$$\hat{q}^4 = \alpha^4 \left(a^4 + 4a^3 a^\dagger + 6a^2 a^{\dagger 2} + 4a a^{\dagger 3} + a^{\dagger 4} + 6a^2 + 12aa^\dagger + 6a^{\dagger 2} + 3 \right), \quad (\text{G.6})$$

one finds

$$\begin{aligned}
\hat{q}^4 |\psi_n\rangle = \alpha^4 & \left[3(2n^2 + 2n + 1) |\psi_n\rangle + 2(2n + 3)\sqrt{(n+1)(n+2)} |\psi_{n+2}\rangle \right. \\
& + 2(2n - 1)\sqrt{n(n-1)} |\psi_{n-2}\rangle \\
& + \sqrt{(n+1)(n+2)(n+3)(n+4)} |\psi_{n+4}\rangle \\
& \left. + \sqrt{n(n-1)(n-2)(n-3)} |\psi_{n-4}\rangle \right], \tag{G.7}
\end{aligned}$$

with negative indices understood to give vanishing contributions. In the even subspace we write

$$\langle \psi_{2m} | \hat{q}^4 | \psi_{2n} \rangle = \left(\frac{\hbar}{2m\Omega} \right)^2 M_{mn}, \tag{G.8}$$

with

$$\begin{aligned}
M_{mn} = & 3(8n^2 + 4n + 1) \delta_{m,n} \\
& + 2(4n + 3)\sqrt{(2n+1)(2n+2)} \delta_{m,n+1} \\
& + 2(4n - 1)\sqrt{2n(2n-1)} \delta_{m,n-1} \\
& + \sqrt{(2n+1)(2n+2)(2n+3)(2n+4)} \delta_{m,n+2} \\
& + \sqrt{(2n-3)(2n-2)(2n-1)(2n)} \delta_{m,n-2}. \tag{G.9}
\end{aligned}$$

Using the energy differences $E_{2n} - E_{2n} = 0$, $E_{2n} - E_{2n\pm 2} = \mp 2\hbar\Omega$, $E_{2n} - E_{2n\pm 4} = \mp 4\hbar\Omega$, the correlator contains only the harmonics $0, \pm 2\Omega, \pm 4\Omega$. It is convenient to factor out the overall power of $\frac{\hbar}{2m\Omega}$ and define normalized coefficients $\alpha_4(T)$, $\gamma_4^{(\pm)}(T)$, $\delta_4^{(\pm)}(T)$ through

$$\begin{aligned}
\langle \hat{q}^4(x_0) \rangle_{\text{D.B.}(T)} = & \left(\frac{\hbar}{2m\Omega} \right)^2 \left[\alpha_4(T) + \gamma_4^{(-)}(T)e^{-i2\Omega x_0} + \gamma_4^{(+)}(T)e^{+i2\Omega x_0} \right. \\
& \left. + \delta_4^{(-)}(T)e^{-i4\Omega x_0} + \delta_4^{(+)}(T)e^{+i4\Omega x_0} \right]. \tag{G.10}
\end{aligned}$$

Explicitly,

$$\alpha_4(T) \equiv \frac{\sum_{n=0}^{\infty} 3(8n^2 + 4n + 1) e^{+\frac{i}{\hbar}E_{2n}T} |\psi_{2n}(0)|^2}{D(T)}, \quad (\text{G.11})$$

$$\gamma_4^{(+)}(T) \equiv \frac{\sum_{n=0}^{\infty} 2(4n+3) \sqrt{(2n+1)(2n+2)} e^{+\frac{i}{\hbar}E_{2n+2}T} \psi_{2n+2}(0) \psi_{2n}(0)}{D(T)}, \quad (\text{G.12})$$

$$\gamma_4^{(-)}(T) \equiv \frac{\sum_{n=0}^{\infty} 2(4n+3) \sqrt{(2n+1)(2n+2)} e^{+\frac{i}{\hbar}E_{2n}T} \psi_{2n}(0) \psi_{2n+2}(0)}{D(T)}, \quad (\text{G.13})$$

$$\delta_4^{(+)}(T) \equiv \frac{\sum_{n=0}^{\infty} \sqrt{(2n+1)(2n+2)(2n+3)(2n+4)} e^{+\frac{i}{\hbar}E_{2n+4}T} \psi_{2n+4}(0) \psi_{2n}(0)}{D(T)}, \quad (\text{G.14})$$

$$\delta_4^{(-)}(T) \equiv \frac{\sum_{n=0}^{\infty} \sqrt{(2n+1)(2n+2)(2n+3)(2n+4)} e^{+\frac{i}{\hbar}E_{2n}T} \psi_{2n}(0) \psi_{2n+4}(0)}{D(T)}. \quad (\text{G.15})$$

For generic T the five coefficients in Eq. (G.10) are independent complex functions of ΩT .

G.2 \hat{q}^6

For \hat{q}^6 we again start from the normalized spectral representation

$$\langle \hat{q}^6(x_0) \rangle_{\text{D.B.}(T)} = \frac{1}{D(T)} \sum_{n,m=0}^{\infty} \langle \psi_m | \hat{q}^6 | \psi_n \rangle \psi_m^*(0; T) \psi_n(0; 0) e^{-\frac{i}{\hbar}(E_n - E_m)x_0}, \quad (\text{G.16})$$

restrict to even levels and use

$$\hat{q}^6 = \alpha^6 (a + a^\dagger)^6. \quad (\text{G.17})$$

A straightforward but lengthy calculation gives

$$\begin{aligned} \hat{q}^6 | \psi_n \rangle &= \alpha^6 \left[A_n | \psi_n \rangle + B_n | \psi_{n+2} \rangle + B_{n-2} | \psi_{n-2} \rangle \right. \\ &\quad + C_n | \psi_{n+4} \rangle + C_{n-4} | \psi_{n-4} \rangle \\ &\quad \left. + D_n | \psi_{n+6} \rangle + D_{n-6} | \psi_{n-6} \rangle \right], \end{aligned} \quad (\text{G.18})$$

with

$$A_n = 20n^3 + 30n^2 + 40n + 15, \quad (\text{G.19})$$

$$B_n = 15(n^2 + 3n + 3) \sqrt{(n+1)(n+2)}, \quad (\text{G.20})$$

$$C_n = (6n+15) \sqrt{(n+1)(n+2)(n+3)(n+4)}, \quad (\text{G.21})$$

$$D_n = \sqrt{(n+1)(n+2)(n+3)(n+4)(n+5)(n+6)}, \quad (\text{G.22})$$

and negative indices understood to give vanishing contributions. Restricting to even levels we write

$$\langle \psi_{2m} | \hat{q}^6 | \psi_{2n} \rangle = \left(\frac{\hbar}{2m\Omega} \right)^3 N_{mn}, \quad (\text{G.23})$$

with

$$\begin{aligned} N_{mn} = & (160n^3 + 120n^2 + 80n + 15) \delta_{m,n} \\ & + 15(4n^2 + 6n + 3) \sqrt{(2n+1)(2n+2)} \delta_{m,n+1} \\ & + 15(4n^2 - 2n + 1) \sqrt{2n(2n-1)} \delta_{m,n-1} \\ & + (12n+15) \sqrt{(2n+1)(2n+2)(2n+3)(2n+4)} \delta_{m,n+2} \\ & + (12n-9) \sqrt{(2n-3)(2n-2)(2n-1)(2n)} \delta_{m,n-2} \\ & + \sqrt{(2n+1)(2n+2)(2n+3)(2n+4)(2n+5)(2n+6)} \delta_{m,n+3} \\ & + \sqrt{(2n-5)(2n-4)(2n-3)(2n-2)(2n-1)(2n)} \delta_{m,n-3}. \end{aligned} \quad (\text{G.24})$$

Using $E_{2n} - E_{2n \pm 2k} = \mp 2k\hbar\Omega$ for $k = 1, 2, 3$ we find that only the harmonics $0, \pm 2\Omega, \pm 4\Omega, \pm 6\Omega$ appear. Factoring out $(\hbar/2m\Omega)^3$ we define normalized coefficients $\alpha_6(T)$, $\gamma_6^{(\pm)}(T)$, $\delta_6^{(\pm)}(T)$, $\epsilon_6^{(\pm)}(T)$ via

$$\begin{aligned} \langle \hat{q}^6(x_0) \rangle_{\text{D.B.}(T)} = & \left(\frac{\hbar}{2m\Omega} \right)^3 \left[\alpha_6(T) + \gamma_6^{(-)}(T) e^{-i2\Omega x_0} + \gamma_6^{(+)}(T) e^{+i2\Omega x_0} \right. \\ & + \delta_6^{(-)}(T) e^{-i4\Omega x_0} + \delta_6^{(+)}(T) e^{+i4\Omega x_0} \\ & \left. + \epsilon_6^{(-)}(T) e^{-i6\Omega x_0} + \epsilon_6^{(+)}(T) e^{+i6\Omega x_0} \right], \end{aligned} \quad (\text{G.25})$$

where each coefficient is the corresponding even–level spectral sum divided by the Dirichlet amplitude $D(T)$. Explicitly,

$$\alpha_6(T) \equiv \frac{\sum_{n=0}^{\infty} (160n^3 + 120n^2 + 80n + 15) e^{+\frac{i}{\hbar} E_{2n} T} |\psi_{2n}(0)|^2}{D(T)}, \quad (\text{G.26})$$

$$\gamma_6^{(+)}(T) \equiv \frac{\sum_{n=0}^{\infty} 15(4n^2 + 6n + 3) \sqrt{(2n+1)(2n+2)} e^{+\frac{i}{\hbar} E_{2n+2} T} \psi_{2n+2}(0) \psi_{2n}(0)}{D(T)}, \quad (\text{G.27})$$

$$\gamma_6^{(-)}(T) \equiv \frac{\sum_{n=0}^{\infty} 15(4n^2 + 6n + 3) \sqrt{(2n+1)(2n+2)} e^{+\frac{i}{\hbar} E_{2n} T} \psi_{2n}(0) \psi_{2n+2}(0)}{D(T)}, \quad (\text{G.28})$$

$$\delta_6^{(+)}(T) \equiv \frac{\sum_{n=0}^{\infty} (12n + 15) \sqrt{(2n+1)(2n+2)(2n+3)(2n+4)} e^{+\frac{i}{\hbar} E_{2n+4} T} \psi_{2n+4}(0) \psi_{2n}(0)}{D(T)}, \quad (\text{G.29})$$

$$\delta_6^{(-)}(T) \equiv \frac{\sum_{n=0}^{\infty} (12n + 15) \sqrt{(2n+1)(2n+2)(2n+3)(2n+4)} e^{+\frac{i}{\hbar} E_{2n} T} \psi_{2n}(0) \psi_{2n+4}(0)}{D(T)}, \quad (\text{G.30})$$

$$\epsilon_6^{(+)}(T) \equiv \frac{\sum_{n=0}^{\infty} \sqrt{(2n+1)(2n+2)(2n+3)(2n+4)(2n+5)(2n+6)} e^{+\frac{i}{\hbar} E_{2n+6} T} \psi_{2n+6}(0) \psi_{2n}(0)}{D(T)}, \quad (\text{G.31})$$

$$\epsilon_6^{(-)}(T) \equiv \frac{\sum_{n=0}^{\infty} \sqrt{(2n+1)(2n+2)(2n+3)(2n+4)(2n+5)(2n+6)} e^{+\frac{i}{\hbar} E_{2n} T} \psi_{2n}(0) \psi_{2n+6}(0)}{D(T)}. \quad (\text{G.32})$$

For generic T these seven quantities are independent complex functions of ΩT .

H Resonant enhancement of Dirichlet correlators on the lattice and relation to truncated even–state sums

We explain here why, for resonant choices of the Dirichlet time extent T , the equal–time correlator measured in the constrained dynamics can grow linearly with the lattice size M . The same mechanism appears in the continuum spectral representation when the Hilbert–space sums are truncated to a finite number of even eigenstates.

We start from the continuum Dirichlet expectation value at $q_i = q_f = 0$,

$$\langle \hat{q}^2(x_0) \rangle_{\text{D.B.}(T)} \equiv \frac{\langle 0, x_0^{\text{f}} | \hat{q}^2(x_0) | 0, x_0^{\text{i}} \rangle}{\langle 0, x_0^{\text{f}} | 0, x_0^{\text{i}} \rangle}, \quad T = x_0^{\text{f}} - x_0^{\text{i}}, \quad (\text{H.1})$$

and recall that inserting completeness leads to the three-harmonic form (Eq. (6.57) in the main text) with coefficients given by even-state sums. In numerical implementations one never samples an infinite tower of states; rather, the effective description is necessarily truncated. It is therefore natural to introduce the truncated, normalised coefficients

$$D_N(T) \equiv \sum_{n=0}^N e^{+\frac{i}{\hbar} E_{2n} T} |\psi_{2n}(0)|^2, \quad (\text{H.2})$$

$$\alpha_N(T) \equiv \frac{\sum_{n=0}^N (4n+1) e^{+\frac{i}{\hbar} E_{2n} T} |\psi_{2n}(0)|^2}{D_N(T)}, \quad (\text{H.3})$$

$$\gamma_{+,N}(T) \equiv \frac{\sum_{n=0}^N \sqrt{(2n+1)(2n+2)} e^{+\frac{i}{\hbar} E_{2n+2} T} \psi_{2n+2}(0) \psi_{2n}(0)}{D_N(T)}, \quad (\text{H.4})$$

$$\gamma_{-,N}(T) \equiv \frac{\sum_{n=0}^N \sqrt{(2n+1)(2n+2)} e^{+\frac{i}{\hbar} E_{2n} T} \psi_{2n+2}(0) \psi_{2n}(0)}{D_N(T)}. \quad (\text{H.5})$$

The truncated Dirichlet “expectation value” is then

$$\langle \hat{q}^2(x_0) \rangle_{\text{D.B.}(T)}^{(N)} = \frac{\hbar}{2m\Omega} \left[\alpha_N(T) + \gamma_{-,N}(T) e^{-i2\Omega(x_0 - x_0^{\text{i}})} + \gamma_{+,N}(T) e^{+i2\Omega(x_0 - x_0^{\text{i}})} \right], \quad (\text{H.6})$$

which reduces to the continuum result as $N \rightarrow \infty$.

The origin of resonant enhancement is that, at special time extents, the phases in the even-state sums cease to oscillate and cancellations are lost. The large- n behaviour of the harmonic-oscillator eigenfunctions at the origin is

$$|\psi_{2n}(0)|^2 = \left(\frac{m\Omega}{\pi\hbar} \right)^{1/2} \frac{(2n)!}{4^n (n!)^2} \sim \left(\frac{m\Omega}{\pi\hbar} \right)^{1/2} \frac{1}{\sqrt{\pi n}}, \quad n \gg 1. \quad (\text{H.7})$$

For generic T the phases $e^{iE_{2n}T/\hbar} = e^{i(2n+\frac{1}{2})\Omega T}$ oscillate rapidly with n , so the partial sums entering Eqs. (H.2)–(H.5) converge efficiently with increasing N despite the slow $n^{-1/2}$ envelope. At resonant times, instead, the phases align. For example, if $T = 4\pi/\Omega$ then $e^{i2\Omega T} = 1$ and all terms add coherently. Equation (H.7) then implies the scaling

$$D_N(4\pi/\Omega) \sim \sum_{n=1}^N n^{-1/2} \propto \sqrt{N}, \quad (\text{H.8})$$

whereas the numerator of α_N carries an additional factor $(4n+1) \sim 4n$,

$$\sum_{n=1}^N (4n+1) e^{+\frac{i}{\hbar} E_{2n}(4\pi/\Omega)} |\psi_{2n}(0)|^2 \sim \sum_{n=1}^N n \cdot n^{-1/2} \propto N^{3/2}. \quad (\text{H.9})$$

Therefore

$$\alpha_N(4\pi/\Omega) \propto \frac{N^{3/2}}{\sqrt{N}} \sim N, \quad (\text{H.10})$$

and the same linear scaling holds for $\gamma_{\pm,N}(4\pi/\Omega)$, since their numerators have the same large- n weight up to subleading factors. The truncated, normalised coefficients thus grow linearly with the truncation level whenever the continuum Dirichlet correlator is resonant.

The lattice exhibits the same phenomenon in a technically different but conceptually identical way: the enhancement arises from a near-zero of the denominator in the mode representation of the lattice propagator. Discretise the Dirichlet interval T into M steps of size a (so $T = Ma$), impose $q_0 = q_M = 0$, and denote the interior sites by $\ell = 1, \dots, M-1$. In complete analogy with the continuum Dirichlet decomposition, the lattice Dirichlet modes are labelled by $n = 1, \dots, M-1$ and correspond to the discrete wave-numbers

$$\kappa_0^{(n)} \equiv \frac{\pi n}{T} = \frac{\pi n}{Ma}, \quad (\text{H.11})$$

while the eigenvalues of the Dirichlet lattice Laplacian are

$$\hat{\kappa}_0^{(n)2} \equiv \frac{4}{a^2} \sin^2\left(\frac{\kappa_0^{(n)} a}{2}\right) = \frac{4}{a^2} \sin^2\left(\frac{\pi n}{2M}\right). \quad (\text{H.12})$$

In this notation the equal-time lattice Dirichlet correlator is

$$\langle q(\ell)^2 \rangle_{\text{D.B.}(T)} = i\hbar \sum_{n=1}^{M-1} \frac{2}{M} \frac{\sin^2\left(\frac{\pi n \ell}{M}\right)}{\hat{\kappa}_0^{(n)2} - \Omega^2}, \quad (\text{H.13})$$

which is equivalent to Eq. (6.74) in the main text.

For a resonant choice such as $T = 4\pi/\Omega$ there exists an integer mode index $n_\star \in \{1, \dots, M-1\}$ such that the lattice eigenvalue $\hat{\kappa}_0^{(n_\star)2}$ lies closest to Ω^2 . The corresponding term in Eq. (H.13) is then enhanced because $|\hat{\kappa}_0^{(n_\star)2} - \Omega^2|$ is small. As M is increased at fixed T (hence at fixed $a = T/M$), the set of available $\hat{\kappa}_0^{(n)2}$ becomes denser and the closest approach to Ω^2 improves; in particular the minimal gap $\min_{1 \leq n \leq M-1} |\hat{\kappa}_0^{(n)2} - \Omega^2|$ decreases. When T is tuned to resonance this produces an overall growth of the correlator amplitude that is observed empirically to be approximately linear in M in the range of parameters considered here. This is the lattice counterpart of the linear growth $\alpha_N, \gamma_{\pm,N} \propto N$ at resonance in the truncated even-state sums, with the identification that the effective number of resolved degrees of freedom (hence the effective truncation scale) increases with lattice resolution, $N \sim \mathcal{O}(M)$.

The numerical signature of this resonant enhancement is that $\langle q(\ell)^2 \rangle_{\text{D.B.}(T)}$ grows linearly with M at fixed resonant T , and therefore the rescaled quantity $\langle q(\ell)^2 \rangle_{\text{D.B.}(T)}/M$ collapses for different M , as shown in Fig. 6 in the main text.

References

- [1] M. Giachello, F. Scardino and G. Gradenigo, *Symplectic quantization: numerical results for the Feynman propagator on a 1+1 lattice and the theoretical relation with quantum field theory*, *JHEP* **09** (2025) 129, [[2403.17149](#)].
- [2] G. Gradenigo and R. Livi, *Symplectic quantization i: dynamics of quantum fluctuations in a relativistic field theory*, *Found. Phys.* **51** (2021) 66, [[2101.02125](#)].
- [3] G. Gradenigo, *Symplectic quantization ii: Dynamics of space-time quantum fluctuations and the cosmological constant*, *Found. Phys.* **51** (2021) 64, [[2101.01795](#)].
- [4] G. Gradenigo, R. Livi and L. Salasnich, *Symplectic quantization iii: Non-relativistic limit*, *Found. Phys.* **54** (2024) 50, [[2401.12355](#)].
- [5] M. Giachello, G. Gradenigo and F. Scardino, *Symplectic quantization and minkowskian statistical mechanics: simulations on a 1+1 lattice*, *PoS LATTICE2024* (2024) 359, [[2412.09162](#)].
- [6] M. Giachello and G. Gradenigo, *Symplectic quantization: A new deterministic approach to the dynamics of quantum fields inspired by statistical mechanics*, *EPJ Web Conf.* **314** (2024) 00028.
- [7] M. Creutz and B. Freedman, *A STATISTICAL APPROACH TO QUANTUM MECHANICS*, *Annals Phys.* **132** (1981) 427.
- [8] G. Parisi and Y.-s. Wu, *Perturbation Theory Without Gauge Fixing*, *Sci. Sin.* **24** (1981) 483.
- [9] P. H. Damgaard and H. Huffel, *Stochastic quantization*, *Phys. Rept.* **152** (1987) 227–398.
- [10] V. de Alfaro, S. Fubini and G. Furlan, *Microcanonical ensemble and quantum field theory*, *Nuovo Cim. A* **74** (1983) 365.
- [11] A. E. Strominger, *Microcanonical quantum field theory*, *Annals Phys.* **146** (1983) 419.
- [12] A. Iwazaki, *Microcanonical formulation of quantum field theories*, *Phys. Lett. B* **141** (1984) 342–348.
- [13] G. Parisi, *On Complex Probabilities*, *Phys. Lett. B* **131** (1983) 393–395.
- [14] D. J. E. Callaway and A. Rahman, *Lattice gauge theory in the microcanonical ensemble*, *Phys. Rev. D* **28** (Sep, 1983) 1506–1514.
- [15] S. Duane, A. D. Kennedy, B. J. Pendleton and D. Roweth, *Hybrid monte carlo*, *Phys. Lett. B* **195** (1987) 216–222.
- [16] R. P. Feynman, *Space-time approach to non-relativistic quantum mechanics*, *Reviews of Modern Physics* **20** (1948) 367–387.
- [17] A. Alexandru, G. Basar, P. F. Bedaque and N. C. Warrington, *Complex paths around the sign problem*, *Rev. Mod. Phys.* **94** (2022) 015006, [[2007.05436](#)].
- [18] M. Cristoforetti, F. Di Renzo and L. Scorzato, *New approach to the sign problem in quantum field theories: High density QCD on a Lefschetz thimble*, *Phys. Rev. D* **86** (2012) 074506, [[1205.3996](#)].
- [19] L. Scorzato, *The Lefschetz thimble and the sign problem*, *PoS LATTICE2015* (2016) 016, [[1512.08039](#)].

- [20] A. Behtash, G. V. Dunne, T. Schäfer, T. Sulejmanpasic and M. Ünsal, *Toward Picard–Lefschetz theory of path integrals, complex saddles and resurgence*, *Ann. Math. Sci. Appl.* **02** (2017) 95–212, [[1510.03435](#)].
- [21] E. Witten, *Analytic Continuation Of Chern-Simons Theory*, *AMS/IP Stud. Adv. Math.* **50** (2011) 347–446, [[1001.2933](#)].
- [22] C. Gattringer and K. Langfeld, *Approaches to the sign problem in lattice field theory*, *Int. J. Mod. Phys. A* **31** (2016) 1643007, [[1603.09517](#)].
- [23] M. Troyer and U.-J. Wiese, *Computational complexity and fundamental limitations to fermionic quantum Monte Carlo simulations*, *Phys. Rev. Lett.* **94** (2005) 170201, [[cond-mat/0408370](#)].
- [24] E. Y. Loh, J. E. Gubernatis, R. T. Scalettar, S. R. White, D. J. Scalapino and R. L. Sugar, *Sign problem in the numerical simulation of many-electron systems*, *Phys. Rev. B* **41** (1990) 9301–9307.
- [25] M. Blau and G. Thompson, *Chern-Simons Theory with Complex Gauge Group on Seifert Fibred 3-Manifolds*, 3, 2016.
- [26] E. Witten, *A New Look At The Path Integral Of Quantum Mechanics*, 9, 2010.
- [27] A. Alexandru, P. F. Bedaque, H. Lamm and S. Lawrence, *Finite-Density Monte Carlo Calculations on Sign-Optimized Manifolds*, *Phys. Rev. D* **97** (2018) 094510, [[1804.00697](#)].
- [28] M. Baldovin, G. Gradenigo, A. Vulpiani and N. Zanghì, *On the foundations of statistical mechanics*, *Phys. Rept.* **1132** (2025) 1–79, [[2411.08709](#)].
- [29] L. S. Schulman, *Techniques and Applications of Path Integration*. Dover Publications, Mineola, N.Y., 2005.
- [30] M. Giachello, G. Gradenigo and F. Scardino, *Symplectic quantization ii: free scalar field theory*, *in preparation* (2025) .
- [31] M. Giachello, F. Scardino and G. Gradenigo, *Symplectic quantization: the anharmonic oscillator*, *in preparation* (2025) .